Studies on geochemical behavior of environmental radioisotopes and their applications to sedimentology

(天然放射性核種の地球化学的挙動とその堆積学への応用に関する研究)

Yutaka Kanai

金井豊

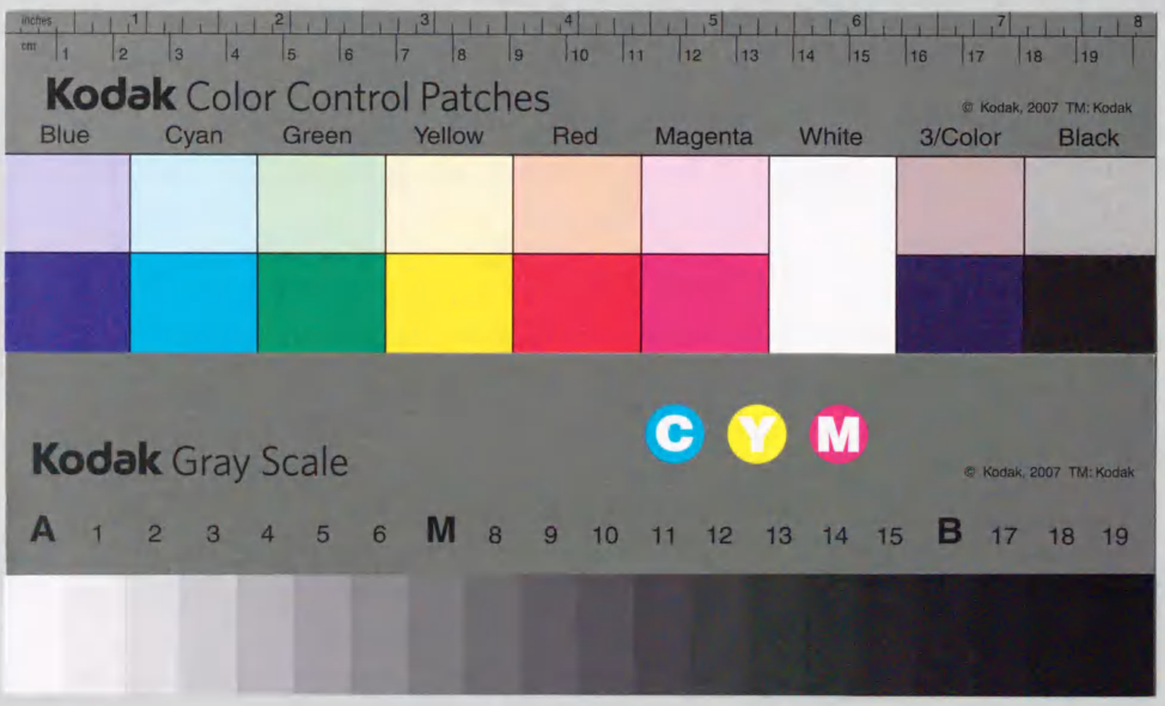

Studies on geochemical behavior of environmental radioisotopes and their applications to sedimentology

（天然放射性核種の地球化学的挙動と
その堆積学への応用に関する研究）

Yutaka Kanai

金 井 豊

Contents

Abstract

Studies on geochemical behavior of environmental radioisotopes and their applications to sedimentology

Yutaka Kanai

In chapter 1 and 2, the radionuclides in environment, especially U series nuclides are listed and the improved analytical methods for determination, radioactivity measurement, and selective chemical leaching methods are shown as introductory chapters.

In chapter 3, the geochemical behavior of uranium, radium and radon in the Masutomi spring district were studied at first. This is a case study on water-rock interaction and water geochemistry. The U concentrations in the Masutomi spring waters are relatively low, while its daughter nuclides Ra-226, Rn-222 are in excess. The U-234/U-238 activity ratios (ARs) are > 1, show an inverse correlation with U-238. These results are explained by reducing water condition and alpha recoil dissolution of Th-234. In this way, the dissolution process of U is important and a part of the water-rock system is elucidated.

Secondly, U impurity in Al reagents motivated me to study bauxite deposits at Yangwa mine in China as a case study, and geochemical behavior and sedimentation process were studied using not only bulk but also fractional compositions obtained by chemical leaching method. U had a strong correlation with Al_2O_3. Most of U in the bauxite is in “HF soluble” and "resistate" fractions whose ARs were < 1 and have a good correlation with the fractional U content, while the ARs of "HCl soluble" U were > 1 and have an inverse correlation with the fractional U content. This suggests that constant amount of mobile U-234 was present. The deposit is thought to be sedimentary in origin. The clay minerals changed reversibly to gibbsite and diaspore. Th-234 was ejected from U-containing mineral and was adsorbed as HCl soluble form in the ore deposits.

Thirdly as a case study on oxidation states, the diagenetic behavior of U(IV, VI) in apatite-bearing sedimentary rocks at Nakamaruke was studied. U content in the strata showed two peaks, the most prominent one at the phosphatic layer with ARs of < 1 and another small one at the lower part of the outcrop (> 0.3 m away from the phosphatic

layer) with ARs of > 1. "U(IV)", "U(VI)" and "residue" fractions were obtained. About 50 % of total U was in "U(VI)" fraction, whose ARs were > 1, so U(VI) is inferred to be bound relatively weakly and move easily. The ARs of "U(IV)" and "residue" fractions showed the same trend as total U. The ARs of the "residue" fraction composed of silicate and clay minerals suggest that some U moved and was adsorbed by phyllosilicates.

Next a selective chemical leaching technique was applied to the granitic conglomerate from the Tono uranium mine to elucidate the processes of migration. The fact that the Th-230/U-234 activity ratios are > 1, suggests partial migration of U. By the selective chemical leaching experiment, it is inferred that carbonates and iron oxides play an important role in U ore genesis. The ion exchangeable U is bound weakly and exchangeable with U in the surrounding water with AR > 1. The ARs of residue fraction varied with the grain size, indicating that the injection effect is advantageous for the coarser grain while the ejection effect is advantageous for the finer grain. The organic/sulfide fraction is depleted in Th-230 compared with U. It suggests that U was secondarily enriched without Th and continued to elute, and that pyrites adsorbed a portion of the eluted U and helped the secondary fixation of U in modern times.

Finally I applied Pb-210 and Cs-137 to the dating of sediments because the dating of geological events is very important. In this section, the sedimentation rates and sedimentary environment in Lake Shinji are studied and several cautions for application are elucidated. The sedimentation rates in the western area are larger than those in the eastern and central areas, which indicates that most of the sediments supplied by the Hii River deposited in the western area. The inventories of excess Pb-210 and Cs-137 were larger in the western area, and are in a positive correlation each other. While the bioturbation and mixing change the profile of radionuclides, some sedimentation rates are obtained using Berger and Heath model.

In chapter 4, concluding remarks are expressed. By analyzing behavior of natural radioactive nuclides as useful tracers in combination with selective chemical leaching methods, the sedimentary environment and diagenetic process are clearly elucidated in detail, and furthermore the dating is also possible for the lake and sea sediments.

KEYWORDS : radioisotopes, uranium series nuclides, U-238, U-234, Th-230, Ra-226, Rn-222, Pb-210, disequilibrium, geochemistry, sedimentology, spring water, bauxite, apatite, uranium mine, sedimentation rate

Chapter 1 Environmental radioisotopes

1.1 Introduction

Natural radiation is everywhere. We suffer about 2.4 mSv of radiation per year from environment. Radioisotopes that exist and are produced on the earth, are classified as follows.

(1) Uranium series nuclides, thorium series nuclides, and actinium series nuclides, that make decay chains.

(2) Radioisotopes that are produced at the production time of elements and didn't disappear because of their long half-lives. K-40, Rb-87 and Re-187 are such nuclides.

(3) Radioisotopes that are produced by cosmic rays, mainly in the stratosphere and come through tropopause. Be-7, Si-32 and Cl-36 belong to this category.

(4) Artificial radioisotopes that are formed by atmospheric testing of nuclear weapons and nuclear reactors. Cs-137, Sr-90 and Pu-239 are examples.

Among these nuclides, uranium series nuclides are one of the most important and well-known sources of natural radioactivity. These are shown in Table 1-1 with other natural decay series. The parent nuclide, U-238, is popular as uranium element, and uranium ores have been explored and surveyed for the use of nuclear reactor fuel. So, uranium geochemistry is of much concern for geochemical exploration, mining, and recently nuclear waste management.

Uranium in environment is considered to be one of the natural tracers because the geological environmental condition in various media such as water, rocks, ores and sediments, controls its behavior with other elements. Furthermore, uranium has a decay chain and its daughter nuclides make radioactive equilibria or disequilibria (The details are written below). The relationships among chain nuclides give good suggestions for geochemical and geological events.

On the other hand, uranium is one of the important natural analog nuclides for the disposal of the high level radioactive waste (HLW). The management of the HLW is at present one of the most important problems, and uranium geochemistry is expected to provide some knowledge for the radionuclide migration and retardation assessment

(Brookins, 1984; Chapman and Smellie,1986; Finnegan and Bryant, 1987). Uranium has two major chemical valences, oxidation state U(VI) and reduced state U(IV). These chemical states have different physicochemical properties such as solubility. The HLW contains much trans-uranium nuclides. As their geochemical behavior resemble to that of uranium in many cases, uranium is considered to be one of the best analogs for the trans-uranium nuclides, and the knowledge about the geochemical behavior of in-situ uranium gives the information about geochemical behavior of trans-uranium nuclides without the direct handling in the field (The details are also written below). Therefore, it has been much important to study geochemical behavior of uranium in various kinds of geological media.

Table 1-1 Natural decay series nuclides. Nuclides in the same line become in radioactive equilibrium easily.

(1) Uranium series

4.47×10^{9}y	^{238}U	→	^{234}Th	→	^{234}Pa	→					
			(24.1d)		(6.75h)						
2.45×10^{5}y	^{234}U	→									
7.52×10^{4}y	^{230}Th	→									
1.60×10^{3}y	^{226}Ra	→	^{222}Rn	→	^{218}Po	→	^{214}Pb	→	^{214}Bi	→	^{214}Po →
			(3.82d)		(3.05m)		(26.8m)		(19.7m)		(164 μ s)
22.3y	^{210}Pb	→	^{210}Bi	→							
			(5.01d)								
138d	^{210}Po	→									
stable	^{206}Pb										

(2) Thorium series

1.41×10^{10}y	^{232}Th	→									
5.76y	^{228}Ra	→	^{228}Ac	→							
			(6.13h)								
1.91y	^{228}Th	→	^{224}Ra	→	^{220}Rn	→	^{216}Po	→	^{212}Pb	→	^{212}Bi → ^{208}Tl ^{212}Po →
			(3.66d)		(55.6s)		(0.15s)		(10.6h)		(60.6m) (3.0m) (0.3 μ s)
stable	^{208}Pb										

(3) Actinium series

7.04×10^{8}y	^{235}U	→	^{231}Th	→							
			(25.5h)								
3.28×10^{4}y	^{231}Pa	→									
21.8y	^{227}Ac	→	^{227}Th	→	^{223}Ra	→	^{219}Rn	→	^{215}Po	→	^{211}Pb → ^{211}Bi → ^{207}Tl →
			(18.7d)		(11.4d)		(3.96s)		(1.78ms)		(36.1m) (2.15m) (4.77m)
stable	^{207}Pb										

1.2 Radioactive equilibria

Uranium disequilibrium study in natural substances was initiated by Cherdyntsev in 1955. Then many studies have elucidated the radioactive disequilibria in rocks, deposits and waters, and a variety of applications have been developed on the basis of the phenomena (Ivanavich and Harmon, 1982; 1992). In most cases, disequilibrium is caused by water movement, change of environment, or physicochemistry of daughter nuclide produced.

Daughters belonging to the uranium or thorium decay chain have different half-lives. If the half-life of daughter nuclide is shorter than that of its precursor, then the activity of daughter nuclide grows up and becomes at constant level (so called "transient equilibrium"), and if the half-life of daughter nuclide is much shorter, then the activity of daughter nuclide becomes as high as that of its precursor after the time several times of its half-time (so called "secular equilibrium"). Table 1-1 shows the groups of daughters that easily become in radioactive equilibrium. In such case, if some geochemical and geological events such as alteration or diagenesis occur, daughter nuclide may behave differently because of different physicochemical characteristics. For example, thorium-230 (so called ionium) with half-life of about 7.52×10^4 y, is a daughter of U-234 whose half-life is about 2.45×10^5 y, which is much longer enough to become radioactive equilibrium among them. The former is thorium and the latter is uranium, so if chemical fractionation occurs, radioactive disequilibrium takes place among decay chain. This is used for the ionium dating of volcanic rocks.

In this study, the relationships among the U-234/U-238 activity ratio and the Th-230/U-234 activity ratio are used as is shown in Fig.1-1. The area of U-234/U-238 activity ratio < 1 and the Th-230/U-234 activity ratio > 1 means U-234<U-238, Th-230, and implies that uranium is readily

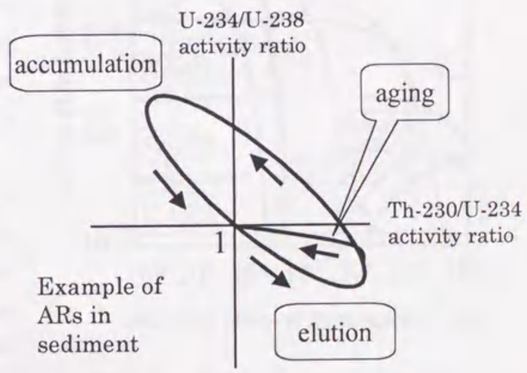

Fig.1-1 Relationships between U-234/U-238 and Th-230/U-234 activity ratios.

removed. Once the system becomes in disequilibrium, it takes over than 300 thousand years to recover equilibrium after the system becomes a closed system (Fig.1-2).

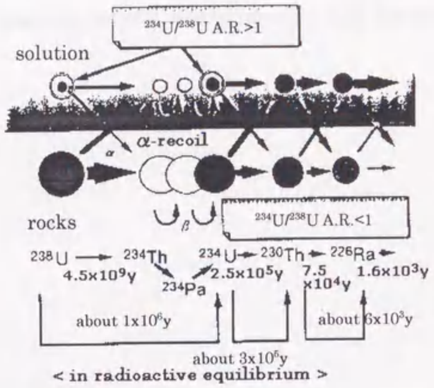

Fig.1-2 Outline of alpha recoil and radioactive disequilibrium in geological media such as water and rocks.

1.3 Natural analog

High level radioactive wastes (HLW) are produced from nuclear reactors and contain several trans-uranium elements whose half-life are as long as several million years (Fig.1-3). These wastes must be disposed far from human life and it is planned to dispose them in deep underground (Brookins, 1984).

The prediction how the nuclides in the wastes behave in future of several million years is difficult because the time is extraordinarily longer than man can expect. By the way, nature has experienced various events for a long time. Therefore, we can learn the prediction from the nature. It is called as "natural analog study".

The natural analog nuclides are listed in Table 1-2. Uranium, thorium and rare earth elements are considered to be good analogs. Especially, uranium is a more important analog because it has two oxidation states and serves as substitutes of many other elements.

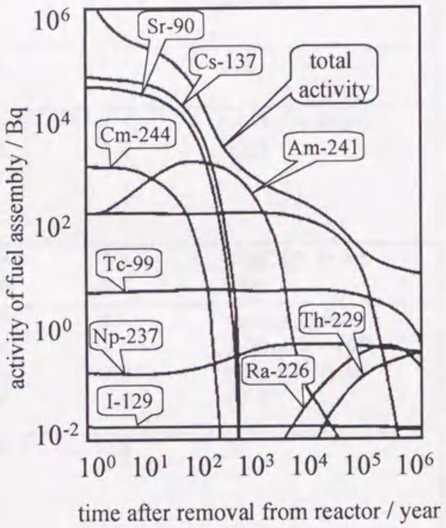

Fig.1-3 Estimated change of radio-activities of the high level radioactive wastes with time.

A variety of geochemical studies can support natural analog studies and further studies are necessary in the future.

Table 1-2 Possible chemical analogs for the long–lived nuclides present in HLW. Modified after Chapman and Smellie (1986).

Element half-life (y)	Oxidation state	Ionic radius (VI coordination·A)	Hydrolysis coeff. (log K 1)	Possible chemical analog
^{99}Tc 2.14×10^5	red. IV ox. VII	0.64		Re(IV)? Re(VIII)?
^{231}Pa 3.28×10^4	red. V ox. V	0.78	9.5	(Th, U(IV))
^{233}U 1.59×10^5 ^{234}U 2.45×10^5 ^{235}U 7.04×10^8 ^{238}U 4.47×10^9	red. IV ox. VI	0.76 0.73	13.4 8.2	U(IV), (Th, Zr, Hf) U(VI)
^{237}Np 2.14×10^6	red. IV ox. V	0.87 0.75	12.5 5.1	U(IV), (Th, Zr, Hf) U(VI)
^{238}Pu 8.77×10 ^{239}Pu 2.41×10^4 ^{240}Pu 6.57×10^3	red. III IV ox. IV V	1.00 0.86 0.86 0.74	6.5 13.5 13.5 4.3	lanthanide (Nd) U(IV), (Th, Zr, Hf) U(IV), (Th, Zr, Hf) U(VI)
^{229}Th 7.34×10^3 ^{230}Th 8.0×10^4 ^{232}Th 1.41×10^{10}	red. IV ox. IV	0.94	10.8	Th
^{241}Am 4.33×10^2 ^{243}Am 7.37×10^3	red. IV ox. III	0.98	6.5	lanthanide
^{244}Cm 1.81×10	red. III ox. III	0.98	(6.5)	lanthanide

Chapter 2 Commonly used analytical methods

2.1 Determination of uranium in geological materials

As uranium concentrations in water and rock samples are low, the pre-treatments such as separation and concentration are in most cases necessary for the determination. Determination of U is sometimes achieved by colorimetry with Arsenazo III (Kanai *et al.*, 1985), fluorimetry with fluoride (Kanai *et al.*, 1986). Recently inductively coupled argon plasma spectrometry (ICP) or ICP mass spectrometry has been used without any separation. However, the separated and purified fraction is necessary for alpha spectrometry (that will be written in detail below), so the chemical analysis with separation and purification procedures is used in this study as follows.

(1) water samples

Uranium in water is coprecipitated with aluminum phosphate, dissolved with H_2SO_4, and poured into an anion exchange column (5cm long) pre-conditioned with 10% H_2SO_4. The column is washed with 6M HCl and uranium is eluted with 0.1-1M HCl. The elution curves of uranium and thorium are shown in Fig.2-1. An aliquot of the uranium solution is taken in a Pt

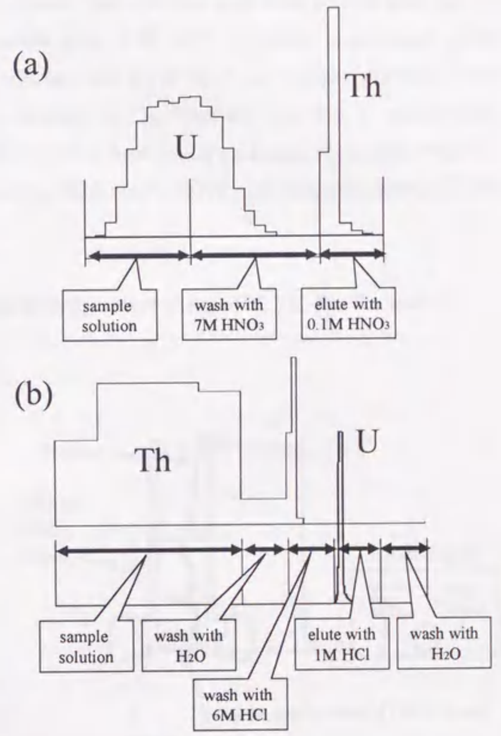

Fig.2-1 Elution curve of uranium and thorium in Amberlite CG 400 (100-200mesh).
(a) NO_3-form anion exchange resin
(b) SO_4-form and Cl-form anion exchange resin

dish and dried. Fused with 2g of flux mixed with Na_2CO_3, K_2CO_3 and NaF, and the uranium is determined fluorimetrically (Kanai *et al.*, 1986) using a fluorimeter (Aloka FMT-4B).

(2) sediments and rocks

The powdered samples are decomposed with alkali hydroxide such as KOH in Ni crucible or alkali peroxide such as Na_2O_2 in Al_2O_3 crucible. The decomposed materials are dissolved with HCl, precipitated twice as ferric and aluminum hydroxides with ammonium hydroxide after the addition of ^{232}U-^{228}Th and ^{229}Th spikes if necessary, and then dissolved with HCl. In case of Fe rich materials, Fe that interferes the analysis, is discarded by extraction with acetyl acetone. The solution is at first poured into the Cl-form anion exchange resin and washed with 6 M HCl. Uranium is retained while thorium is not adsorbed. Then U is eluted with 0.1 M HCl and further purified using SO_4-form anion exchange resins as written in (1). Thorium fraction is evaporated, dissolved with HNO_3, and then purified by NO_3-form anion exchange resins (see Fig.2-1). The U and Th contents are determined by fluorimetry (U) or alpha spectrometry (U, Th) as written below.

2.2 Measurement of radioactivity and activity ratios (ARs) of U, Th, Ra, Rn and Pb

2.2.1 U and Th

The purified U and Th fractions are evaporated gently on a hot plate with 2 ml of nitric acid and 0.25 ml of sulfuric acid until sulfuric acid fumes. Then add 1.5 ml of deionized water and a drop of thymol blue solution, and blow ammonium gas into the solution until red color changes to yellow (pH 2). Transfer the solution into the cell shown in Fig 2-2, and electrodeposit on a stainless steel planchet (Talvitie,

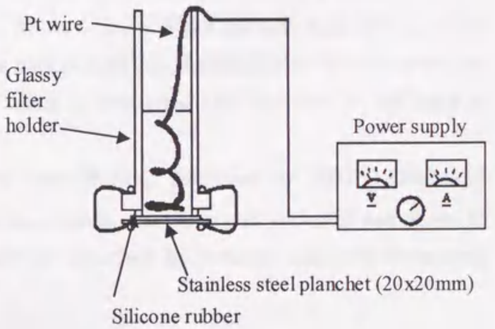

Fig.2-2 Apparatus used for electro-deposition of U and Th in this study.

1972; Kanai, 1986a). The recoveries of uranium in ammonium sulfate media in this system are examined and 2hours at 0.7 A in 1-5 mM ammonium sulfate media gave the best recovery (Kanai, 1986a).

Each activities and activity ratios of U-238, U-234, Th-232, Th-230, and Th-228 were measured by an alpha spectrometer with silicon surface barrier semi-conductor detectors (SSB; effective areas are 450 - 600 mm^2). Typical spectra of U and Th fractions are shown in Fig.2-3.

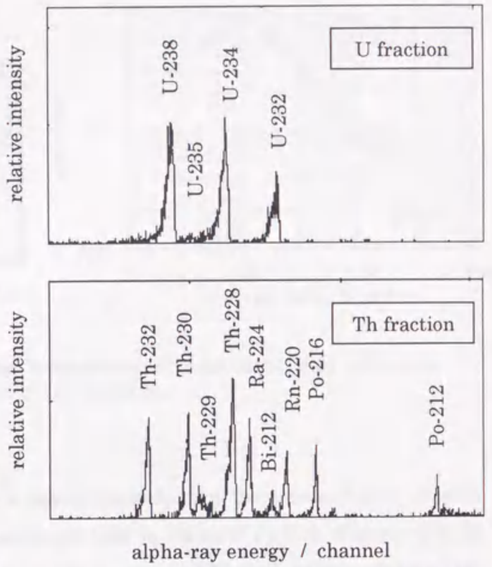

Fig.2-3 Typical alpha spectra of U and Th fractions of geological materials spiked with U-232 (U fraction) and Th-229 (Th fraction).

2.2.2 Ra-226 and Rn-222

Dissolved radon (Rn-222) in water is extracted into toluene solution containing scintillator (0.1g POPOP and 4g POP in 1 liter toluene) by shaking water sample in a glass bottle. The separation time and the water temperature are recorded. Rn-222 decays with half-life of 3.8 days, and its descendants become in equilibrium in about 3 hours. Then the activities of Rn and its descendants are measured using a low background liquid scintillation counter (Packard Tri-Carb 1550). Activity of dissolved radon is calculated and corrected at the time of sampling.

Radium (Ra-226) is coprecipitated with $BaSO_4$, dissolved by EDTA · 4Na, and transferred into a Curie Bottle. After one month, the generated radon in gas phase in equilibrium with radium in solution is absorbed by toluene solution containing scintillator, and measured as well.

2.2.3 Pb-210

Lead-210 is a beta decay nuclide, and its daughter nuclides such as Bi-210 and Po-210

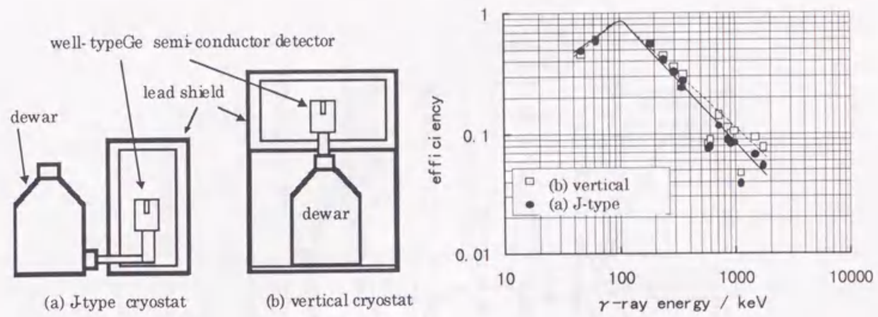

Fig.2-4 Outline of gamma-ray measurement instrument and efficiency curves of various types of Ge detectors.

readily attain radioactive equilibrium in several months. For the determination of lead-210, there are three methods. One is alpha particle counting of Po-210. Another is beta ray counting of Bi-210. The last is gamma ray counting of Pb-210. Alpha spectrometry has merits of low background noise and high sensitivity, but needs chemical pre-treatment as beta spectrometry. Gamma spectrometry is non-destructive, needs no special pre-treatment. So gamma spectrometry is adopted in this study.

As the gamma emission ratio of Pb-210 is only 4 % of decay, the most important problem for measurement is how to increase sensitivity. In this study, the low background well type Ge semi-conductor detector and a thick lead shield box are used (Fig.2-4). The background counts and the efficiency of used detector are checked. Shielding by thicker lead and usage of J-type cryostat were useful as is seen in Fig.2-5. As the efficiency changes with the amount of sample owing to self-absorption and arrangement, the relationships between the efficiency and sample height is studied and the measured activity is corrected by sample height (Kanai, 1993a).

2.3 Selective chemical leaching method

Bulk chemical composition is the first step to be determined. In such a case, not only the amount of each element but also its chemical state is necessary to be specified in detailed study. Selective chemical leaching technique is one of the speciation analytical methods, and developed by Tessier *et al.* (1979). It is applied to the study of soils, clay minerals and sediments. A variety of methods depending on the subjects and objectives

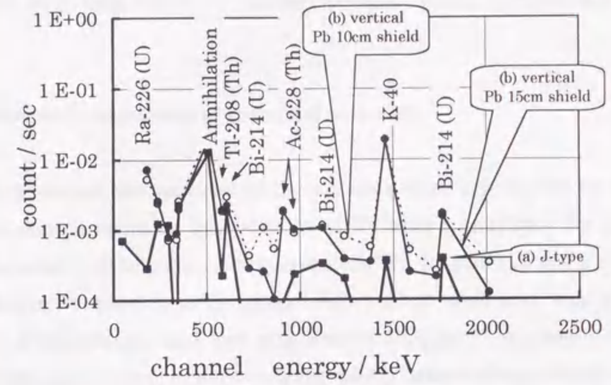

Fig.2-5 Background peak counts of various types of Ge detectors (see Fig.2-3).

are proposed (Kanai, 1993b; 1995). I have applied this technique to the sediments and elucidated the sedimentary environments by using some trace elements (for example, Kanai, 1986b ; 1992a ; 1994; Kanai *et al.*, 1990a). The method is varied according to the kind of samples.

Preliminary test of selectivity showed that sodium acetate solution did not dissolve heavy metals and alkali earth metals except for some hydroxides or sulfates, and acetate with acetic acid solution (pH 5.0) dissolved carbonate efficiently (Kanai *et al.*, 1996). Therefore, the typical scheme used in this study is modified as follows.

Approximately 1.5g of powdered sample is progressively leached with 100ml of : (1) 1M sodium acetate at room temperature (RT) for a week, (2) 1M sodium acetate with acetic acid (pH 5.0) at RT for a week, (3) 0.04M hydroxylamine hydrochloride with 25% acetic acid at about 90 ° C in water bath for 6 hrs., (4) 30% hydrogen peroxide (pH 1) at about 85 ° C in water bath for 5 hrs. The leachate after each treatment is evaporated to dryness with nitric acid, dissolved with hydrochloric acid, and then its composition is determined by ICP and atomic absorption spectrometry (AAS). The fractions will be referred to as (a) sodium acetate soluble fraction, which consists of exchangeable ions, (b) sodium acetate/ acetic acid soluble fraction, whose main constituent is presumed to be carbonate, (c) hydroxylamine hydrochloride soluble fraction, which are the Fe-Mn oxide complexes, and (d) hydrogen peroxide soluble fraction, which is considered to consist of organic matter and sulfide. The residual material after the treatment with (4)

is analyzed as well, and named (e) residue fraction, which is composed of silicate materials.

2.4 General chemical composition of geological materials

Most of the chemical compositions of the samples were determined by inductively coupled argon plasma emission spectrometry (ICP) after Imai(1986). Na and K were determined by atomic absorption spectrometry (AAS). In general, 0.1 g of powdered sample is taken in Pt vessel or teflon beaker. Add 1 ml of nitric acid, 3 ml of perchloric acid and 5 ml of hydrofluoric acid, and evaporate to dryness. Then dissolve the residue with 2.5 ml of 6N hydrochloric acid by warming gently. After cooling, transfer it to 50 ml volumetric flask and make up with distilled water. Major and minor elements such as Al_2O_3, TiO_2, total Fe_2O_3, MnO, MgO, CaO, P_2O_5, Zn, Co, Ni, Cr, V, Cu, Sr and Ba are determined using SEIKO SPS 1200 ICP spectrometer. An aliquot is taken and added with Sr solution to avoid interference. Then Na_2O, K_2O are determined using JAPAN JARREL ASH AA-8500 spectrometer.

Chapter 3 Application of radioisotopes to sedimentology

3.1 Uranium series nuclides in the Masutomi spring, Yamanashi Prefecture

3.1.1 Introduction

The Masutomi spring is located in the northern part of Yamanashi Prefecture (Fig.3-1-1), and famous for the high radon content of the spring waters. 12,000 Mache of radon content was observed in this district, and this value is the highest in Japan, and the second in the world (Mihune, 1981).

The basement of this district is called Masutomi Formation composed of sandstone and slate of Cretaceous Period (Fujimoto *et al.*, 1958). A biotite-rich granite intruded into this formation in the same Period (Fujimoto *et al.*, 1958) or Tertiary Period (Kato, 1968). Later several large faults were formed, along which the springs studied in this section are located.

Many geochemical studies have been achieved in this district (for example, Nakai, 1940; Kuroda, 1944; Nakanishi, 1948; Yokoyama, 1955; Sugihara, 1967; Iwasaki, 1968). Most of them are on radon or radium, but few studies have been done for their precursors, *i.e.* uranium isotopes; only three data on uranium concentrations of the Masutomi spring waters and deposits were reported by Nakanishi(1948). Therefore, the concentrations of uranium, as well as radium and radon in the waters from the Masutomi spring district, and the

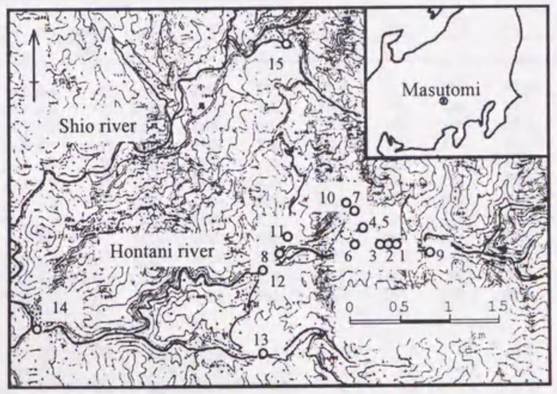

Fig.3-1-1 Sampling locations of spring waters (1-8) and river waters (9-15) in the Masutomi district.

relationships among them are studied in this section.

3.1.2 Samples

Twelve spring waters were collected from eight locations (No.1-8 in Fig.3-1-1), and seven river waters were sampled from the Hontani River and surrounding rivers (No.9-15 in Fig.3-1-1). Four samples from Togetsuan and two samples from Niusawa were collected along short length streams (2.4, 6.0 m each). Rn was extracted in the field and brought back to laboratory. Each sample water was packed in two bottles; one was for general water quality analysis and the other was acidified with HCl(1+1) for uranium and radium analysis. They were brought back to laboratory and analyzed.

3.1.3 Results and discussions

General water qualities

General water qualities (Table 3-1-1) show that main components of the Masutomi spring waters are sodium and chloride ions, being plotted in the area of non-carbonate

Table 3-1-1 Chemical compositions of spring waters and river waters in the Masutomi district, Yamanashi Prefecture, central Japan.

No.	Location	Name	F	Tw	pH	Redox	HCO_3	Cl	SO_4	Na	K	Ca	Mg	Cond.
			l/m	°C		mV				mg/l				μS/cm
	(spring waters)													
1-1	Togetsuan(outlet)	88030104	4.8	26.2	6.4	-44	1440.	4010.	820.	2730.	243.	299.	22.8	13900.
1-2	Togetsuan(1.8m from outlet)	88030205		25.2	7.0	-57	1400.	4010.	848.	2730.	259.	309.	23.1	13700.
1-3	Togetsuan(2.4m from outlet)	88030103		24.0	7.1	-71	1380.	3990.	816.	2710.	283.	289.	22.6	13200.
1-4	Togetsuan(pool)	88030206		21.8	6.5	-37	1390.	3940.	798.	2710.	205.	290.	22.5	13200.
2	Tsuganero	88030207		26.5	6.6	-38	1420.	4250.	671.	2860.	210.	279.	21.6	13600.
3	Dairokuten no izumi	88030208	3.2	19.3	6.3	19	1020.	3140.	486.	2030.	134.	220.	20.8	9970.
4	Furokaku Iwaburo	88030311		16.5	6.4	57	1330.	4010.	588.	2630.	296.	279.	22.5	11900.
5	Furokaku Iwaburo(side)	88030310		12.0	6.5	9	842.	2350.	377.	1620.	119.	150.	13.7	6800.
6	Furokaku Boring	88030312			6.5		1660.	3940.	590.	2650.	206.	261.	22.5	
7-1	Niusawa(outlet)	88030317		21.0	6.6		1270.	3320.	516.	2220.	159.	259.	20.5	
7-2	Niusawa(6.0m from outlet)	88030315			8.1	-110	976.	3430.	518.	2160.	185.	99.6	20.9	8760.
8	Kouseiryo Outlet	88030313	33.	36.2	7.7	-58	2060.	4490.	592.	2960.	262.	164.	39.4	19300.
	(river waters)													
9	Hontani(Hiuke-bashi)	88030102	3600.	2.1	7.1	172	12.2	8.3	1.6	8.9	1.7	4.0	0.6	48.3
10	Niusawa upstream	88030316		2.6	7.2		27.4	1.6	1.0	4.7	0.9	6.7	1.6	
11	Kouseiryo upstream	88030314	2.0		7.2	103	33.3	1.1	0.7	4.5	1.3	5.3	1.4	41.1
12	Hontani(Hikage-ohashi)	88030309		2.4	7.1	38	35.4	67.4	21.8	51.9	7.4	8.5	1.1	208.
13	Hyuga	88030419	30.	0.6	7.1	213	14.6	3.0	0.3	4.4	0.8	2.5	0.5	24.3
14	Hontani downstream	88030420	100.	1.0	7.3	90	45.8	73.0	22.2	55.0	7.5	10.1	1.3	220.
15	Shiokawa branch	88030421	0.5	0.3	7.2	86	28.7	0.8	0.5	3.5	0.8	6.0	1.4	40.5

The symbols of F, Tw, Cond, and Redox indicate flow rate, water temperature, conductivity, and redox potential respectively

alkali type in the key diagram. On the other hand, most of the river waters are plotted in the area of carbonate hardness type. The pHs of spring waters range from 6.3 to 8.1 and those of river waters range from 7.1 to 7.3. The large variation of pHs of spring waters compared with those of river waters may be due to bicarbonate ion which is easily lost by airing.

The relationships between the concentrations of sodium ion and chloride ion of the spring waters show a good linear relation (the correlation coefficient is 0.999). The atomic ratio of these two ions of the samples is almost identical to unity. The linear relationship suggests that the spring waters have the same origin with a high NaCl concentration and that the original water was diluted to various extent by extremely dilute groundwaters or surface waters.

Behavior of radium

The concentrations of Ra-226 in the spring waters range from 0.222 to 1.48 Bq/l (6.06 - 40.4 pg/l) and that in the river waters from 0.051 to 0.146 Bq/l (Table 3-1-2). The ultimate source of radium is assumed to be the intruded granite rocks because there are no other rocks in this district that may supply radium as well as other radioactive

Table 3-1-2 Uranium contents, activities of radium and radon, and activity ratios among them in spring waters and river waters from the Masutomi district, Yamanashi Prefecture, central Japan.

No.	Location	Name	U-228	Ra-226	Rn-222	Activity Ratio			
			μg/l	Bq/l	Bq/l	U-234/U-238	Ra-226/U-238	Rn-222/U-238	Rn-222/Ra-226
	(spring waters)								
1-1	Togetsuan(outlet)	88030104	0.16	1.21(3)	5.88(3)	1.09(9)	610.(11)	2900.(20)	4.86(11)
1-2	Togetsuan(1.8m from outlet)	88030205	0.05	1.21(3)	4.10(3)	1.50(18)	1900.(33)	6500.(40)	3.39(8)
1-3	Togetsuan(2.4m from outlet)	88030103	0.19	1.07(3)	2.04(2)	0.98(2)	450.(9)	860.(8)	1.91(6)
1-4	Togetsuan(pool)	88030206	0.07	1.40(3)	14.1(1)	1.51(18)	1600.(25)	16000.(50)	10.1(2)
2	Tsuganero	88030207	0.05	1.42(3)	2.34(2)	2.42(80)	2300.(35)	3700.(30)	1.65(4)
3	Dairokuten no izumi	88030208	0.34	0.681(23)	591.(1)	1.10(7)	160.(5)	140000.(70)	849.(25)
4	Furokaku Iwaburo	88030311	2.07	0.997(25)	10.6(1)	1.00(2)	39.(1)	400.(1)	10.6(2)
5	Furokaku Iwaburo(side)	88030310	0.13	0.566(22)	129.(1)	1.90(16)	350.(12)	77000.(80)	228.(8)
6	Furokaku Boring	88030312	0.07	1.48(3)		2.17(26)	1700.(25)		
7-1	Niusawa(outlet)	88030317	0.11	0.228(19)		1.38(14)	170.(14)		
7-2	Niusawa(6.0m from outlet)	88030315	0.02	0.222(20)			890.(76)		
8	Kouseiryo Outlet	88030313	0.01	0.654(23)	0.131(6)		5300.(160)	100.(46)	0.20(2)
	(river waters)								
9	Hontani(Hiuke-bashi)	88030102	0.33	0.087(19)	0.090(7)	1.10(7)	21.(4)	22.(2)	1.04(31)
10	Niusawa upstream	88030316	0.01	0.090(18)			720.(140)		
11	Kouseiryo upstream	88030314	0.01	0.146(20)			1200.(160)		
12	Hontani(Hikage-ohashi)	88030309	0.08	0.092(19)	0.952(13)	1.09(15)	93.(19)	930.(13)	10.3(22)
13	Hyuga	88030419	0.02	0.071(18)			290.(73)		
14	Hontani downstream	88030420	0.01	0.104(19)			840.(150)		
15	Shiokawa branch	88030421	0.00	0.051(8)					

nuclides.

Ra-226 is a descendant of U-238. The Ra-226/U-238 activity ratios in the samples are more than 21, which indicates that Ra-226 is enriched more than that expected from its parent U-238. If radioactive equilibrium in the source rock is assumed, this disequilibrium in the waters would be caused by the difference in solubility of two nuclides. The chloride ion concentration is an indicator of mixing processes because the concentrations of sodium ion and chloride ion of the spring waters show a good linear relation. Figure 3-1-2 shows the relation between Ra and chloride ion concentrations. A positive correlation is observed between them (correlation coefficient is 0.828 in overall, 0.966 if the deviated data on samples from Niusawa and Kouseiryo (No.7-1, 7-2 and 8) are excluded). The deviated three samples are from near iron oxide precipitates or carbonate precipitates. A part of radium may have been removed from the spring waters by coprecipitation with iron oxides. The linear relation indicates that the primary Ra-226 rich solution was diluted by mixing with surface waters or dilute groundwaters.

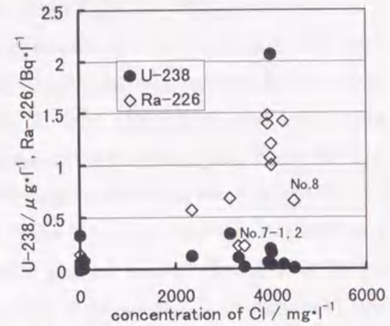

Fig.3-1-2 Correlation between Cl concentration and U-238 content and Ra-226 activity in waters from Masutomi district.

Behavior of radon

Rn-222 is the daughter of Ra-226. The Rn-222 activities are much higher than those expected from Ra-226 activities (Table 3-1-2). The largest Rn-222 /Ra-226 activity ratio (849) was observed at No.3 spring. It is difficult to explain the origin of Rn-222 only from the dissolved Ra-226. A large emanation from the source rock may be estimated.

According to the experiment by Barretto *et al.* (1975), average emanation rate of Rn from granite rocks is only about 7.5 %. Taking this emanation rate and assuming that U-238, Ra-226 and Rn-222 in the source granite rocks are in equilibrium, the ratio of Ra-226 in water to Ra-226 in rock is estimated to be about 0.01 % (because $(^{222}Rn_W+0.075x^{222}Rn_R)/^{226}Ra_W=849$, $^{222}Rn_W=^{226}Ra_W$, $^{222}Rn_R=^{226}Ra_R$; where the subscripts W and R indicate activities in water and rock, respectively). However, the source of Ra-226, *i.e.* U-238, is not so highly concentrated in granitic rocks in this district. The high activity of Rn-222 may be attributed to a high rock/water ratio in the system, that is,

Rn-222 is extracted by water which runs through micro fractures of the granite rocks.

Kuroda(1944) observed a daily variation of Rn-222 concentration in some springs and proposed "sinter theory" that Rn-222 was supplied from ocherous deposits located near surface through which spring waters ascended. In fact, there are some iron oxide precipitates with high Ra-226 contents around the springs (Kanai, 1989). These Ra-226 rich precipitates are thought to supply Rn-222 into spring waters to some extent.

For explaining the high Rn-222 concentration in the Masutomi springs, Horiuchi and Murakami (1978) proposed a mixing with "Rn rich ground water". However, so far as the correlation of Rn-222 and chloride concentrations is considered, the behavior of Rn-222 can not be explained by a simple mixing model. The origin of high content Rn-222 is ascribed to both the source granite rocks and the Ra-226 rich precipitates.

Behavior of uranium

U-238 concentrations in the spring waters range from 0.01 to 2.07 ppb (average 0.27 ppb arithmetically) (Table 3-1-2). Nakanishi(1948) reported the U concentration at A8 spring as 0.3 ppb. Average U-238 concentration in the river waters is 0.06 ppb ranging from 0 to 0.51 ppb, a little lower than that in the spring waters.

Uranium concentration in spring water varies according to water chemistry, pH, surrounding rocks, geology, etc.. Most of the springs in Japan are poor in U-238. The reported U concentration in springs in Japan ranges from 0.02 to 1.5 ppb (Torii *et al.*, 1958), from 0 to 2.8 ppb (Noguchi and Imahashi, 1967), from 0.02 to 0.15 ppb (Itakura, 1968), and from 0 to 0.16 ppb (Koga, 1959). The data in this study fall in these range. The U-238 activity is much lower than those expected from Ra-226 or Rn-222.

Uranium(VI) exists as uranyl ion in waters and it easily makes a complex with sulphate or carbonate ion. In groundwaters from the Tsukuba Tunnel, a linear relation between U and bicarbonate ion concentrations is observed as shown in Fig.3-1-3 (Kanai

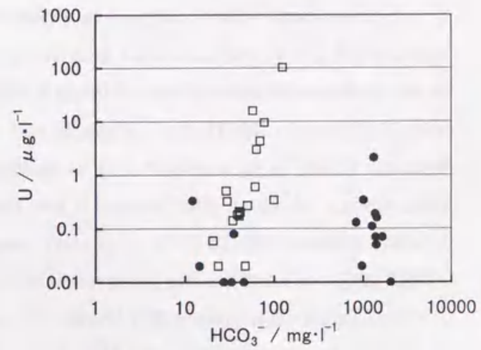

Fig.3-1-3 Correlation between bicarbonate concentration and uranium concentration in waters from Masutomi district (●) and the Tsukuba Tunnel(□).

et al., 1993). Andrews and Kay(1983) also found a linear relation between U and bicarbonate ion concentrations in oxic groundwaters. Although bicarbonate ion is the second largest anion constituent of the Masutomi spring waters, no clear relation with the U concentration was observed (Fig.3-1-3). However, reduction-oxidation potential seems to have a correlation with the U-238 concentration (Fig.3-1-4). The U-238 concentration increases as the redox potential becomes high. U has two oxidation states; tetravalent U(IV) and hexavalent U(VI). The distribution of U between the two oxidation states may be controlled by pH, redox potential, temperature, pressure and other coexisting ions. In a neutral solution with low redox potential like the samples in this study, U(IV) is stable. Since U(IV) is difficult to dissolve, the low U concentration in the Masutomi spring waters is ascribed to their reducing environment.

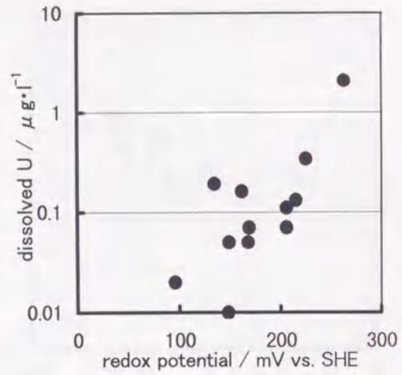

Fig.3-1-4 Correlation between redox potential and U concentration in spring waters from the Masutomi district, Yamanashi Prefecture, central Japan.

In this study no relation is observed between U-238 content and chloride ion as is shown in Fig.3-1-2. Therefore, it is difficult to apply a simple mixing model that Mitsuda *et al.* (1983) suggested for the groundwater samples from Musashino-daichi.

Most of U-234/U-238 activity ratios are above 1 as shown in Table 3-1-2. They range from 0.98 to 2.42. The extent of U-234/U-238 disequilibrium found in this study is not so large as those observed in other springs. For example, Szabo(1982) reported a highly fractionated U-234/U-238 activity ratio as large as 15.6. Sandoval *et al.* (1987) reported 9.94 in a spring in Venezuela, and Sakanoue and Hayashi (1982) found the activity ratio of 8.41 at the Tatsunokuchi spring, Japan. Generally, U-234/U-238 activity ratio of water samples is above 1 and explained by the alpha recoil effect (Fleischer, 1980; 1982).

Figure 3-1-5 shows a reverse correlation of U-234/U-238 activity ratio with U-238; U-234/U-238 activity ratio decreases with increase in U-238 concentration. As shown in Table 1-1, U-234 is produced by decay of U-238 via Th-234 ($T_{1/2}$ = 24.10 days) and Pa-234 ($T_{1/2}$ = 6.75 hours). During the decay, Th-234 atoms suffer alpha recoil and some are ejected into solution (Kigoshi, 1971). Schematic diagram is shown in Fig.3-1-6. Because Th has only one valence (Th(IV)), the amount of Th-234 dissolved into the solution may

not be much influenced by the redox conditions. Therefore U-234 produced from ejected Th-234 would be constant (Th-234 may precipitate or adsorb in suspended matters in a short time). In a solution of relatively oxidative condition, U-234 formed in this process is less important because the proportion of U-234 dissolved by ordinary chemical process becomes larger. However it is much important when the solution becomes reductive, in which environment both U-238 and U-234 are difficult to dissolve. The U-234/U-238 activity ratio in such condition becomes larger than that in high U concentration. The reverse correlation observed in this study indicates that the ejection of Th-234 by alpha recoil effect plays an important role. In this way, the process of dissolution of U is the most important for U disequilibrium in water.

In summary, U-238 and its descendants, U-234, Ra-226 and Rn-222, in the Masutomi spring district behave differently. The same behavior are observed in the waters at the Tono mine area (see Table 3-4-4). The cause of the difference is attributed to the chemical characteristics of those nuclides and the radiochemical recoil effects.

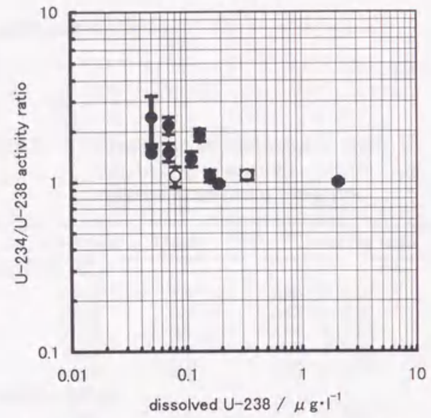

Fig.3-1-5 Correlation between U-238 concentration and U-234/U-238 activity ratio in spring waters (●) and river waters (○) from the Masutomi district, Yamanashi Prefecture, central Japan.

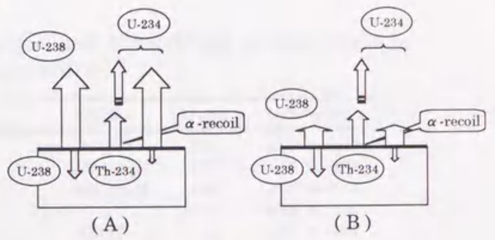

	U-238 concentration	U-234 / U-238 activity ratio
(A) oxidative	high	small
	∨	∧
(B) reductive	low	large

Fig.3-1-6 Schematic diagram of dissolution mechanism of U-238 and U-234 under oxidative and reducing conditions.

3.2 Radionuclides in bauxite deposits in Yangwa mine, China

3.2.1 Introduction

Aluminum nitrate is often used for salting-out reagent in the extraction procedure of U analysis. However aluminum nitrate sometimes contains considerable amount of U with various U-234/U-238 activity ratios (Kanai, 1992b). Table 3-2-1 is a list of uranium contents and U-234/U-238 activity ratios in commercial reagents and aluminum foils.

Table 3-2-1 Uranium concentration and U-234/U-238 activity ratio in various aluminum reagents.

Company	Al reagent	U / ppb	^{234}U / ^{238}U activity ratio
A	$Al(NO_3)_3 \cdot 9H_2O$		
	No.1	9.4	1.26 ± 0.02
	No.2	2.2	1.48 ± 0.06
	No.3	2.7	1.48 ± 0.11
	No.4	2.7	2.29 ± 0.19
	No.5	12.1	4.29 ± 0.18
B	$Al(NO_3)_3 \cdot 9H_2O$		
	No.1	9.6	1.22 ± 0.07
	No.2	9.2	1.24 ± 0.06
C	$Al(NO_3)_3 \cdot 9H_2O$		
	No.1	0.9	1.50 ± 0.22
	No.2	3.1	1.41 ± 0.15
	Al plate	680.	1.04 ± 0.03
D	Al rod	40.0	1.07 ± 0.06
E	Alumina	330.	1.06 ± 0.03
F	Al kitchen foil	310.	0.94 ± 0.03

Table 3-2-2 Uranium concentration and U-234/U-238 activity ratio in bauxite from various countries.

No.	country	location	Ref.No.	U / ppm	Activity Ratio
1	Australia	Pinjarra Mine	M14617	2.89	1.00 ± 0.03
2	Australia	Pinjarra Mine	A31-17075	2.07	1.04 ± 0.03
3	Australia	Pinjarra Mine	A31-14614	4.96	0.99 ± 0.03
4	Australia	west Jarrahdale		12.3	0.95 ± 0.02
5	Australia		M8647	7.28	0.97 ± 0.04
6	China	Shan Dong	M3852	5.67	0.95 ± 0.01
7	China	Fu Zhou	M5215	11.5	0.98 ± 0.02
8	France	Tombarel Mine	M11469	10.9	0.99 ± 0.03
9	France	Tombarel Mine	M11462	5.13	0.99 ± 0.03
10	France	Bedavieux, Herault	A31-11664	20.2	1.01 ± 0.01
11	Ghana			2.37	1.02 ± 0.03
12	India		A31-860	6.34	1.04 ± 0.06
13	Indonesia	Bintan	M5214	8.46	0.89 ± 0.01
14	Italy	Capo La, Carmona Lato , Nord	M11463	3.42	1.13 ± 0.02
15	Italy	Capo La, Carmona Lato , Sud.	M114641	3.80	1.00 ± 0.02
16	Italy	Millevallelonga	M11461	4.57	0.96 ± 0.03
17	Japan	Kagawa Pref.	M2741	6.33	1.20 ± 0.02
18	Japan	Tottori Pref.	10341	1.69	0.97 ± 0.04
19	Malaysia	Seaba		5.07	0.90 ± 0.02
20	Malaysia	Ramunia		5.37	0.96 ± 0.02
21	U.S.A.	Najine, Georgia	M11465	2.91	0.94 ± 0.03
22	U.S.A.	near Chattanooga	A31-11466	7.42	0.98 ± 0.01
23	U.S.A.	Hawaiian Island	M11470	0.86	0.99 ± 0.05

Furthermore, it has recently become apparent that aluminum metal used in a semi-conductor device is contaminated by trace amount of uranium and that alpha particles emitted from contaminated uranium produce "memory error" in the semi-conductor devices. As aluminum is manufactured from bauxite ores, such uranium may be originated from the bauxite deposit. In this way, a bauxite deposit was investigated. The U contents and U-234/U-238 activity ratios in various bauxite ores in the world were determined and the results are listed in Table 3-2-2.

Bauxite deposits are formed typically by chemical weathering of igneous, sedimentary and metamorphic rocks under humid tropical conditions. Some elements are dissolved and removed from the parent rocks and some are retained. The studies on the weathering process, bauxitization and elemental mobility have been conducted in many locations such as Malaysia (Wolfenden, 1965), Jamaica (Comer, 1974), Brazil (Kronberg *et al.*, 1979, 1982), Suriname (Topp *et al.*, 1984/1985), Taiwan (Chen *et al.*, 1988), America (Gordon and Murata, 1952; Hotz, 1964), Australia (White, 1976), and Italy (Bardossy *et al.*, 1977). Few studies on uranium in bauxite deposits, however, have been conducted.

3.2.2 Details of samples and analytical methods

The analyzed samples in this study were collected from the Yangwa mine at Jiaozuo area in Henan Province, China. This bauxite deposit is thought to be of the sedimentary type, which is distributed on a continental platform of the Sino-Korea massif. The sediments deposited on an Ordovician limestone basement. The main ore bodies deposited during the middle Carboniferous period. The geological map with sampling locations is shown in Fig.3-2-1.

Eleven samples were collected: two from the Majiagou Formation (1a-b, limestone), five from the lower Benxi Formation (2a-e), three from the high-alumina Benxi Formation (3a-c), and one from the upper Benxi Formation (4a). The samples were air-dried, pulverized with an automatic agate mortar.

Most of the chemical components of these samples were determined by AAS (for Na, K) and ICP (for Si, Ti, Al, Fe, Mn, Mg, Ca, P, Zn, Ni, Cr, V, Cu, Sr and Ba). Uranium and thorium were separated and purified with Cl, SO_4, NO_3-form anion exchange resins after addition of the proper spikes, then the activities and activity ratios were measured by an alpha spectrometer. Uranium contents in the leachates (described later) were also determined by the fluorimetry.

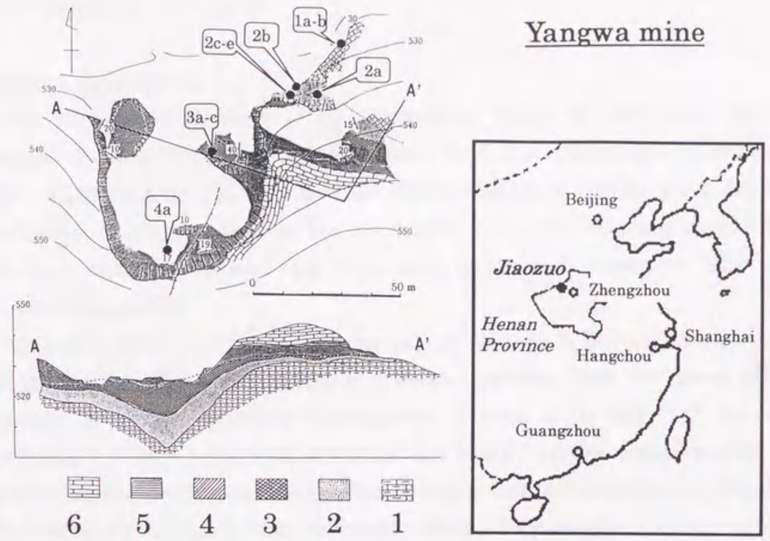

Fig.3-2-1 Geological map and sampling locations of bauxite from the Yangwa mine at Jiaozuo area in Henan Province, China.
1: Majiaoguo Formation (limestone)
2: lower Benxi Formation
3: high-alumina Benxi Formation
4: upper Benxi Formation
5: Benxi Formation (shale)
6: Taiyuan Formation (limestone)

The samples were successively leached to provide simply three fractions termed "(1) HCl soluble", "(2) HF soluble" and "(3) resistate" as follows.

(1) HCl soluble

0.5 g of sample was boiled with 10 ml of 12 M HCl to dryness. The residue was taken up in 5 ml of 6 M HCl and filtered. The filtrate providing the "HCl soluble fraction".

(2) HF soluble

5 ml of HNO_3, 5ml of $HClO_4$ and 10 ml of HF were added to the residue of (1) and the solution boiled to dryness. The residue was taken up in 5 ml of 6 M HCl and filtered. The filtrate providing the "HF soluble fraction".

(3) Resistate

The residue of (2) was totally dissolved by fusion with KOH followed by solution in 6 M HCl, the solution providing the "resistate fraction".

3.2.3 Results and discussion

Chemical compositions

The chemical compositions of the samples are shown in Table 3-2-3. The major mineral compositions are also shown in Table 3-2-4. The content of U range from 3-29 ppm, which are larger than the average crustal abundance (Taylor, 1964). Adams and Richardson (1960) also observed the enrichment of U in the Arkansas bauxite, though Kronberg *et al.* (1982) stated that 30 elements including U maintained their average crustal concentration.

Al_2O_3 contents in the main ore body range from 50 to 80 %, being the highest at 3a-b. On the contrary, Fe_2O_3 is abundant in samples 2a-b taken from the bottom of the ore deposits. A negative correlation is observed between Al_2O_3 and Fe_2O_3 (correlation coefficient = -0.83, significant at 98% confidence level). A vertical sequence of the in situ bauxite deposits originated from the Fe-rich parent rock is characteristic of Fe cap over the bauxite ore (Maynard, 1983). In the surveyed ore deposits, there is some enrichment of Fe at the bottom of bauxite deposit. Sedimentary beds were also observed. It is, therefore, suggested that the ore deposit is sedimentary origin, of type "allochthonous" (Valeton, 1972).

Correlation coefficients among the determined elements of the bauxite samples show that the elements are classified into three groups. The first group is composed of Al, Ti, Cr, U and V, which have strong positive correlation with Al. The second is composed of Fe, Mn, Ca and Cu. The element of the first group is also in a negative correlation with

Table 3-2-3 Chemical composition of samples from Yangwa mine, China.

No.	SiO_2	TiO_2	Al_2O_3	Fe_2O_3	MnO	MgO	CaO	Na_2O	K_2O	P_2O_5	Zn	Cr	V	Cu	Sr	Ba	U
	/%										/μg·l^{-1}						
1a	19.8	0.54	11.8	2.43	0.03	1.86	34.7	0.10	2.42	0.13	21	45	70	68	109	134	5.87
1b	11.8	0.15	3.23	2.54	0.07	9.85	33.9	0.04	0.84	0.04	7	10	17	13	80	50	3.19
2a	6.87	0.14	4.49	76.2	0.10	0.32	0.79	0.02	0.02	0.24	158	15	42	753	84	42	7.22
2b	20.6	0.81	20.5	46.5	0.08	2.32	0.22	0.02	0.01	0.04	217	83	58	<1	32	97	7.26
2c	35.3	2.34	52.0	4.09	0.01	0.35	0.27	0.10	0.61	0.28	141	160	253	39	269	64	16.3
2d	43.0	1.57	42.4	0.67	<0.01	0.43	0.23	0.31	6.24	0.20	50	151	490	10	373	211	14.0
2e	32.0	1.58	50.4	5.27	<0.01	0.50	0.16	0.25	4.44	0.24	182	156	276	20	280	95	24.1
3a	8.42	4.02	82.7	0.95	<0.01	0.18	0.05	0.12	0.97	0.03	67	501	606	<1	39	25	28.5
3b	4.33	3.09	82.3	7.06	<0.01	0.18	0.05	0.10	0.47	0.11	80	215	378	<1	97	18	28.8
3c	28.2	2.27	56.7	2.04	<0.01	0.45	0.27	0.06	0.31	0.05	94	285	348	6	53	27	19.3
4a	31.4	2.41	60.8	0.55	<0.01	0.37	0.14	0.06	0.10	0.24	106	230	274	10	243	21	27.3

Table 3-2-4 Mineral composition of samples from the Yangwa mine, China. Relative intensities by X-ray diffraction analysis are shown.

No.	Formation	Cal.	Dol.	Dia.	Pyr.	Chl.	Kao.	Mus.	Hem.	Qz.
1a	Majiagou	+++++	trace					+		+
1b		+++	+++++					trace		+
2a	Benxi (lower part)					trace			++	
2b						+			trace	trace
2c				++	+++	+	+	trace		
2d				trace	+	+	+	++++		+++
2e				++	trace	trace	+	+		+
3a	Benxi (high-alumina)			+++++	+		trace	+		+
3b				++++			trace		trace	
3c				++		++	+			
4a	Benxi (upper part)			+++	+++	+	+			

Cal:Calcite Dol:Dolomite Dia:Diaspore
Pyr:Pyrophillite Chl:Chlorite Kao:Kaolinite
Mus:Muscovite Hem:Hematite Qz :Quartz

that of the second group because Al has a strong negative correlation with Fe as mentioned above. On the contrary, Na, K, Sr and Ba form another group, which are alkali and alkaline earth elements, and are depleted in the ore.

Fractional composition by leaching techniques

To make a better understanding of the elemental distribution, selective chemical leaching technique was applied. Figure 3-2-2 shows the typical X-ray diffraction patterns of the raw sample, after HCl treatment, and after HNO_3-$HClO_4$-HF treatment. Table 3-2-4 also indicates the major mineral composition of raw samples. It is observed that hematite and some of clay minerals are decomposed by HCl treatment, and that quartz, clay minerals, pyrophillite are decomposed by HNO_3-$HClO_4$-HF treatment.

Uranium contents in each fraction are shown in Fig.3-2-3.

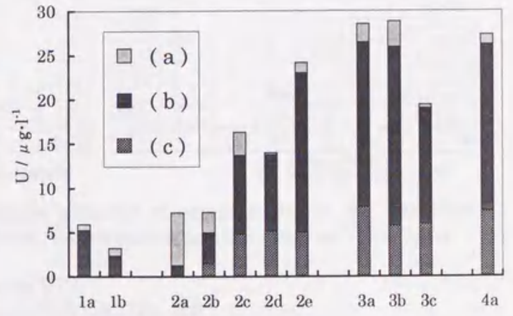

Fig.3-2-3 Total and fractional uranium contents in samples from the Yangwa mine, China.
(a): HCl soluble fraction
(b): HF soluble fraction
(c): resistate fraction

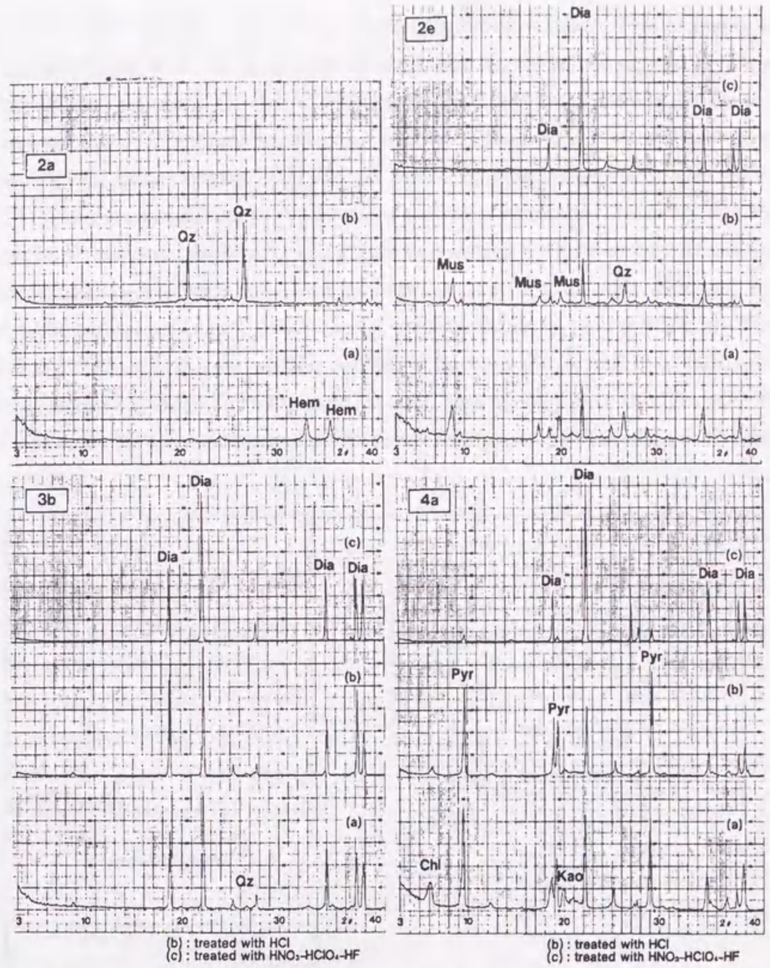

Fig.3-2-2 Typical X-ray diffraction patterns of samples (2a, 2e, 3b, 4a) from Yangwa mine, China. Abbreviations are the same as Table 3-2-4.
(a) raw sample,
(b) after treatment with HCl,
(c) after treatment with HNO_3-$HClO_4$-HF

Most of the U is present in the silicate ("HF soluble fraction"). Bardossy *et al.* (1977) treated the Italian bauxite with HNO_3 and demonstrated that U is mainly contained in resistant minerals of volcanic origin. In this study it is revealed that U is contained both in the silicate and resistate fractions.

Most of Fe, Mn, Mg, Ca, and Sr were in "HCl soluble fraction". This suggests that these elements are from the hydroxide precipitates, a part of the clay minerals and soluble postgenic minerals. On the other hand, Ti, Na and K are contained mainly in the clay and silicate ("HF soluble fraction"), probably in the original source materials of bauxite deposits. Much of the Ti, Al, Zn, Cr and V in samples 3a-b is in the resistate phase, probably corresponding to the diaspore and other refractory minerals. Ti, Cr and V contents of "resistate fraction" have a good correlation with Al content of the same fraction. A good correlation is also observed between those of bulk compositions.

The relationships between U contents and other elements in each fraction are shown in Fig.3-2-4. Although the correlation coefficient between Al_2O_3 and U in HCl soluble fraction is 0.20, that between Fe_2O_3 and U is 0.82, high enough to be significant at 98 % confidence level. This may indicate a preferential precipitation of U with iron hydroxide

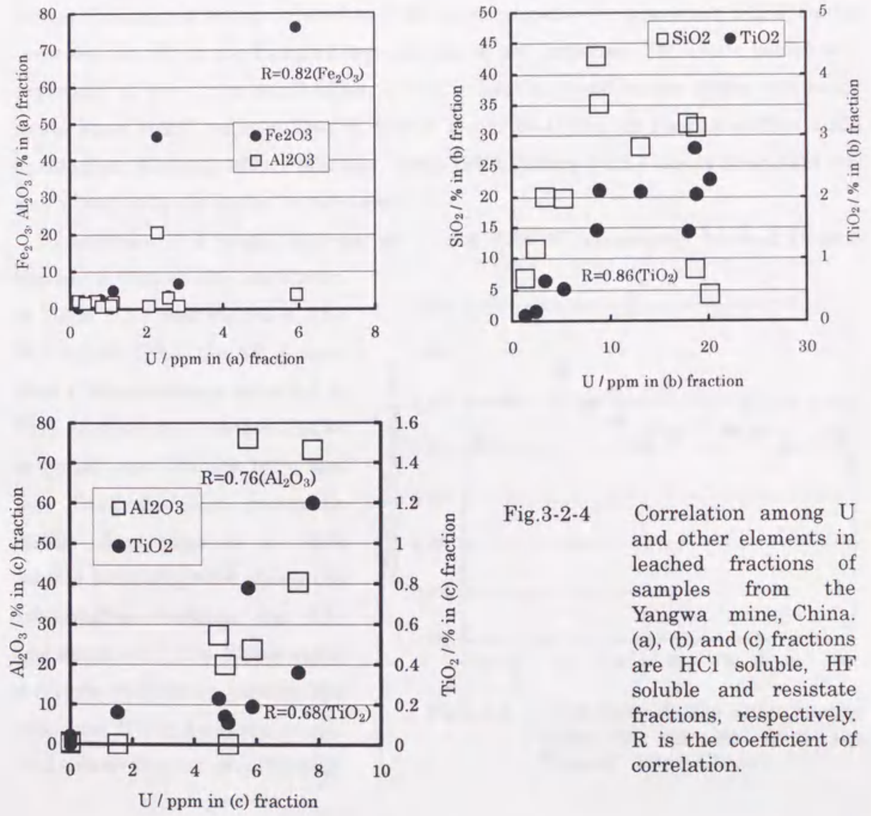

Fig.3-2-4 Correlation among U and other elements in leached fractions of samples from the Yangwa mine, China. (a), (b) and (c) fractions are HCl soluble, HF soluble and resistate fractions, respectively. R is the coefficient of correlation.

rather than with aluminum hydroxide. U contents of "HF soluble fraction" in the ore parts range from 18% to 75%, and have a good correlation with SiO_2 contents except for the sample 3a-b. Some amount of U in the sample 3a-b may derive from the non-silicate minerals such as Ti bearing minerals, because the dissolved U is in good correlation with dissolved TiO_2 (correlation coefficient = 0.86). Most of U in the basement limestone (1a-b) is contained in the silicate fraction. The ratios of U of "resistate fraction" to bulk content range from 0.20 to 0.36. U contents are relatively in a good correlation with insoluble Al_2O_3 contents and relative X-ray diffraction intensities of diaspore. Uranium in this fraction is thought to be contained in a diaspore lattice.

U-234/U-238 activity ratios

The bulk U-234/U-238 activity ratios (ARs) in the bauxite samples are shown in Fig.3-2-5. The upper and main parts of bauxite ore body, 3(a-c) and 4a, have the AR values of about 0.8, being depleted in U-234 with respect to its precursor U-238. On the contrary, the ARs at the Fe rich lower part (2a-e) are increased. The U-234 depletion is explained by the alpha recoil effect. U-234 is loosely bound to the lattice and easily moves than U-238 because Th-234, which decays to U-234 via Pa-234, suffers alpha recoil effect (Kigoshi, 1971; Fleischler, 1980; 1982). Mobile U-234 moved downward and was adsorbed by the lower Fe rich layer.

To understand a detail behavior of U, the ARs of successively leached U were measured. The results are shown in Table 3-2-5 and Fig.3-2-6. The HCl soluble U has the AR of more than 1. The maximum value is 3.3. This implies that excess U-234 migrated over the ore body and was fixed by iron hydroxide and/or clay minerals as HCl soluble form. Fig.3-2-6 shows the relationships between the ARs and dissolved U-238. There exists a reverse correlation between the ARs and U-238 contents in the HCl soluble fraction (Fig.3-2-6(a)),

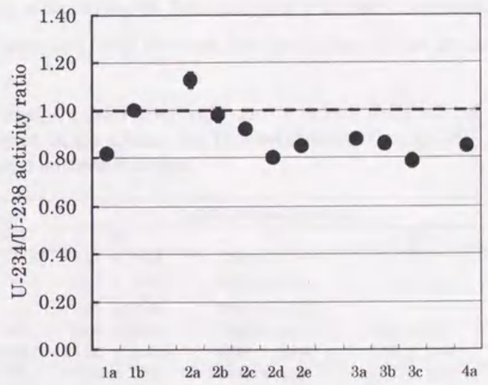

Fig.3-2-5 Bulk U-234/U-238 activity ratios (ARs) in samples from the Yangwa mine, China.

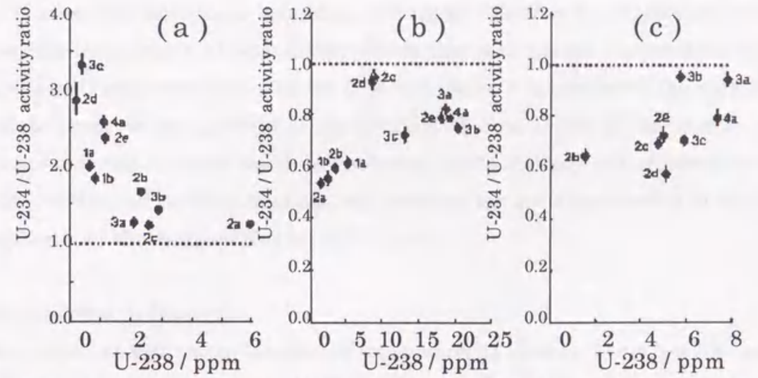

Fig.3-2-6 Correlation between U content and U-234/U-238 activity ratios in leached fractions of samples from the Yangwa mine, China.
(a) HCl soluble fraction
(b) HF soluble fraction
(c) resistate fraction

suggesting that the amount of mobile U-234 is almost constant. On the other hand, the ARs of HF soluble and resistate U are less than unity. This is explained by the effect of leaching out by groundwater. Some U-234 atoms may be dissolved into the interstitial water by contact with water for a long period or recoil ejection of Th-234 from the mineral grain (Kigoshi, 1971). The ARs of HF soluble and resistate fractions have a positive correlation with the U-238 contents of each fraction (Fig.3-2-6(b) and (c))

Lowson *et al.* (1986) studied the ARs of the samples from lateritic weathered uranium ore body in Alligator Rivers region, Australia, and showed the similarity of ARs in the

Table 3-2-5 U-234/U-238 activity ratios (ARs) in bulk and leached fractions of samples from the Yangwa mine, China; (a) HCl soluble fraction, (b) HF soluble fraction, and (c) resistate fraction.

No.	bulk activity ratios	relative U content*			fractional activity ratios		
		(a)	(b)	(c)	(a)	(b)	(c)
1a	0.82 ± 0.02	0.179	0.821	–	1.83 ± 0.07	0.66 ± 0.02	–
1b	1.00 ± 0.02	0.329	0.671	–	1.78 ± 0.05	0.55 ± 0.03	–
2a	1.13 ± 0.03	0.822	0.178	–	1.25 ± 0.03	0.53 ± 0.02	–
2b	0.98 ± 0.03	0.316	0.474	0.210	1.65 ± 0.04	0.59 ± 0.02	0.64 ± 0.03
2c	0.92 ± 0.02	0.159	0.547	0.294	1.23 ± 0.05	0.95 ± 0.03	0.69 ± 0.02
2d	0.80 ± 0.02	0.015	0.620	0.365	2.86 ± 0.21	0.93 ± 0.03	0.57 ± 0.03
2e	0.85 ± 0.01	0.047	0.746	0.207	2.35 ± 0.07	0.79 ± 0.02	0.72 ± 0.03
3a	0.88 ± 0.01	0.072	0.653	0.275	1.28 ± 0.03	0.82 ± 0.02	0.94 ± 0.03
3b	0.86 ± 0.02	0.099	0.701	0.200	1.42 ± 0.03	0.75 ± 0.02	0.95 ± 0.02
3c	0.79 ± 0.02	0.021	0.676	0.303	3.32 ± 0.14	0.72 ± 0.03	0.70 ± 0.02
4a	0.85 ± 0.01	0.040	0.691	0.269	2.56 ± 0.07	0.79 ± 0.01	0.79 ± 0.03

*: (a)+(b)+(c)=1

ground water and amorphous iron phase, and higher ARs than 1 in clay/quartz resistate phase. The latter result is rather different from that in this study. They showed that the majority of U was associated with the iron rich phase, and attributed the high ARs in resistate phase to the injection of Th-234 (U-234) from U-238 in the surface of the resistate minerals by alpha recoil. In this study, as the majority of U is associated with the HF soluble and resistate fractions, the reason of the low ARs observed in this study is explained by the ejection effect by alpha recoil.

Genesis of bauxite deposits

Most of the studies on the bauxite ore focussed on its genesis. There are four ways to be formed as bauxite ore: (a) autochthonous, (b) parautochthonous, (c) allochthonous, and (d) crypto-autochthonous (Maynard, 1983). Chinese bauxite was studied in the Gun district in Honan (Henan) Province by Schuller (1957) and he showed that the source rock was a chloritic to muscovitic slate (Valeton, 1972).

Considering that there is much organic matter on the upper part of the Yangwa ore (Kamitani, 1987) and that there is not any iron cap, this ore deposit must be deposited allochthonously. On the karstic Ordovician limestone, terra rossa was deposited, causing the Fe rich layer at the bottom of the ore deposit. The sedimentation condition must have been oxidative because in a reducing condition Fe exists as Fe^{2+} and is readily removed away while Fe^{3+} precipitates and is retained. Afterwards the weathered materials of Pre-Cambrian basement were transported and deposited on the basin repeatedly. Most of them must have been chloritic or muscovitic materials as the clay minerals were observed by X-ray diffraction analysis. The depositional condition became reducing like a swamp by bio-activities or plants. This is necessary for genesis of iron poor Al hydroxide. Then clay minerals changed to gibbsite, diaspore:

$$H_4Al_2Si_2O_9 + 5H_20 = 2Al(OH)_3 + 2H_4SiO_4$$

kaolinite gibbsite

This reaction is reversible, and depends on the concentration of H_4SiO_4. At times higher rainfall or river water would dilute the H_4SiO_4 concentration and accelerate the formation of gibbsite, and at other times H_4SiO_4 concentration would rise and accelerate the reverse reaction. The reverse correlation between kaolinite and diaspore in the samples is observed as shown in Fig.3-2-7. Diaspore must have formed from gibbsite in diagenetic process. The ore body was again overlain by the Carboniferous limestone.

The variable uranium content, *i.e.*, high content at ore body and low at the bottom, is explained by the redox condition. At the bottom where iron oxide was formed under

oxidative condition, the U would have existed as soluble uranyl ion UO_2^{2+}. Under these conditions, the uranium would have been fixed by adsorption. At the deposition point the ore body was reducing, U was in the U^{4+} form, which is less soluble and was easily concentrated with Al hydroxide. During later diagenesis, some U-234 was removed from mineral surface, and relocated as HCl soluble form.

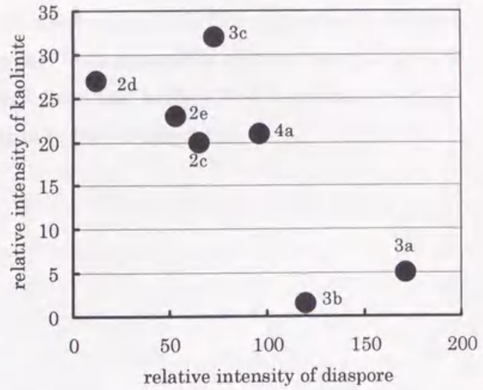

Fig.3-2-7 Correlation between intensities of kaolinite and diaspore by X-ray diffraction analysis of samples from the Yangwa mine, China.

3-2-4. Conclusion

By the study of uranium and other elements in bauxite deposits in Yangwa mine at Jiaozuo area in Henan Province, China, the characteristics of chemical composition, the behavior of uranium and the genesis of bauxite deposits are elucidated.

An inverse correlation between two major components, Al_2O_3 and Fe_2O_3, was observed. Uranium as well as Ti, Cr, V has a strong correlation with Al_2O_3 and Mn, Ca, Cu with Fe_2O_3. Uranium, Cr and V were enriched in the deposits compared with the crustal abundance, whereas SiO_2, MnO, MgO, CaO, Na_2O, Cu, Sr and Ba were depleted in the ore.

By selective chemical leaching method, "HCl soluble", "HF soluble" and "resistate" fractions are obtained. Most of the U in the bauxite is in the silicate fraction (18-75 %), and 20-36 % of the U was in "resistate fraction". The U-234/U-238 activity ratios of those fractions were less than unity, and have a good correlation with the fractional U content. It suggests that U-234 was depleted from the surface of the mineral grain. On the other hand, the activity ratios of HCl soluble U were more than unity, have an inverse correlation with the fractional U content. This suggests that an almost constant amount of mobile U-234 was present in the ore deposits.

The bauxite ore deposit is thought to be sedimentary in origin. It was at first formed as a terra rossa deposit on the karstic Ordovician limestone. The deposit was rich in Fe_2O_3 under relatively oxidative condition. Afterwards, the weathered materials of Pre-Cambrian basement were transported and deposited repeatedly. The deposition

condition was reducing, favoring for the concentration of U. The clay minerals such as kaolinite changed to gibbsite and diaspore. This reversible change depends on the H_4SiO_4 concentration. Th-234 was ejected from the surface of U-containing mineral grain and was adsorbed as HCl soluble form in the ore deposits.

3.3 Uranium species in apatite-bearing sedimentary rocks at Nakamaruke district, Niigata Prefecture

3-3-1 Introduction

Uranium has two major oxidation states; tetravalent U(IV) and hexavalent U(VI). The behavior of U in such different oxidation states are of much concern for studies on various geochemical phenomena and natural analog. As U in a phosphorite shows various oxidation states, phosphorite is a proper material for such research.

Phosphorite deposits have been found along the continental margins of the world, typically associated with upwelling waters (McKelvey, 1967). Phosphorites contain relatively much amount of uranium ranging from 3 to 8300 ppm after Altschuler *et al.* (1958), which is associated with the apatite. Kolodny and Kaplan (1970) studied the U-234/U-238 activity ratios (ARs) in sea-floor phosphorites. They found that tetravalent U (U(IV)) was 38-84 % of total U and that the average ARs of U(IV) and hexavalent U (U(VI)) were 0.71 and 1.57, respectively. They also proposed a fractionation mechanism of uranium isotopes in phosphorites. About 30% of radiogenic U(IV)-234 are oxidized to U(VI)-234. Roe and Burnett (1985) studied island phosphorites and showed that hexavalence (+6) is the predominant oxidation state of U and that AR of U(IV) is larger than that of U(VI) in these rocks.

Most of the U-234/U-238 disequilibrium studies on marine phosphorites, phosphatic nodules, and sediments are concerned with the genesis, age, and the sedimentation rate (Veeh *et al.*, 1974; Veeh and Burnett, 1978; Kress and Veeh, 1980; Kim and Burnett, 1985), few studies have, however, been conducted on the diagenetic or alteration behavior of uranium in the phosphatic sediment. Giresse *et al.* (1986) studied the diagenesis in Tchivoula, Congo in terms of uranium contents, and they found that mobilization and secondary concentration of U was led by hydrolysis of apatite and authigenic minerals that are characteristic of tropical climate. However, systematic studies of U-234/U-238 activity ratio in phosphatic sediment under mild climatic condition have not yet been conducted.

3.3.2 Geology and sample locations

The Nakamaruke area is located in the northern part of Niigata Prefecture, central Japan (see Fig.3-3-1). The basement rocks of this area are composed of Paleozoic slate

and porphyritic biotite granite that intruded in late Cretaceous (Hamachi and Obi, 1969). The Kamagui Formation, Shimoseki Formation and Uchisugawa Formation were formed sequentially during the Neogene Period. The samples for this study were collected from the Kamagui Formation, which consists of conglomerate and sandstone, mainly sandstone in the studied area. The occurrence of phosphorite is restricted to the uppermost part of Kamagui Formation. Very fine sandstone (A), tuffaceous siltstone (B), medium grain sandstone (C), medium grain arkose sandstone (D-0, D-1, D-2), tuffaceous siltstone (E-1), tuffaceous fine grain sandstone (E-2, E-3), and coarse grain arkose sandstone (F-0, F-1, F-2, G, H) were collected from the outcrop as shown in Fig.3-3-2.

Niigata, the nearest meteorological station, is in a monsoon climate area with 1778 mm of annual rainfall. Monthly average temperature ranges from 2 to 26° C, averaging 13.2° C. As the sampling point in this study is

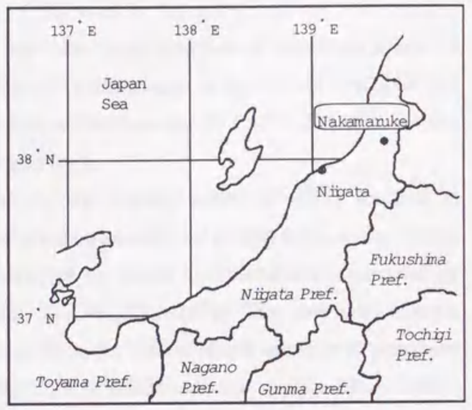

Fig.3-3-1 Location of Nakamaruke in Niigata Prefecture, central Japan.

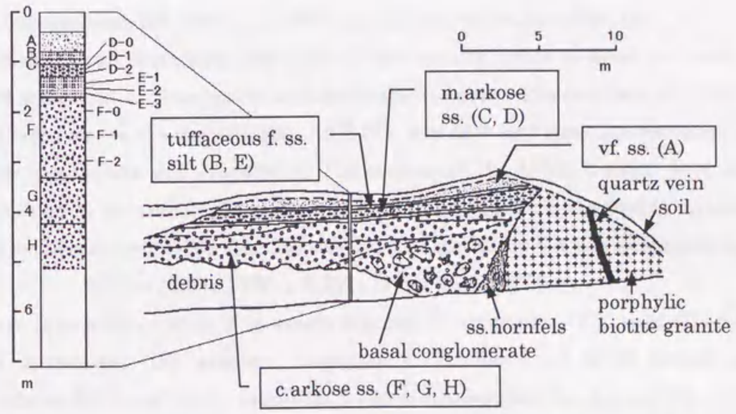

Fig.3-3-2 Sketch of studied outcrop and sample locations at Nakamaruke, Niigata prefecture, central Japan.

located 220 m above sea level and the water table is low, diffusion by underground water is negligible. Rain water from the surface of the hill percolates into the column, and probably plays the most important role in the diagenesis and remobilization of uranium in this study.

3.3.3 Analytical method for U(IV) and U(VI)

The collected samples were air-dried, and the sandy fraction of less than 2 mm in diameter was pulverized for analysis. Weight percentages of the sandy fractions are 100 % for A, D-0, D-1, D-2, E-1, E-2, and E-3, while those for B, C, F-0, F-1, F-2, G, and H are 47, 82, 92, 70, 66, 86, and 75 %, respectively.

Anderson (1984) used U(IV)-232 spike for the determination of U(IV) fraction in natural waters and found that most of the tracer was oxidized before spiking. So, in this study the tetravalent uranium was separated by using the technique described by Clarke and Altschuler (1958), and Kolodny and Kaplan (1970). The powdered sample (0.5g) was taken into a 100 ml beaker cooled in an ice bath under a nitrogen atmosphere to avoid oxidation, and 50 ml of 1.5 M H_3PO_4 was added into the beaker. After 1 hour, the solution was filtered through a glass filter by suction and 3 ml of Ti carrier and 3 ml of 6% cupferron were added to the filtrate. After standing in a refrigerator for 15 minutes, uranium (IV) cupferrate was separated by suction filtration. The cupferrate was decomposed and ashed with HNO_3 and $HClO_4$ (U(IV) fraction). The filtrate was assumed to contain the U(VI) fraction. The glass filter with insoluble residue was decomposed with HF, HNO_3 and $HClO_4$ to produce the residual fraction.

Uranium concentrations and U-234/U-238 activity ratios in total and each fraction were measured by fluorimetry and alpha spectrometry. The recovery of U(VI) fraction was low because the concentration of H_3PO_4 was high and some precipitation occurred when the filtrate was evaporated. The content of the U(VI) fraction was, therefore, calculated by subtraction from total U. Relative errors are estimated to be under 10%. The activity ratio of U(VI) fraction was not only measured but also calculated by

$$R(VI) = [R(T) - F(IV) \times R(IV) - F(r) \times R(r)] / F(VI)$$

where R is activity ratio, F is weight fraction of hexavalent (VI), total (T), residue (r) and tetravalent (IV) uranium, respectively. The observed R(VI) agreed with the calculated R(VI) within the estimated 2 sigma errors except for one sample.

3.3.4 Results and discussion

Uranium contents

The chemical compositions and relative mineral compositions of the samples are shown in Table 3-3-1. The samples D-0, D-1, D-2 contain a large amount of U, Ca and P_2O_5. The mineralogical study of samples from D layer by X-ray diffraction analysis (XRD) revealed the presence of apatite. Most of the uranium is fixed into apatite structure under marine conditions by replacement of Ca^{2+} because of the similarity of their ionic radii. The uranium was in the tetravalent state. The correlation coefficient between Ca and P_2O_5 among all the samples is 0.917, and the correlation coefficients of U-Ca and U-P_2O_5 are 0.967 and 0.947, respectively.

The content of U in the outcrop samples is highest in D, but a second smaller maximum at G is observed. This may be explained by (i) a change of sedimentary conditions in which the phosphatic sediment was formed, and/or (ii) the redistribution of U during diagenesis and alteration. The fine sandy fraction is more abundant in G than in F-1, F-2 and H. This implies that the sedimentation environment changed. The P_2O_5 content in G is, however, less than in F-1 and F-2. The second explanation (ii) suggests the movement of U from the upper layer (probably D) to G after sedimentation. A leaching experiment of Pacific island apatite with $(NH_4)_2CO_3$ performed by Roe and Burnett(1985) indicates that preferential dissolution of U from apatite is possible. Thus, some U in the D layer might have dissolved into interstitial water, been brought to G

Table 3-3-1 Chemical compositions and relative mineral compositions of samples at Nakamaruke, central Japan.

	A	B	C	D-0	D-1	D-2	E-1	E-2	E-3	F-0	F-1	F-2	G	H
lithofacies	very fine sandstone	tuffaceous silt	medium sandstone	medium arkose sandstone	medium arkose sandstone	medium arkose sandstone	tuffaceous silt	tuffaceous fine sandstone	tuffaceous fine sandstone	coarse arkose sandstone	coarse arkose sandstone	coarse arkose sandstone	coarse arkose sandstone	coarse arkose sandstone
(%)														
Al_2O_3	18.78	18.38	11.05	15.42	14.81	13.41	17.39	18.92	16.54	12.27	15.43	15.29	20.10	18.24
TiO_2	0.41	0.51	0.43	0.35	0.35	0.30	0.33	0.39	0.42	0.43	0.43	0.38	0.37	0.36
Fe_2O_3	5.37	3.65	5.59	2.02	2.25	2.15	7.77	4.17	4.33	3.25	2.89	2.29	5.45	2.68
MnO	0.01	0.01	0.02	0.02	0.02	0.02	0.03	0.16	0.07	0.03	0.05	0.03	0.02	0.02
MgO	2.48	2.38	0.96	0.88	0.79	0.70	1.62	2.08	1.55	0.97	1.00	0.83	0.56	0.70
CaO	0.02	0.03	0.10	4.07	4.45	4.52	0.69	0.04	0.05	0.20	0.58	0.49	0.04	0.04
Na_2O	0.05	0.09	0.28	1.42	1.47	1.48	0.23	0.15	0.26	0.79	1.48	1.50	0.32	0.36
K_2O	1.05	0.99	3.91	3.53	3.68	4.75	2.18	2.16	2.93	5.54	4.97	4.60	3.47	4.41
P_2O_5	0.09	0.07	0.25	3.80	3.98	4.03	3.00	1.01	0.72	0.32	0.60	0.40	0.32	0.12
(ppm)														
U	4.48	11.5	16.9	88.9	84.8	78.1	35.3	13.2	16.1	7.40	8.44	11.0	22.0	10.2
Quartz*	+	+	+++++	++	+++	+++	+	+	++	+++++	++++	++++	++	+++
Clay#.*	-	-	+	-	+	++	-	-	+	+	++	++	+	++++

* : - trace, + relative intensity
\# : d = 10 Å

and adsorbed on finer particles such as clay minerals, organic matters, and oxyhydroxides.

Fractional uranium and activity ratio

Table 3-3-2 shows the U contents and the U-234/U-238 activity ratios of total U, U(IV), U(VI) and residual fractions. U(VI) fraction ranges from 9 to 77 % of total U (average 50 %). Residual fraction ranges from 11 to 89 % (average 42 %). Uranium in the samples exists mainly in U(VI) and residual fractions. U(IV) is abundant in D, phosphatic sediments.

In D layer sediments, the ratios of U(IV) to [U(IV) + U(VI)] range from 0.38 to 0.47. Marine phosphorite comprises U(IV) of 0.03-0.91 (Clarke and Altschuler, 1958), 0.38-0.86 (Kolodny and Kaplan, 1970), and 0.40-0.89 (Burnett and Veeh, 1977) of total U, and the D samples in this study contain U(IV) within marine phosphorite range. ARs of total U in D are less than unity, ranging from 0.92 to 0.95. ARs of U(IV) range from 0.75 to 0.81. In contrast, ARs of U(VI) in D are more than unity. The order of fractional ARs, R(IV) < R(T) < R(VI), is in good agreement with the U fractionation model of sea floor phosphorites proposed by Kolodny and Kaplan (1970), Burnett and Veeh(1977). The small enrichment of U at G consists of mainly U(VI) and residual fractions. No apatite was observed by XRD analysis and the contents of U(IV) and P_2O_5 at G were low.

Table 3-3-2 Uranium contents and U-234/U-238 activity ratios of total U, U(IV), U(VI) and residual fractions in samples at Nakamaruke, central Japan.

U / Sample	U content (ppm)				U-234/U-238 activity ratio			
	Total	U(IV)	U(VI)	residue	R(T) ± σ	R(IV) ± σ	R(VI) ± σ	R(r) ± σ
A	4.48	0.06	0.42	4.00	0.92 ± 0.03	0.81 ± 0.14	1.15 ± 0.04	0.93 ± 0.02
B	11.5	0.06	2.75	8.69	0.88 ± 0.02	1.45 ± 0.23	1.06 ± 0.08	0.89 ± 0.02
C	16.9	0.10	5.80	11.0	1.02 ± 0.02	0.91 ± 0.11	1.07 ± 0.04	0.98 ± 0.02
D-0	88.9	29.8	47.7	11.4	0.92 ± 0.02	0.75 ± 0.01	1.03 ± 0.03	0.82 ± 0.02
D-1	84.8	30.5	43.5	10.8	0.92 ± 0.01	0.78 ± 0.02	1.12 ± 0.02	0.84 ± 0.02
D-2	78.1	32.9	36.7	8.49	0.95 ± 0.01	0.81 ± 0.02	1.18 ± 0.02	0.81 ± 0.02
E-1	35.3	0.29	25.7	9.34	0.93 ± 0.01	0.86 ± 0.08	0.99 ± 0.02	0.80 ± 0.02
E-2	13.2	0.08	5.89	7.23	0.95 ± 0.02	1.02 ± 0.10	1.06 ± 0.04	0.89 ± 0.02
E-3	16.1	0.13	8.43	7.54	1.02 ± 0.02	1.09 ± 0.10	1.13 ± 0.05	0.96 ± 0.02
F-0	7.40	0.14	4.56	2.70	1.11 ± 0.02	0.85 ± 0.07	1.09 ± 0.03	0.98 ± 0.02
F-1	8.44	0.09	5.91	2.44	1.06 ± 0.02	1.15 ± 0.12	1.00 ± 0.03	1.14 ± 0.04
F-2	11.0	0.14	8.48	2.38	1.04 ± 0.02	1.21 ± 0.10	1.09 ± 0.03	1.05 ± 0.03
G	22.0	0.08	11.1	10.8	1.11 ± 0.01	1.15 ± 0.14	1.20 ± 0.03	1.10 ± 0.02
H	10.2	0.03	5.11	5.06	1.03 ± 0.02	1.20 ± 0.45	1.02 ± 0.07	1.03 ± 0.02

σ : statistical counting error

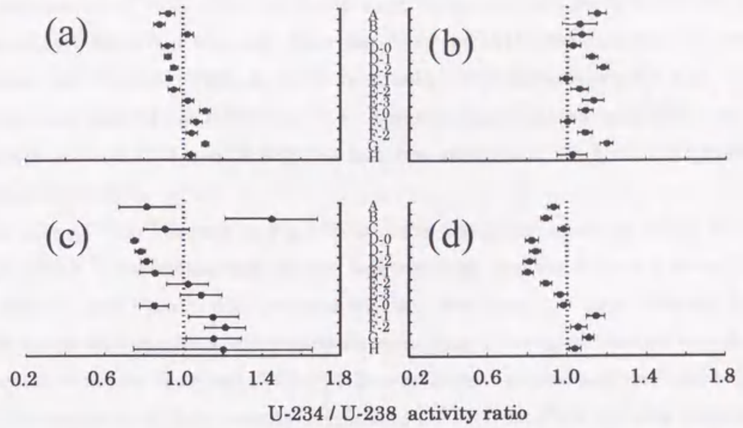

Fig. 3-3-3 Vertical variations of U-234/U-238 activity ratios of total U, U(IV), U(VI) and residual fractions in sedimentary phosphatic strata at Nakamaruke, central Japan.
(a) : total uranium (b) : U(VI) fraction
(c) : U(IV) fraction (d) : residue fraction

Redistribution of uranium in the deposits

The sampled outcrop is in a highly weathered zone of a monsoon climate. Thus, one purpose of the study in this section is focused on the movement of U under this condition, as discussed before.

Figure 3-3-3(a) shows the vertical variations of ARs of total U in the sampled outcrop. In the strata above level E-2, ARs of total U are < 1, while ARs of the strata below E-2 are > 1. If the ARs of the sediments were the same as that of U in seawater (e.g. 1.14, Ku *et al.*, 1977; Chen *et al.*, 1986) and the old strata behaved as a closed system after sedimentation, present ARs should be unity. U-234 (its half-life is 2.45×10^5 y) is preferentially leached by water, because its precursor Th-234 is ejected from the grain surfaces by alpha recoil effect (Kigoshi, 1971; Fleischer, 1980; 1982; Eyal and Fleischer,1985; Eyal and Olander, 1990). Thus, the result of Fig.3-3-3a may appear to be simply explained by relatively recent weathering. Although the stratum is an open system and U-234 has moved, why do all the ARs of the strata samples not become less than unity? Some other mechanism must control the behavior of U in the strata.

Fig.3-3-3(b) shows the vertical variation of ARs of the U(VI) fractions. In this case, all ARs of U(VI) in the strata samples are > 1 within 1σ counting error. This indicates

the enrichment of U(VI)-234. U(VI)-234 is produced not only from U(VI)-238 after 3 steps of disintegration but also from the decay of U(IV)-238 followed by oxidation (Kolodny and Kaplan, 1970). As U(VI) is soluble, U(VI) has a relatively high mobility. The fact that present AR of U(VI) is > 1 suggests that U is moving through the strata in steady state or that soluble U is not lost, but retained in the sediments during the weathering process.

The ARs of U(IV) shown in Fig.3-3-3(c) have the same trend as those of total U (Fig.3-3-3(a)). U associated with apatite is tetravalent, and the AR is < 1, as is D. Some ARs are > 1, and their U (IV) contents are low , less than 0.14 ppm. Roe and Burnett (1985) found that insular apatite contains more than 2 % organic matter and that this may serve to reduce the recoil U(VI)-234. In comparison, marine apatite is formed under reducing condition within the stability field of U(IV). One of the possible explanations may be that U(IV)-234 was fixed into sediments by the reduction of hexavalent U after completing migration. However, the present content of organic matter in all the outcrop samples is less than 0.12 w/w %. The sedimentary rocks might not have reached strongly reducing condition during diagenesis after U(VI) migration under oxidative conditions. Therefore, the U(IV) fractions with AR > 1 are not associated with apatite and are not reduced from U(VI). The other explanation is that they may probably be acid-soluble components of immobile U.

ARs of residual fraction (R(r)) are also shown in Fig.3-3-3(d). The U content of residual fraction ranges from 11 to 89 % of total U, average 42 %, and R(r) has the same tendency as R(T) (Fig.3-3-3(a)). The residual fraction is considered to consist mainly of silicate minerals including some accessory clay minerals. The fact that the R(r) is less than unity is explained by the weathering process of silicates. The recoil U-234 from silicate lattice is very labile and easily lost by weathering. In such case, AR becomes less than unity. The enrichment of U-234 (AR >1) at lower horizon was observed in this study. This needs another explanation. Considering that U(VI) is soluble, U(VI) might migrate downward and be fixed by the residual fraction component. X-ray diffraction analysis showed that the samples F, G, and H contain relatively large amounts of clay minerals (see Table 3-3-1). Burnett and Deetae (1987) has shown that highly weathered phosphate rock in Florida contains nearly half of its activity within finest ($<63\,\mu$ m) fraction. Shirvington (1983) has shown that dissolution of U-234 in the Alligator Rivers region depends on the clay minerals. So, the enrichment of U at G in this study may be explained by transportation of U and adsorption on clay minerals.

3.3.4 Conclusion

The study of U contents and U-234/U-238 activity ratios in the sedimentary rocks associated with apatite deposits at Nakamaruke, central Japan, elucidated the diagenetic behavior of uranium. Uranium content in the outcrop deposits showed two peaks (89 ppm and 22 ppm), a large one at the phosphatic layer and another small one at the 0.3m lower part of the strata, which suggests some uranium has migrated vertically through the deposits.

The U-234/U-238 activity ratios (ARs) of total U in the phosphatic layer were < 1, and > 1 in the lower part of the outcrop. About 50 % of total U is in the U(VI) fraction, and its AR was > 1 in all the samples. This suggests that U(VI)-234 produced from recoil Th-234 is bounded relatively weakly in the minerals.

ARs of U(IV) and residual fraction in the strata varied similarly to those of total fraction. The AR of U(IV) in the phosphatic layer, D, was < 1 as in typical marine phosphorite. U(IV) is abundant in the D layer, while the average U content ratio of the residual fraction in all the samples is 42 % of total U. The ARs of residual fraction composed of silicate including clay minerals also suggest that some amount of uranium moved and was adsorbed by clay minerals.

3.4 Radioisotopes in the Tono uranium deposit in Gifu Prefecture

3.4.1 Introduction

The Tono uranium mine is located in Gifu Prefecture, central Japan (see Fig.3-4-1). It is sedimentary uranium ore deposit and its general formation process is thought to be that U was dissolved from the granitic rocks in the basement of the sedimentary basin, transported by groundwater, and concentrated in a fluvial lignite-bearing formation under a reducing environment (Yamamoto *et al.*, 1974; Sakamaki, 1985). The fact that such uranium deposit formed more than ten million years ago in the late Miocene exists almost unchanged macroscopically, supplies an important information of the geological environment for the preservation of U and behavior of U structures. A microscopic study as well as macroscopic studies, is necessary for understanding the U migration behavior through geological media, for example, a study for leaching - adsorption behavior of uranium series nuclides from U-containing minerals. In such a case, not only the amount of each nuclide but also its chemical state is needed to be specified. Selective chemical leaching technique is one of the speciation analytical methods. Although this technique provides an important information about the phase and existing elements, only a few studies concerning uranium ore deposit are reported. The study of this section is focused on the granitic conglomerate in the Tono uranium mine, central Japan, and the micro-behavior of uranium series nuclides is studied by using selective chemical leaching method.

3.4.2 Outline of geology and sampling location

A high radioactivity was observed in the Tono area during the carborne survey in 1962. Detailed studies in this area revealed the presence of large-scale, sandstone-hosted uranium deposits and associated smaller ore bodies. The Tsukiyoshi ore body is the largest in this area. The geology of the uranium deposits has been reported by Sakamaki (1985), Sato *et al.* (1987) and Kobayashi (1989). The basement is the Cretaceous biotite granite (so called "Toki granite") dated 70 Ma by K-Ar method. The overlying sediments are, in the ascending order, the Miocene Mizunami Group and the Plio-Pleistocene Seto Group. The ore bodies are mostly formed in the Toki Lignite-bearing Formation which lies in the lowest of the Mizunami Group. The age of U mineralization is considered to be 10 Ma, based on the fission track dating on the Jorinji

ore body just in the south of the Tsukiyoshi ore body (Ochiai *et al.*, 1989).

The sample was taken from a newly cut branch of the main gallery (-126m from the ground level) of the Tono uranium mine (Fig.3-4-1). The sample, weighed about 3 kg, was a fresh, slightly consolidated conglomerate in the basal part of the Toki Lignite-bearing Formation which unconformably overlies the granitic basement. The conglomerate was mainly composed of boulders of biotite granite. The sandy matrix, which occupied the interstice of granite boulders, contained a large amount of slightly altered feldspar and biotite derived from the weathered granitic basement. The granitic conglomerate was weakly mineralized in uranium, probably at the same time as the formation of the Tsukiyoshi ore body.

In the laboratory, the sample was crushed and sieved into fractions as ϕ>2mm, 1mm< ϕ <2mm, 500 μ m< ϕ <1mm, 250 μ m< ϕ <500 μ m, 125 μ m< ϕ <250 μ m, 63 μ m< ϕ <125 μ m, and ϕ <63 μ m. Each fraction was 70.0, 6.60, 10.2, 4.97, 3.72 and 2.25 by w/w%. The divided 7 samples are pulverized by an agate motor and supplied to the mineral, chemical and radioactivity analyses.

3.4.3 Analytical method

Mineral analysis was carried out by using JEOL JDX-8030W X-ray diffractometer with Cu tube (40kV, 40mA). Chemical bulk composition was determined by ICP and AAS after the decomposition with nitric acid, hydrofluoric acid and perchloric acid (Kanai *et al.*, 1996).

The selective chemical leaching scheme used in this study is written in chapter 2. Approximately 1.5g of powdered sample was progressively leached. The fractions will be referred to as (a) sodium acetate soluble fraction, which consists of exchangeable ions, (b) sodium acetate/ acetic acid soluble fraction, whose main constituent is presumed to be carbonate, (c) hydroxylamine hydrochloride soluble

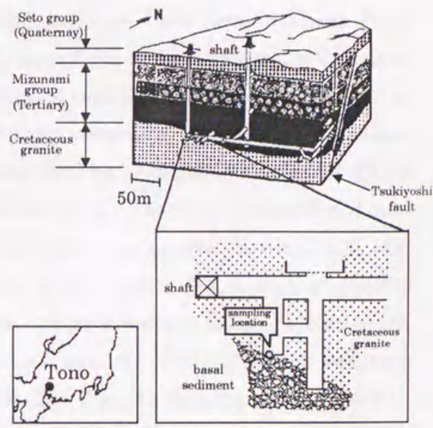

Fig.3-4-1 Location of samples and outline of geology at the Tono uranium mine area.

fraction, which are the Fe-Mn oxide complexes, and (d) hydrogen peroxide soluble fraction, which is considered to consist of organic matter and sulfide. The residual material after the treatment with (4) was analyzed as well, and named (e) residue fraction, which is composed of silicate materials.

Uranium series nuclides such as U-238, U-234 and Th-230, were determined by alpha spectrometry. U-232 and Th-229 spikes were added to the decomposed sample and uranium and thorium fractions were separated and purified by the combination of anion exchange resins of nitrate, chloride and sulfate forms. Purified radionuclides were electrodeposited on a stainless steel planchet and their radioactivities were measured by alpha spectrometers with silicon surface barrier detectors and/or passivated implanted planar silicon detectors (Kanai, 1986a).

3.4.4 Results and discussion

Chemical bulk compositions in sieved samples

The bulk concentrations of U (U-238) and Th (Th-232) before sieving were 65ppm (0.80 Bq/g) and 16ppm (0.064 Bq/g), respectively. The U concentration is one order higher than the average in granite (*i.e.*, 3ppm by Turekian and Wedepohl, 1961), while Th concentration falls within range. The U concentration in the ore body is as high as several %, so the bulk U concentration in the sample is 2-3 orders lower than that in the ore bodies.

Figure 3-4-2 and Table 3-4-1 show the amounts of U and Th in sieved samples. Their amounts in the fine-grained sample are larger than those of the coarse-grained sample. Mineralogical study indicates that the fine-grained sample contains a large amount of biotite while the coarse-grained sample contains abundant quartz and plagioclase (Fig.3-4-3). The U and Th contents in the sieved samples have positive correlation with the amount of biotite (their correlation coefficients are 0.76 and 0.66, respectively), and negative correlation with plagioclase. The U also has a good correlation with Ti, Al, Mn, Mg, P, Cr, V and Li (Kanai *et al.*, 1996). The heterogeneous distribution of mineral species in the sieved samples may be due to the selective decomposition of biotite in the weathered granite; biotite brakes down to finer particles while the more resistant quartz and plagioclase remains coarse-grained. The U in the fine-grained sample may exist on the surface of detrital grains and/or within altered biotite grains. The enrichment of U in the fine soil particles was observed by Megumi and Mamuro (1977) and they explained it by the surface adsorption. The SEM analysis shows that the U

Table 3-4-1 Chemical composition of sieved samples of granitic conglomerate from Tono uranium mine.

components / grain size(ϕ)	TiO_2	Al_2O_3	Fe_2O_3	MnO	MgO	CaO	Na_2O	K_2O	P_2O_5	Zn	Pb	Co	Ni	Cr	V	Cu	Sr	Ba	Li	Rb	^{238}U	^{232}Th
	(%)									(ppm)											(Bq/g)	
ϕ <63 μ m	0.51	16.16	4.55	0.13	0.64	3.60	3.36	2.49	0.05	101	41	5	15	15	60	30	59	151	113	67	3.14	0.36
63 μ m< ϕ <125 μ m	0.36	13.80	4.31	0.10	0.53	2.92	3.65	2.87	0.03	91	38	5	9	7	40	16	63	158	85	76	1.51	0.20
125 μ m< ϕ <250 μ m	0.26	13.76	2.72	0.08	0.39	2.44	3.28	3.56	0.03	73	26	0	27	7	26	15	62	179	57	104	0.90	0.11
250 μ m< ϕ <500 μ m	0.15	10.98	1.52	0.05	0.23	1.53	2.32	4.27	0.02	33	11	2	9	5	13	13	48	179	38	111	0.51	0.04
500 μ m< ϕ <1mm	0.09	10.85	0.94	0.03	0.14	1.08	2.13	5.02	0.02	19	6	1	9	5	7	4	45	211	28	130	0.36	0.03
1mm< ϕ <2mm	0.07	12.29	0.72	0.03	0.11	1.34	2.58	6.23	0.02	29	20	2	14	3	5	15	50	266	23	167	0.32	0.01
2mm< ϕ	0.08	10.98	1.08	0.07	0.16	4.47	2.47	5.02	0.03	27	12	0	7	6	8	7	54	239	29	121	0.83	0.06

content is high in the biotite grains and that U is gathered around the surface of pyrites, so the biotite itself is considered to be one of the main reservoir of U (Kanai *et al.*, 1998a). This indicates that the U concentration is associated with the fine pyrite grains.

Uranium concentration in leached fraction

Selective chemical leaching technique was applied to 3 sieved samples (grain size (ϕ) : 500 μ m< ϕ <1mm, 125 μ m< ϕ <250 μ m, and ϕ <63 μ m) and the fractional U concentrations were determined. The results were shown in Table 3-4-2 and Fig. 3-4-4. A large proportion of the uranium was in the (b)sodium acetate/ acetic acid soluble fraction and (c)hydroxylamine hydrochloride soluble fraction. The fraction (b) is called the "carbonate fraction" because the X-ray diffraction peaks of calcite disappeared after

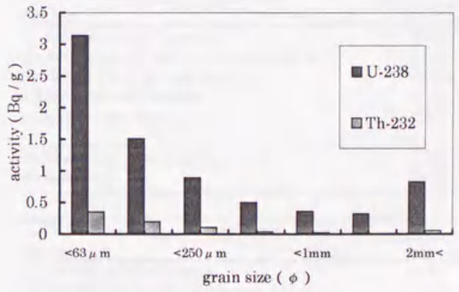

Fig.3-4-2 U and Th contents in sieved samples of granitic conglomerate from the Tono uranium mine.

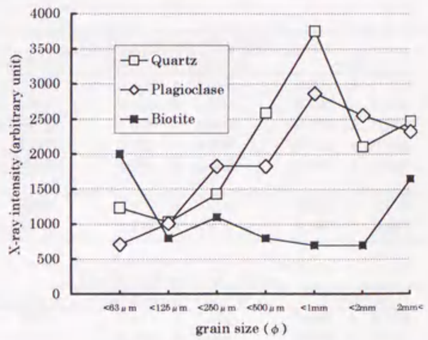

Fig.3-4-3 Variation of mineral composition of sieved samples of granitic conglomerate from the Tono uranium mine.

the treatment of sodium acetate-acetic acid (pH 5.0) solution (Fig.3-4-5). In the mineralized zone of the Tono mine, calcite was often observed (Yoshida, 1994), and a large amount of U in the mineralized sample was eluted in a sodium acetate-acetic acid solution (Sato *et al.*, 1987). Fraction (c) is considered to be "iron oxide fraction" because a large amount of iron is dissolved by the reducing reagent. Therefore, the carbonate and iron oxides are thought to play an important role for U ore genesis.

Table 3-4-2 Fractional U-238, U-234, Th-232 and Th-230 radioactivities in sieved samples from the Tono mine, Gifu Prefecture.

grain size / fraction	U-238 radioactivity (Bq/g)		
	500 μm<φ<1mm	125 μm<φ<250 μm	φ<63 μm
(a) AcONa soluble fraction	0.039 ± 0.001	0.092 ± 0.002	0.182 ± 0.005
(b) AcONa-AcOH soluble fraction (pH 5)	0.139 ± 0.004	0.249 ± 0.009	0.537 ± 0.020
(c) $NH_2OH \cdot HCl$ soluble fraction	0.068 ± 0.002	0.199 ± 0.007	0.725 ± 0.028
(d) H_2O_2 soluble fraction	0.031 ± 0.002	0.068 ± 0.003	0.325 ± 0.014
(e) Residue fraction	0.052 ± 0.002	0.239 ± 0.012	1.443 ± 0.054
Total activity (calculated)	0.329 ± 0.006	0.846 ± 0.017	3.212 ± 0.066
Bulk activity	0.364 ± 0.010	0.899 ± 0.033	3.140 ± 0.090

grain size / fraction	U-234 radioactivity (Bq/g)		
	500 μm<φ<1mm	125 μm<φ<250 μm	φ<63 μm
(a) AcONa soluble fraction	0.040 ± 0.001	0.101 ± 0.003	0.184 ± 0.005
(b) AcONa-AcOH soluble fraction (pH 5)	0.114 ± 0.003	0.218 ± 0.008	0.451 ± 0.017
(c) $NH_2OH \cdot HCl$ soluble fraction	0.050 ± 0.002	0.144 ± 0.005	0.460 ± 0.018
(d) H_2O_2 soluble fraction	0.010 ± 0.001	0.020 ± 0.001	0.094 ± 0.004
(e) Residue fraction	0.068 ± 0.003	0.274 ± 0.014	1.285 ± 0.049
Total activity (calculated)	0.282 ± 0.005	0.757 ± 0.017	2.475 ± 0.055
Bulk activity	0.325 ± 0.009	0.834 ± 0.031	2.550 ± 0.080

grain size / fraction	Th-232 radioactivity (Bq/g)		
	500 μm<φ<1mm	125 μm<φ<250 μm	φ<63 μm
(a) AcONa soluble fraction	0.000 ± 0.000	0.000 ± 0.000	0.001 ± 0.000
(b) AcONa-AcOH soluble fraction (pH 5)	0.014 ± 0.014	0.019 ± 0.001	0.027 ± 0.002
(c) $NH_2OH \cdot HCl$ soluble fraction	0.009 ± 0.009	0.022 ± 0.002	0.025 ± 0.004
(d) H_2O_2 soluble fraction	0.000 ± 0.000	0.002 ± 0.000	0.010 ± 0.000
(e) Residue fraction	0.021 ± 0.021	0.065 ± 0.002	0.257 ± 0.006
Total activity (calculated)	0.044 ± 0.027	0.109 ± 0.003	0.320 ± 0.007
Bulk activity	0.034 ± 0.007	0.110 ± 0.010	0.380 ± 0.020

grain size / fraction	Th-230 radioactivity (Bq/g)		
	500 μm<φ<1mm	125 μm<φ<250 μm	φ<63 μm
(a) AcONa soluble fraction	0.002 ± 0.000	0.007 ± 0.000	0.006 ± 0.000
(b) AcONa-AcOH soluble fraction (pH 5)	0.236 ± 0.003	0.402 ± 0.004	0.653 ± 0.008
(c) $NH_2OH \cdot HCl$ soluble fraction	0.088 ± 0.004	0.246 ± 0.008	0.256 ± 0.012
(d) H_2O_2 soluble fraction	0.006 ± 0.000	0.016 ± 0.001	0.087 ± 0.001
(e) Residue fraction	0.163 ± 0.003	0.617 ± 0.008	2.523 ± 0.018
Total activity (calculated)	0.495 ± 0.006	1.288 ± 0.012	3.524 ± 0.023
Bulk activity	0.430 ± 0.020	1.320 ± 0.100	4.300 ± 0.150

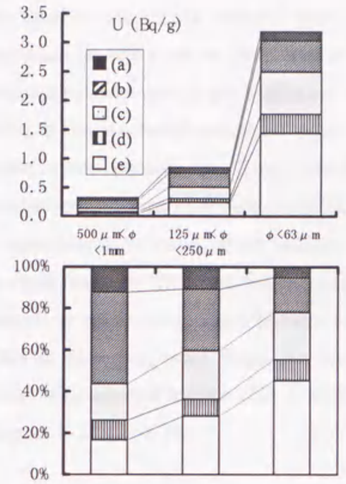

Fig.3-4-4 Fractional U-238 radioactivities in sieved samples of granitic conglomerate from Tono uranium mine.

(a) AcONa soluble fraction
(b) AcONa-AcOH soluble fraction
(c) $NH_2OH \cdot HCl$ soluble fraction
(d) H_2O_2 soluble fraction
(e) residue fraction

A relatively large amount of Ca was found in (a)sodium acetate soluble fraction, Ca, Mn and Zn in the (b)sodium acetate/ acetic acid soluble fraction, and Fe, Mn, Mg, P, Zn and V in the (c)hydroxylamine hydrochloride soluble fraction (Kanai *et al.*, 1996). Most of the elements were dissolved with the Fe and Mn, which suggests that they coprecipitated with iron and manganese oxides, possibly derived from the altered biotite.

The percentages of fractional content against

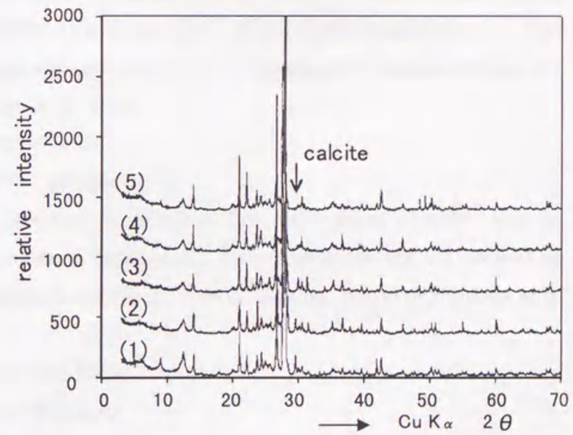

Fig.3-4-5 X-ray diffraction patterns of untreated and treated samples of sieved granitic conglomerate (ϕ <63 μ m) by successive chemical leaching.

(1) untreated
after treatment with
(2) 1M AcONa solution
(3) 1M AcONa/AcOH solution
(4) 0.04M $NH_2OH \cdot HCl$/25%AcOH solution
(5) 30% H_2O_2 (pH2)

the total content (bulk content) shown in Fig.3-4-4, indicate that the leached U (sum of fractions (a)-(d)) is more than half of the bulk content. The fine-grained samples have smaller percentages of the leached U than the coarse-grained ones. The U concentration ratio of the leached fraction between the finest and coarsest samples was about 6. The fine-grained sample has larger surface area than the coarse-grained one and the leached component may be correlated with the surface of the grain. On the contrary, the U concentration ratio of (e) residue fraction was about 28, bigger than that of the leached fraction. This fact indicates that the U in the silicate fraction of the fine-grained sample is concentrated much more than expected from the grain size and surface area. This is also suggested from the fact that the fine-grained sample contains a large amount of altered biotite that is rich in U, and less quartz and plagioclase which are poor in U (Fig.3-4-3).

Absorption density

The elements in the reducing reagent soluble fraction (c), may be adsorbed by the iron oxyhydroxides. Adsorption density (Γ) is one index of this geochemical behavior. The adsorption model at the surface of iron oxyhydroxide is assumed as follows (Balistrieri and Murray, 1982, 1983; Tessier *et al.*, 1985),

$$SOHx + M^{z+} = SOM^{(z-x)+} + xH^{+}$$

$$^{*}Ka = [SOM^{(z-x)+}][H^{+}]^{x} / \{[SOHx][M^{z+}]\},$$

where SOHx, SOM and $^{*}Ka$ are the free surface site, the surface complex and an apparent overall equilibrium constant, respectively. If the iron concentration present as oxyhydroxide is denoted as [Fe]total, and the number of sites per iron oxyhydroxide as n, then

$$[SOHx] + [SOM] = [SOHx]total$$
$$= n \cdot [Fe]total.$$

Adsorption density Γ is defined as $\Gamma = [SOM] / [Fe]total$. ---- (1)

Therefore, $^{*}Ka = \Gamma \cdot [H]^{x} / \{(n - \Gamma) \cdot [M]\}$

$$\Gamma = n \cdot {}^{*}Ka \cdot [M] / \{{}^{*}Ka \cdot [M] + [H]^{x}\},$$ ---- (2)

depending on the solute composition and pH. The adsorption densities of U calculated from the equation (1) are shown in Fig.3-5-6, using the metal concentrations of fraction(c) as [SOM] and [Fe]total. They are the lower limits because some loosely bound U may be leached during the procedures preceding (c). It is indicated that the calculated adsorption density of U tends to increase with decreasing grain size, while

those of Na, Mg, Ca, Mn, Zn and V almost unchange and those of Al, K, P, Ti, Ba and Sr decrease with decreasing grain size. This tendency is confirmed by upper limits of adsorption densities calculated using fractions (a) and (c) (The fraction (b) is excluded from calculation because it was strongly associated with carbonate). This tendency of U is not concordant with the adsorption model because it requires a constant adsorption density when U is fixed only by the adsorption on the iron oxyhydroxide. Yoshida (1994) observed U minerals in the cleavage of biotite mineral in ore body, so this tendency may be because the fine U minerals are formed and abundant in fine-grained samples. Alternatively, U concentration around the complexing site of iron oxyhydroxides may have become locally high, because the adsorption density is a function of metal concentration as shown in the equation (2).

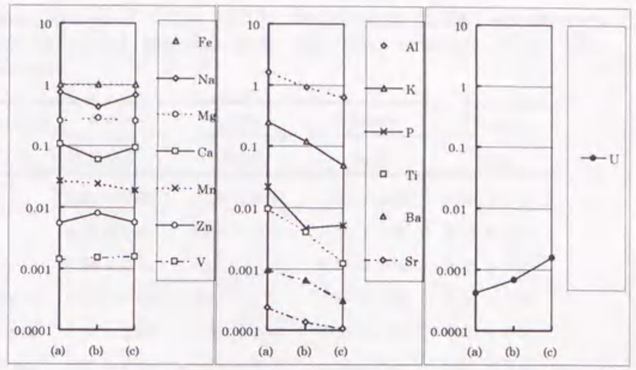

Fig.3-4-6 Variation of adsorption density (Γ) with grain size.
(a) 500 μ m< ϕ <1mm
(b) 125 μ m< ϕ <250 μ m
(c) ϕ <63 μ m

Uranium series nuclides in sieved samples

The U-238, U-234, Th-230 and Th-232 radioactivities, and U-234/U-238 and Th-230/U-234 activity ratios in samples of the different grain size are shown in Table 3-4-1 and Table 3-4-3. The U-234 and Th-230 are abundant in the fine-grained samples as well as U-238 and Th-232, as was shown before. The bulk U-234/U-238 activity ratio is 0.95±0.05, indicating that U-234 is in a little disequilibrium with U-238. The bulk Th-230/U-234 activity ratio is 1.36±0.06. For the sieved samples of 2mm> ϕ , U-234/U-238 activity ratios are less than 1, and Th-230/U-234 activity ratios are more than 1. The data are plotted in $^{234}U/^{238}U$-$^{230}Th/^{234}U$ diagram (Fig.3-4-7), which shows the uranium mobility (Ivanovich and Harmon, 1992). It indicates that U is eluted from the matrix of the conglomerate. It is inferred that uranium series nuclides in the matrix of

Table 3-4-3 Radioactivities of U-238, U-234, Th-230 and Th-232 and activity ratios in sieved samples from the Tono uranium mine, Gifu Prefecture.

nuclides / grain size	U-238 (Bq/g)	U-234 (Bq/g)	Th-230 (Bq/g)	Th-232 (Bq/g)
2mm< ϕ	0.83 ± 0.04	0.82 ± 0.04	1.06 ± 0.03	0.06 ± 0.00
1mm< ϕ <2mm	0.32 ± 0.01	0.28 ± 0.01	0.33 ± 0.01	0.03 ± 0.00
500 μ m< ϕ <1mm	0.36 ± 0.01	0.33 ± 0.01	0.43 ± 0.02	0.03 ± 0.01
250 μ m< ϕ <500 μ m	0.51 ± 0.02	0.43 ± 0.01	0.70 ± 0.02	0.05 ± 0.00
125 μ m< ϕ <250 μ m	0.90 ± 0.03	0.83 ± 0.03	1.32 ± 0.10	0.11 ± 0.01
63 μ m< ϕ <125 μ m	1.51 ± 0.05	1.32 ± 0.04	2.37 ± 0.07	0.20 ± 0.01
ϕ <63 μ m	3.14 ± 0.09	2.55 ± 0.08	4.30 ± 0.15	0.38 ± 0.02

grain size / activity ratio	U-234/U-238	Th-230/U-234	Th-230/Th-232	U-238/Th-232
2mm< ϕ	0.99 ± 0.01	1.29 ± 0.07	16.6 ± 1.1	13.0 ± 1.0
1mm< ϕ <2mm	0.87 ± 0.05	1.17 ± 0.06	9.7 ± 0.6	9.5 ± 0.7
500 μ m< ϕ <1mm	0.89 ± 0.03	1.32 ± 0.07	12.6 ± 2.7	10.7 ± 2.2
250 μ m< ϕ <500 μ m	0.85 ± 0.04	1.62 ± 0.07	14.0 ± 1.2	10.1 ± 0.9
125 μ m< ϕ <250 μ m	0.93 ± 0.05	1.58 ± 0.13	12.3 ± 1.6	8.4 ± 0.9
63 μ m< ϕ <125 μ m	0.87 ± 0.04	1.80 ± 0.08	11.9 ± 0.7	7.6 ± 0.5
ϕ <63 μ m	0.81 ± 0.04	1.69 ± 0.08	11.3 ± 0.6	8.3 ± 0.4

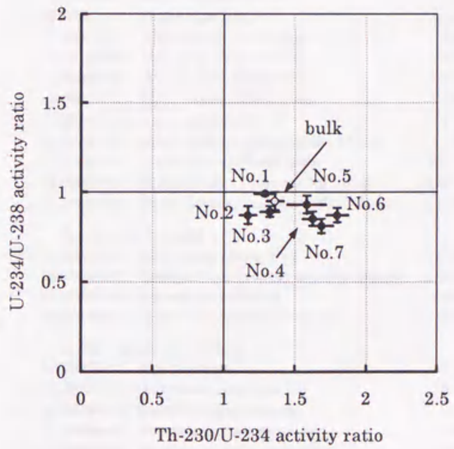

Fig.3-4-7 $^{234}U/^{238}U$ and $^{230}Th/^{234}U$ activity ratios in sieved samples of granitic conglomerate from the Tono uranium mine, Gifu Prefecture.

No.1: ϕ >2mm,
No.2:1mm< ϕ <2mm,
No.3: 500 μ m< ϕ <1mm,
No.4:250 μ m< ϕ <500 μ m,
No.5:125 μ m< ϕ <250 μ m,
No.6:63 μ m< ϕ <125 μ m,
No.7: ϕ <63 μ m.

conglomerate are not in equilibrium within 300,000 y, because they, if in a closed system,

would become in radioactive equilibrium in 300,000 y at the longest based on the half-life of Th-230 (Ivanovich and Harmon, 1992). The radioisotopes such as U, Ra and Rn in groundwaters in the Tono area were surveyed (Kanai *et al.*, 1990b) and shown in Table 3-4-4. Considering the fact that U-234/U-238 activity ratios in the groundwater in this area are more than 1 and those in the conglomerate are less than 1, U is inferred to migrate microscopically through the matrix of conglomerate. Uranium mineralization is considered to be occurred on the clay minerals and organic materials in the ore bodies (Yamamoto *et al.*, 1974), therefore a portion of the eluted U is assumed to be adsorbed and fixed by the clay minerals and organic materials during the flow.

Nohara *et al.* (1992) studied the uranium series nuclides in the samples at the mineralized zone. They found that their activity ratios gathered at the center of $^{234}U/^{238}U$-$^{230}Th/^{234}U$ diagram and that the daughters were almost in equilibrium, indicating no transportation macroscopically. Our study showed that U is leached microscopically in the granitic conglomerate at the basement of ore forming formations.

Table 3-4-4 Uranium, radium and radon concentrations in waters in the Tono area, Gifu Prefecture.

No.	Name	Location	U μg/l	Ra Bq/l	Rn Bq/l	U-234/U-238 activity ratio
	(waters in the pit)					
1	89022806	Sublevel gallery, A+C	0.02	0.04 ± 0.01	0.7 ± 0.1	
2	89022807	Sublevel gallery, B	0.56	0.02 ± 0.01	0.1 ± 0.1	0.93 ± 0.04
5	89022704	Main gallery, 65m boring	0.02	0.03 ± 0.01	118. ± 1.	2.76 ± 0.41
6	89122702	Main gallery, 70m boring	< 0.01	0.07 ± 0.01	94.1 ± 0.2	1.47 ± 0.39
7	89022701	Main gallery, 95m boring	0.01	0.02 ± 0.01	193. ± 1.	2.84 ± 0.70
8	89022703	Main gallery,120m boring	0.10	0.27 ± 0.16	368. ± 1.	1.55 ± 0.14
9	89022811	North gallery, End	0.06	0.03 ± 0.01	4.6 ± 0.1	5.07 ± 0.49
10	89022705	Under gallery, Higashidobira boring	0.06	0.02 ± 0.01	670. ± 1.	6.12 ± 0.59
11	89022809	Under gallery, Ki-eki drain	233.	0.10 ± 0.01	500. ± 1.	4.61 ± 0.10
12	89022810	Under gallery, Cross-cut No.1 west	1140.			3.67 ± 0.04
13	89022808	Under gallery, Tsukiyoshi-Fault Drop	2.00			3.58 ± 0.10
	(waters out of the pit)					
15	89030113	Matsunoike boring No.1	1.27	0.09 ± 0.01	77.5 ± 0.1	1.97 ± 0.05
16	89030112	Tsukiyoshi community center(Kimei 81)	0.19	0.02 ± 0.01	126. ± 1.	1.69 ± 0.15
17	89030115	Kiguchi No.81 boring	0.01	0.03 ± 0.01	20.2 ± 0.1	1.79 ± 0.56
18	89030222	Oniiwa Onsen (Shosen-kaku)	0.84	0.08 ± 0.01	37.2 ± 0.1	3.34 ± 0.15
	(surface wa	(surface waters)				
20	89030217	Kyuroku-bora	0.02			1.79 ± 0.63
21	89030218	Shizu-bora upstream	0.04			3.77 ± 0.48
22	89030216	Shizu-bora downstream	0.39			1.86 ± 0.10
23	89030219	Shomasama-bora upstream	0.03			3.22 ± 0.63
24	89030220	Shomasama-bora downstream	0.09			5.10 ± 0.45
25	89030114	Pool near the No.21 outcrop	239.	0.02 ± 0.01	157. ± 1.	2.94 ± 0.05
26	89030221	Pool at the Obara outcrop	0.07	0.06 ± 0.01		0.99 ± 0.14

(± sigma) indicates statistic counting error

Uranium series nuclides in leached fraction

The fractional U-238 and U-234 radioactivities and U-234/U-238 activity ratios obtained by selective chemical leaching method are shown in Table 3-4-2, Table 3-4-5 and Fig.3-4-8. The sum of each fractional radioactivity is almost in good accordance with the bulk radioactivity. There are two remarkable points in activity ratios. One is that the U-234/U-238 activity ratios of (a)sodium acetate soluble fraction slightly exceed 1, and the other is that the ratios of (e)residue fraction are larger than 1 for coarse-grained samples. U-234/U-238 activity ratios of other fractions ((b)-(d)) are less than 1, which is like the

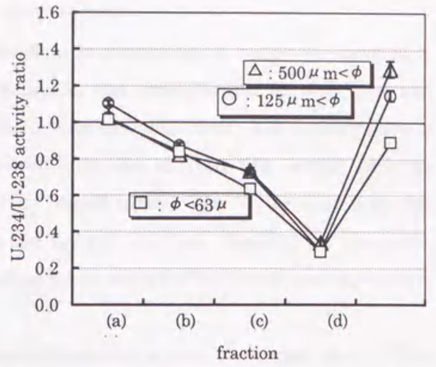

Fig.3-4-8 Fractional U-234/U-238 activity ratios in sieved samples from the Tono uranium mine, Gifu Prefecture.
△: 500 μm< φ <1mm,
○: 125 μm< φ <250 μm
□: φ <63 μm
(a) AcONa soluble fraction
(b) AcONa-AcOH soluble fraction
(c) $NH_2OH \cdot HCl$ soluble fraction
(d) H_2O_2 soluble fraction
(e) residue fraction

Table 3-4-5 Fractional U-234/U-238 and Th-230/U-234 activity ratios in sieved samples from the Tono uranium mine, Gifu Prefecture.

grain size / fraction	U-234/U-238 activity ratio		
	500μm< φ <1mm	125μm< φ <250μm	φ <63μm
(a) AcONa soluble fraction	1.03 ± 0.02	1.10 ± 0.02	1.02 ± 0.01
(b) AcONa-AcOH soluble fraction (pH 5)	0.82 ± 0.01	0.87 ± 0.01	0.84 ± 0.01
(c) $NH_2OH \cdot HCl$ soluble fraction	0.73 ± 0.02	0.73 ± 0.01	0.64 ± 0.01
(d) H_2O_2 soluble fraction	0.34 ± 0.02	0.29 ± 0.01	0.29 ± 0.01
(e) Residue fraction	1.29 ± 0.04	1.15 ± 0.03	0.89 ± 0.01
Total activity ratio (calculated)	0.86 ± 0.02	0.89 ± 0.03	0.77 ± 0.02
Bulk activity ratio	0.89 ± 0.03	0.93 ± 0.05	0.81 ± 0.04

grain size / fraction	Th-230/U-234 activity ratio		
	500μm< φ <1mm	125μm< φ <250μm	φ <63μm
(a) AcONa soluble fraction	0.04 ± 0.00	0.07 ± 0.00	0.03 ± 0.00
(b) AcONa-AcOH soluble fraction (pH 5)	2.07 ± 0.07	1.85 ± 0.07	1.45 ± 0.06
(c) $NH_2OH \cdot HCl$ soluble fraction	1.76 ± 0.10	1.71 ± 0.08	0.56 ± 0.03
(d) H_2O_2 soluble fraction	0.57 ± 0.06	0.83 ± 0.05	0.92 ± 0.04
(e) Residue fraction	2.42 ± 0.12	2.25 ± 0.12	1.96 ± 0.08
Total activity (calculated)	1.75 ± 0.06	1.70 ± 0.08	1.42 ± 0.07
Bulk activity	1.14 ± 0.05	1.28 ± 0.06	1.36 ± 0.08

bulk ratio. The ratio decreases in the order of (b)>(c)>(d).

The U in the (a)sodium acetate soluble fraction is considered to be ion exchangeable and bound weakly. U-234/U-238 activity ratios in the groundwater in this area are reported to be more than 1 (Kanai *et al.*, 1990b). The fact of U-234/U-238 activity ratio > 1 suggests that U-234 is apt to be dissolved into the surrounding water such as interstitial water and groundwater water by recoil effect. The U leached into the (a)sodium acetate soluble fraction may be the uranyl ion that adsorbed on the grain surface and exchangeable with the surrounding water with U-234/U-238 activity ratio > 1.

The U-234/U-238 activity ratios in (e)residue fraction are near 1 or larger than 1. The U-234/U-238 activity ratio in the silicate lattice is decreased by alpha recoil ejection of the Th-234 outside the lattice after U-238 decay (Kigoshi, 1971). On the other hand, the U-234/U-238 activity ratio of the lattice may be increased by alpha recoil through incorporation into the lattice from the surrounding U. Which effect is advantageous and whether the activity ratio becomes less or more than 1, depend on the ratio of U contents between the adjacent phases. When U decays in the low content phase, the loss of recoiled Th-234 is smaller than the case in the high content phase. And the low content phase gets more recoiled Th-234 than the ejection loss, if the content of U in the adjacent phase is higher than in itself. In such case, incorporation effect is advantageous. The results in this study were that the U-234/U-238 activity ratio of the finest sample (ϕ <63 μ m) was a little smaller than 1 and those of the other two samples were larger than 1 (Fig.3-4-8), indicating that the ejection effect is advantageous for the fine-grained sample while the incorporation effect is advantageous for the coarse-grained sample. The fraction (e) is the remained phase, *i.e.* silicate phase. It is consistent with the fact that the coarse-grained sample contains much quartz and plagioclase that are poor in U. Fig.3-4-9 shows the relationships between the U-238 concentration and the U-234/U-238 activity ratio in each fraction. The activity ratios in (e)residue fraction varied largely with U concentration, while those of other fractions varied a little. In particular, the activity ratios in (d)hydrogen peroxide soluble fraction were almost unchanged although the U concentration changed in a larger range.

Sheng and Kuroda (1984; 1986a, b) studied the leaching behavior of radionuclides in pitchblend and carnotite, and observed extremely high activity ratios. They discussed the U-234/U-238 activity ratio using the model of spherical small grain (phase A) surrounded by the phase B. The activity ratio is given as ;

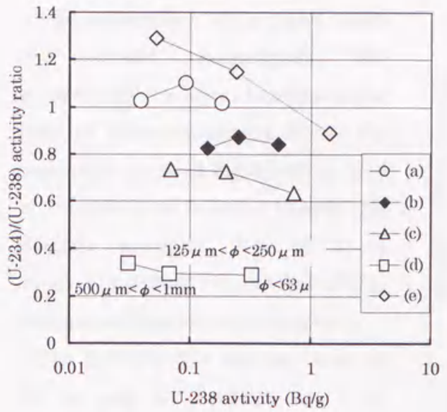

Fig.3-4-9 Relationships between U-238 activity and U-234/U-238 activity ratios in leached fractions.
(a) AcONa soluble fraction
(b) AcONa-AcOH soluble fraction
(c) $NH_2OH \cdot HCl$ soluble fraction
(d) H_2O_2 soluble fraction
(e) residue fraction

$^{234}U/^{238}U=3/4*1/(1+f)*(C_B/C_A-1)*[R/r_A-1/12*(R/r_A)^3]*(1-\exp(-\lambda \cdot T)+(1+f*g)/(1+f)$ --(3)

where f, C, R, r_A, λ, T and g are the contamination factor, uranium concentration in each phase, the range of recoil atom, the radius of the grain, the decay constant of U-234, the age of U-bearing system and the activity ratio of the contamination uranium, respectively. The R of recoiledTh-234 (that disintegrates to U-234) is calculated to be 27.2nm in quartz and 24.7nm in biotite using LLS-theory by Hashimoto *et al.* (1985). So it can be assumed to be less than 0.03 μm in these samples, which is far to small compared to the grain size even if the sample size is <63 μm. When f=0, $R<<r_A$ and $T>>1/\lambda$,the equation (3) becomes

$^{234}U/^{238}U=1+3/4*(C_B/C_A-1)*[R/r_A]$. --(4)

The activity ratio depends on the concentration ratio of adjacent phases (C_B/C_A) and the radius of the grain. In this study the C_B/C_A value (calculated from the ratio of leached U ((a)-(d)) to residue U (e)) ranges from 1.2 to 5.3, so the U-234/U-238 activity ratio becomes more than 1 from the equation (4). However, that of the fine-grained sample is < 1.

This problem may be overcome by assuming that a portion of the U in the grain is also transported outside. Although the U distribution is not uniform and the injection of recoil atom occurs only at the surface, it is assumed that ^{234}U moves from outside into the inside (injection) at the ratio of k_1 and from inside to outside (ejection and elution) at the ratio of k_2. Then U-234/U-238 activity ratio in the grain becomes

$$^{234}Ui=(1-k_2)*^{238}Ui+k_1*^{238}Uo$$

$$^{234}Ui/^{238}Ui=(1-k_2)+k_1*(^{238}Uo/^{238}Ui) \quad \text{-----(5)}$$

where subscripts i and o mean inside and outside, respectively. The equation (5) is a linear function of the ratio of adjacent phases. From the regression curve in Fig.3-4-10, k_1 and k_2 are calculated to be 0.092 and 0.17. Roughly speaking, 1/10 of U is injected into the grain and 2/10 of U is transported outside from the grain.

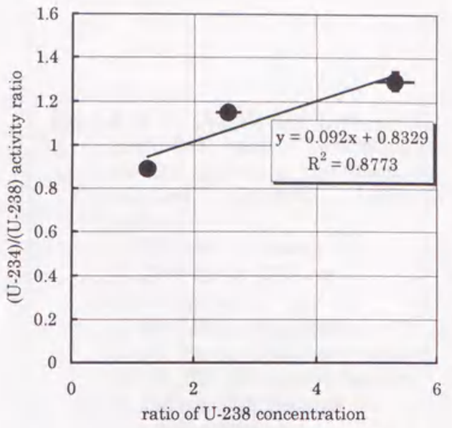

Fig.3-4-10 Relationships between $^{234}U/^{238}U$ activity ratio in residue fraction and ratio of ^{238}U concentration in iron oxide fraction to that in residue fraction.

The U-234/U-238 activity ratios in (b), (c) and (d) fractions are < 1, indicating U-234 deficiencies are probably in the carbonate, iron oxide and sulfide / organic phases. These phases are between the grains and minerals, and the sum of U in these fractions exceeds half of the bulk content. The elution of U from the bulk sediment owes much to these phases. Therefore, it is concluded that a large amount of U-234 was eluted and moved microscopically from the matrix between the grains, and the U-234 in the grain was increased by adsorptive interaction with interstitial water (*i.e.* (a)) and also was enriched by alpha recoil injection effect (*i.e.* (e)).

More than half of the Th is retained in the residue fraction, though the measurement errors for Th are a little larger than for U. A much greater amount of Th was leached in the (b) sodium acetate/ acetic acid soluble and (c) hydroxylamine hydrochloride soluble fractions. A little was dissolved in the (a) sodium acetate soluble fraction, which is expected from the insolubility of Th. Therefore, the Th-230/U-234 activity ratio of the (a) fraction is very low. Those of (b), (c) and (e) fractions are > 1 (the activity ratio of only (c) fraction of the sample ϕ <63 μ m is < 1). The ratio in the (d) hydrogen peroxide soluble fraction was < 1. Fig. 3-4-11 shows the distribution of U-234/U-238 and Th-230/U-234 activity ratios. In this diagram, the data of the (e) residue fraction were plotted in the area of U-234/U-238 > 1 and Th-230/U-234 > 1, indicating the elution of U and enrichment of U-234 by alpha recoil injection. The fraction (d) falls within the area of U-234/U-238 < 1 and Th-230/U-234 < 1, being depleted in Th-230 compared with U (the Th-230/U-234 activity ratios are 0.57-0.92). This fraction is considered to be organic

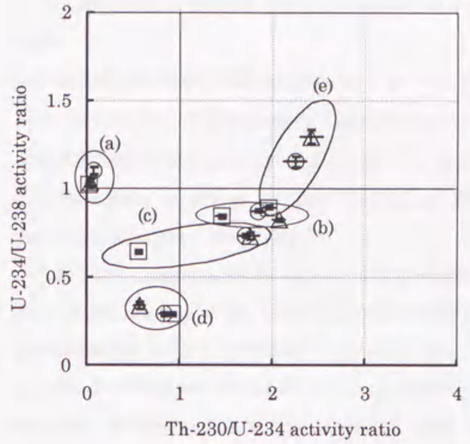

Fig.3-4-10 Correlation between U-234/U-238 and Th-230/U-234 activity ratios in fractions by selective chemical leaching method.
△: 500 μ m< ϕ <1mm,
○: 125 μ m< ϕ <250 μ m
□: ϕ <63 μ m
(a) AcONa soluble fraction
(b) AcONa-AcOH soluble fraction
(c) $NH_2OH \cdot HCl$ soluble fraction
(d) H_2O_2 soluble fraction
(e) residue fraction

or sulfide complex phase, so that the U was enriched without the Th and continued to elute. As U was observed to be enriched in the surface of pyrites, it is supposed that some pyrites may help the secondary mineralization of U in modern times. Supposing that the initial Th-230 was absent and grew up from U-234, then the age of U fixation on pyrite surface is calculated to be 9-27 x10^4 y at the longest.

3.4.5. Conclusion

Uranium series nuclides in the granitic conglomerate in the Tono uranium mine, Gifu prefecture, central Japan, were determined by a selective chemical leaching technique, and the uranium migration behavior through geological media was studied microscopically.

The bulk contents of U and Th in fine-grained sample are larger than those of coarse-grained ones, and have positive correlation with the abundance of biotite. A large amount of U leached in sodium acetate/ acetic acid (pH 5.0) soluble, and hydroxylamine hydrochloride soluble fractions. It is inferred that carbonate minerals and iron oxides play an important role in U ore genesis. The total amount of U eluted by the leaching reagents was more than half. The percentage of the leached U of fine-grained sample is less than that of coarse-grained ones, suggesting that the U concentration in the residue of the fine-grained sample is much higher than expected from the soluble fractions that may correlate with the surface area. The adsorption density tends to increase with decreasing grain size, which suggests that the fine U minerals are abundant and/or the

U concentration around the complexing site of iron oxyhydroxides may have become high.

The bulk U-234/U-238 activity ratio is 0.95±0.05, and the bulk Th-230/U-234 activity ratio is 1.36±0.06. For most of the sieved samples, U-234/U-238 activity ratios are < 1, and Th-230/U-234 activity ratios are > 1, showing that U moved from the sediments. The uranium nuclides in the matrix of conglomelate are inferred to be not in equilibrium within 300,000 y.

The ion exchangeable U, whose U-234/U-238 activity ratio was > 1, is bound weakly and exchangeable with U in the surrounding water such as interstitial water and groundwater with U-234/U-238 activity ratio > 1. The U-234/U-238 activity ratios of residue fraction are less than 1 (fine-grained sample) and larger than 1 (coarse-grained sample), indicating that the injection effect is advantageous for the coarse-grained sample while the ejection effect is advantageous for the fine-grained sample. The U-234/U-238 activity ratios of other fractions are less than 1, which is like the bulk ratio. The ratio decreases in the order of carbonate > iron oxide > organic/sulfide fractions.

The Th-230/U-234 activity ratios is very low in ion exchangeable fraction and > 1 in carbonate, iron oxide and residue fractions. For residue fraction, U-234/U-238 > 1 and Th-230/U-234 > 1 indicate the elution of U and enrichment of U-234 relative to U-238 by alpha recoil injection. The organic/sulfide complex fraction is depleted in Th-230 compared to U-234 and U-238. It suggests that U was secondarily enriched without Th and continued to elute. As U was enriched at the surface of pyrites, it is supposed that pyrites adsorbed a portion of the eluted U and helped the secondary fixation of U in modern times.

3.5 Radioisotopes in core sediment and determination of sedimentation rate

3.5.1 Introduction

Sediment, which is deposited year by year, records the geochemical and geological events. So it is very important to date the sediment. Radionuclide, which decays at a constant rate, provides a good clock. Table 3-5-1 is a list of nuclides used for dating of various geological materials.

Lead-210 is used for a calculation of accumulation rate of sediment younger than one hundred years. It is produced from Rn-222 through Po-218, Pb-214, Bi-214 and Po-214 whose half-life is short. As Rn-222, decay product of Ra-226 that exists in the ground, is gaseous, it goes out from the surface of earth into the atmosphere. In the air, its descendants including Pb-210 are scavenged by the aerosols and particles, and falls down on the surface of earth. The particles with excess Pb-210 are accumulated with detritus on the bottom sediments of ponds, lakes and sea, and the excess Pb-210 decays with its own half-life (22.3 y). Therefore, the activity of excess Pb-210 in sediment decreases with the depth of sediment. The outline is shown in Fig.3-5-1.

Table 3-5-1 Radionuclides used for dating of various geological materials. Time range of dating depends on half-life of nuclide used.

methods	samples	half-life
<disintegration and grow-up>		
^{238}U-^{206}Pb method	igneous rocks (volcanic rock, plutonic rock),	4.47E+09 y
^{232}Th-^{208}Pb method	sedimentary rocks (limestone), meteorites, moon stone, ·····	1.41E+10 y
^{235}U-^{207}Pb method	galena, pitchblende, U-containing minerals,	7.04E+08 y
Pb-Pb method	zircon, monazite, xenotime, epidote, allanite, ·····	7.04E+08 y
^{238}U-^{230}Th method	igneous rocks, magma generation, volcanic products (volcanic glass),	7.52E+04 y
^{234}U-^{230}Th method	zircon, apatite, plagioclase, pyroxene, magnetite, limestone, coral, ····	7.52E+04 y
^{235}U-^{231}Pa method	Mn nodule, foraminifers, hydrothermal deposit, marine phosphorite, phosphate, sulfate, stalactite, calcareous sinter, ·····	3.28E+04 y
<disintegration of excess nuclide>		
excess ^{234}U	natural water, sedimentation rate of sea floor	2.45E+05 y
excess ^{230}Th	sedimentation rate of sea floor, coral, Mn nodule, ·····	7.52E+04 y
excess $^{230}Th/^{232}Th$		7.52E+04 y
excess ^{231}Pa		3.28E+04 y
excess ^{210}Pb	sedimentation rate of lake, sea floor, soil, glacier, ·····	22.3 y
excess ^{234}Th	tracer of marine suspended matter	24.1 d
excess ^{228}Th		1.9 y
excess ^{210}Po		138 d

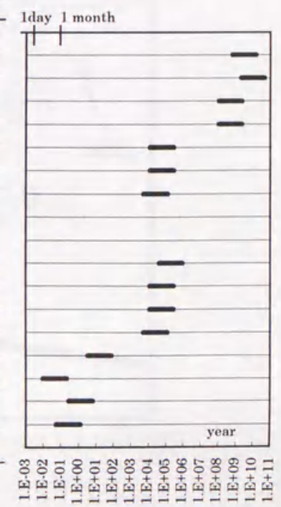

The activity of "excess Pb-210" is obtained by subtracting "supported Pb-210" (produced within the particles) from "total Pb-210" activity. Assuming that the flux of excess Pb-210 (F) and the rate of sedimentation (w) are constant through the depth of core (x), the activity of excess Pb-210 (A) is expressed as follows.

$A=A_0 \cdot \exp(-\lambda x/w)$, $t=x/w$, $\lambda=0.031$ (y^{-1})

Therefore, the logarithmic plot of A versus x becomes linear, with a slope of $-\lambda/w$ and w is obtained.

On the other hand, Cs-137, artificial nuclide produced mainly by the atmospheric testing of nuclear weapons, has been spread worldwide. The profile of annual fall-out is well known to be first detected in 1954 and become maximum in 1963 (Peirson, 1971; Katsuragi, 1983; Katsuragi and Aoyama, 1986). The activity profile in the sediment core is also expected to be the same as that of annual fall-out. Therefore, the average accumulation rate is calculated from the core depth of Cs-137 peak assigned as 1963.

In this study, the sedimentation rates of Lake Suwa, Lake Shinji, river mouth of Shinano River (off Niigata), two lakes in China and two lakes in Nepal were studied by using Pb-210 and Cs-137 radionuclides. The results of Lake Shinji are written in detail in this section.

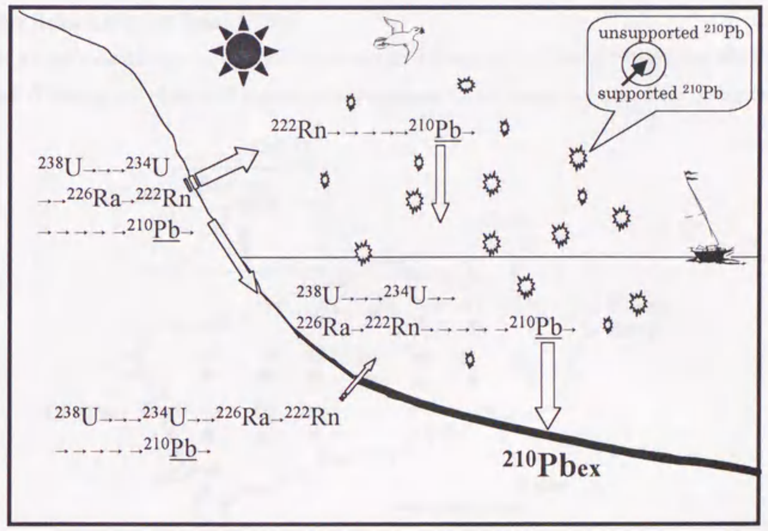

Fig.3-5-1 Outline of method for Pb-210 dating.

3.5.2 Sampling locations and analytical method

Fifteen bottom core samples were obtained from Lake Shinji, Shimane Prefecture on October in 1994 using bottom sampler. The sampling locations are 2 km intervals as shown in Fig.3-5-2. Lake Shinji is surrounded by volcanic and sedimentary rocks of Miocene, and the Chugoku Mountains are composed of Cretaceous - Paleogene granite. The Hii River run into the west of Lake Shinji, and the Ohashi River flows out from the east of the lake and into the Lake Nakaumi, which connect to the Japan Sea through Sakai-Suido.

The core samples are divided by 1cm intervals, dried and pulverized. Four grams of powdered sample is taken in a tube with a cap and sealed for one month. Then, the activities of Pb-210 (peak energy: 46.5 keV), Pb-214 (352 keV), Cs-137 (661.6 keV) and K-40 (1461 keV) are measured by gamma-ray spectrometry. The peak intensities are corrected by sample arrangement (Kanai, 1993a). The activity of excess Pb-210 is calculated by subtracting that of Pb-214 from that of Pb-210, as it is assumed that the supported Pb-210 is in equilibrium with Ra-226 and Pb-214.

3.5.3 Results and discussions

Sedimentation rates in Lake Shinji

The variations of excess Pb-210 activities in 15 stations of Lake Shinji are shown in Fig.3-5-3. Some are observed logarithmic decrease, while some are not. The latter core

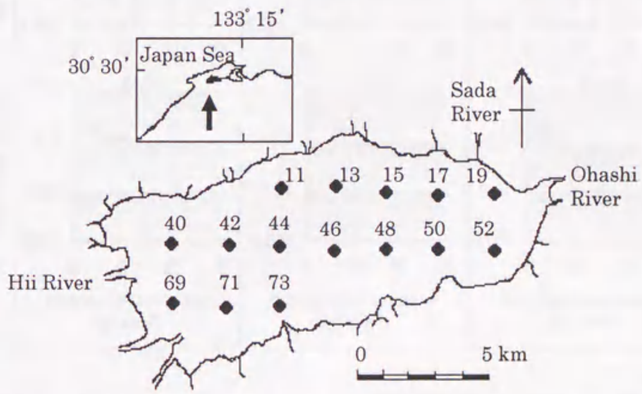

Fig.3-5-2 Sampling locations in Lake Shinji, Shimane Prefecture.

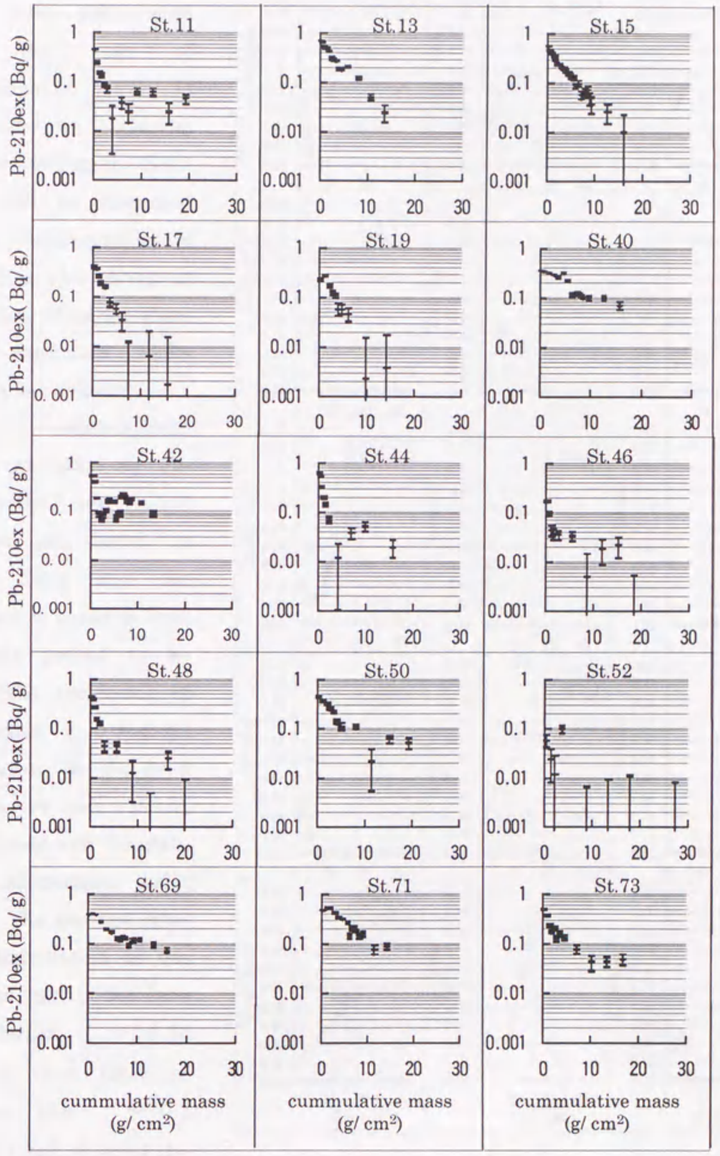

Fig.3-5-3 Variation of excess Pb-210 activities in 15 stations of Lake Shinji, Shimane Prefecture.

samples may be suffered from some disturbance and the rate of sedimentation is calculated by excluding surface sediment. Such case will be discussed later. Depth profiles of Cs-137 is also shown in Fig.3-5-4. Most of them have maximum peaks while some do not.

The sedimentation rates calculated by Pb-210 method and Cs-137 method are listed in Table 3-5-2 and the correlation between both methods proved to be good (the coefficient of correlation is 0.96-0.97) as shown in Fig.3-5-5 (Kanai *et al.*, 1998b; Mitsunashi and Tokuoka, 1988; Matsumoto, 1975; 1987). The average rates of sedimentation at the western part of the lake are larger (～ 0.25 g/cm^2/y) than those of eastern part (～ 0.1 g/cm^2/y) and those of the central part are the lowest (≦0.05 g/cm^2/y).

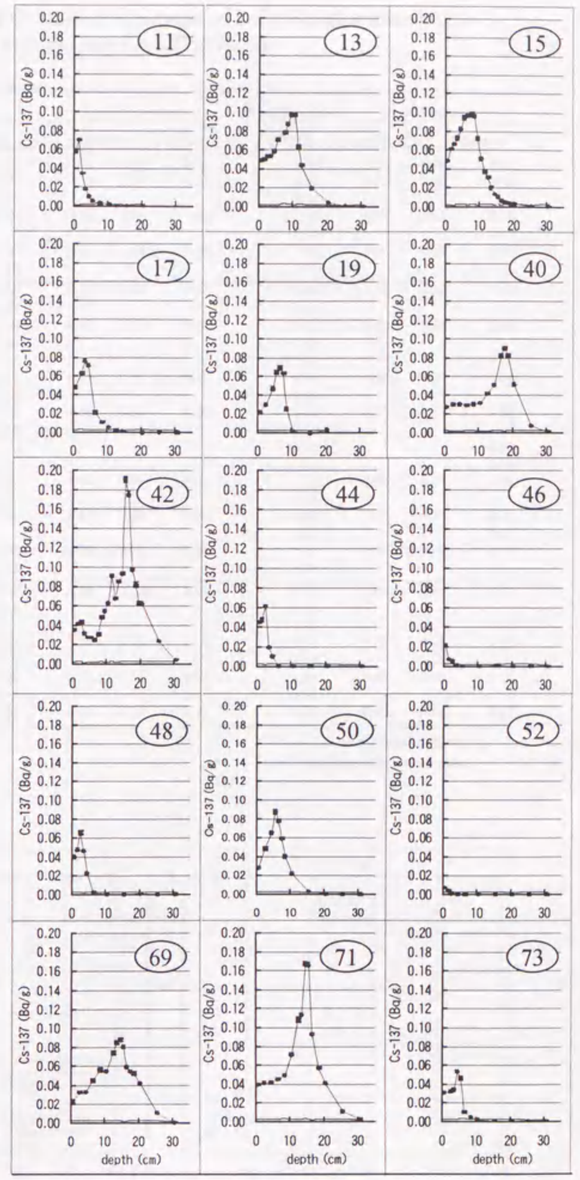

Fig.3-5-4 Variation of Cs-137 activities in 15 stations of Lake Shinji, Shimane Prefecture.

Table 3-5-2 Average sedimentation rates in Lake Shinji estimated by Pb-210 method and Cs-137 method.

location	sed.rate	Pb-210 method #	Pb-210 method cm/y	Cs-137 method range(cm/y)	Cs-137 method average	Pb-210 method g/cm²/y	Cs-137 method range(g/cm²/y)	Cs-137 method average
	40	0-30cm	0.50	0.55 - 0.58	0.56	0.26	0.24 - 0.26	0.25
	69	0-30cm	0.51	0.42 - 0.48	0.45	0.28	0.20 - 0.24	0.22
		3-17cm	0.30			0.16		
western	42		ND	0.48 - 0.55	0.52	ND	0.17 - 0.20	0.18
	SJ85-5 *					0.17		0.17
	71	0-30cm	0.44	0.45 - 0.52	0.48	0.20	0.20 - 0.23	0.21
		2-30cm	0.42			0.19		
	11	0-3cm	0.06	0.03 - 0.07	0.05	0.03	0.01 - 0.03	0.02
		0-8cm	0.07			0.04		
	44	0-5cm	0.08	0.06 - 0.10	0.08	0.02	0.02 - 0.03	0.02
		0-10cm	0.08			0.03		
	SJ85-13 *					0.11		0.06
	73	0-7cm	0.14	0.13 - 0.16	0.15	0.06	0.05 - 0.07	0.06
		0-20cm	0.29			0.14		
	13	0-13cm	0.28	0.29 - 0.36	0.32	0.10	0.10 - 0.12	0.11
central		0-30cm	0.30			0.13		
	SJ85-9 *					0.12		0.09
	SJ85-3 *					0.10		0.08
	46	0-3cm	0.05	0.00 - 0.03	0.02	0.02	0.00 - 0.01	0.01
		0-4cm	0.06			0.03		
	15	0-30cm	0.24	0.16 - 0.29	0.23	0.12	0.05 - 0.10	0.07
	SJ85-1 *					0.09		0.07
	48	0-7cm	0.08	0.06 - 0.10	0.08	0.04	0.02 - 0.04	0.03
		0-15cm	0.13			0.08		
	17	0-30cm	0.14	0.10 - 0.13	0.11	0.09	0.03 - 0.04	0.04
		0-13cm	0.15			0.07		
	SJ85-7 *					0.05		0.02
	50	0-10cm	0.23	0.16 - 0.19	0.18	0.11	0.07 - 0.08	0.08
eastern		0-20cm	0.22			0.13		
	19	0-20cm	0.12	0.19 - 0.23	0.21	0.09	0.10 - 0.12	0.11
		2-10cm	0.13			0.08		
	52	0-3cm	0.04	0.00 - 0.03	0.02	0.03	0.00 - 0.03	0.01

* : Mitsunashi and Tokuoka (1988)
\# : core length used for calculation
ND : not determined

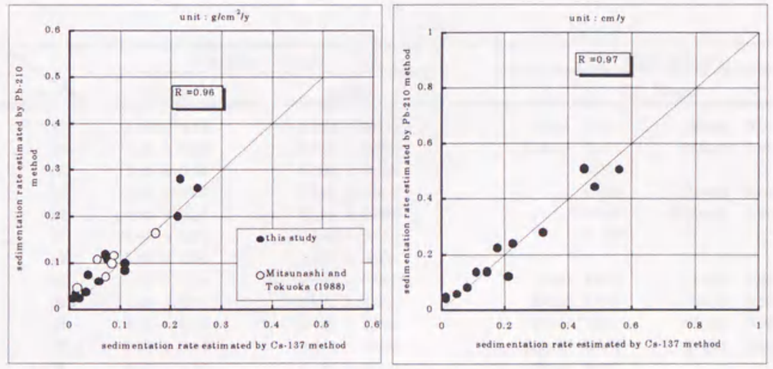

Fig.3-5-5 Correlation between sedimentation rate estimated by Pb-210 method and that by Cs-137 method in Lake Shinji, Shimane Prefecture.

Inventories of radionuclides

The inventories of excess Pb-210 and Cs-137, which indicate the total accumulated input activities, are shown in Table 3-5-3. The tendency of their distributions in the lake is the same as the rates of sedimentation. It is considered that the detritus is conveyed from the Hii River that locates at the west of the lake, and deposits near the mouth of river. The coefficient of correlation between both inventories is 0.78, which suggests that both nuclides behave likely together, probably adsorbed at a constant ratio by suspended particles. It is of interest that both nuclides behave likely together although their sources are different.

Figure 3-5-6 shows the correlation between excess Pb-210 inventories and Cs-137 inventories in Lake Shinji as well as in Lake Suwa (Kanai *et al.*, 1995; 1997), in Lake Nakaumi, in Chinese lakes (Kanai *et al.*, 1998c), in Nepal lakes (Kanai *et al.*, 2000) and in Japan Sea (Kanai and Ikehara, 1995; Suzuki, 1993). It is indicated that the trend in Lake Shinji is the same as those in Lake Suwa and Nepal lakes. It is also shown that the slope of regression curve in Japan Sea is smaller, *i.e.* excess Pb-210 is relatively more abundant in offshore sediment. The trend in Lake Nakaumi is middle among them. These characteristics are probably because Cs-137 fallout is accumulated in inland lakes whereas it is dispersed in open sea. Most of Cs-137 retains in seawater in western Pacific Ocean and only 1-5% is deposited (Nagaya and Nakamura, 1987). On the other

Table 3-5-3 Inventories of excess Pb-210 and Cs-137, and fluxes of excess Pb-210 in Lake Shinji, Shimane Prefecture.

St No.	Inventory (Bq/cm²)		Flux (Bq/cm²/y)			
	Pb-210	Cs-137	Pb-210			
11	1.23 ± 0.06	0.094 ± 0.002	(3cm)	0.014	(8cm)	0.018
13	2.44 ± 0.03	0.304 ± 0.002	(13cm)	0.072	(30cm)	0.084
15	1.86 ± 0.06	0.388 ± 0.003		0.054		
17	0.99 ± 0.07	0.123 ± 0.002		0.032	(13cm)	0.031
19	0.92 ± 0.07	0.194 ± 0.003		0.026	(2-10cm)	0.030
40	2.69 ± 0.04	0.549 ± 0.003		0.094		
42	2.16 ± 0.06	0.676 ± 0.001				
44	1.07 ± 0.06	0.057 ± 0.001	(5cm)	0.018	(10cm)	0.020
46	0.48 ± 0.05	0.021 ± 0.001	(3cm)	0.005	(4cm)	0.006
48	0.91 ± 0.06	0.116 ± 0.002	(7cm)	0.021	(15cm)	0.026
50	2.25 ± 0.08	0.204 ± 0.002	(10cm)	0.053	(20cm)	0.058
52	0.23 ± 0.03	0.012 ± 0.002	(3cm)	0.003		
69	2.63 ± 0.04	0.669 ± 0.003		0.092	(3-17cm)	0.073
71	3.40 ± 0.06	0.447 ± 0.003		0.115	(2-30cm)	0.116
73	1.81 ± 0.07	0.093 ± 0.014	(7cm)	0.032	(20cm)	0.050

( ) : core length used for calculation

hand, Ra-226 concentration in seawater is higher than in river water (Elsinger and Moore, 1983; More and Scott, 1986) and the removal efficiency at seashore is said to be high (Bacon *et al.*, 1976).

The surface sediment is the newest deposit and considered to show the present style of deposition. The excess Pb-210 and Cs-137 concentrations in the surface sediments within the lake showed a good correlation as shown in Fig.3-5-7. The coefficient of correlation is 0.76, which suggests that both nuclides are adsorbed in the surface particles at a constant ratio. Furthermore, Fig.3-5-8 shows the correlation between sand content and radioactivities of excess Pb-210 and Cs-137. The tendency is observed that the higher the sand content becomes, the lower the radioactivities become.

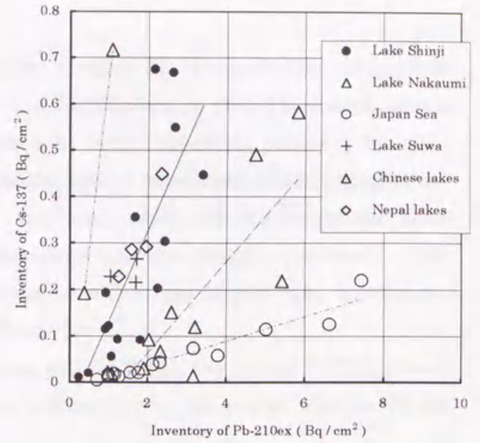

Fig.3-5-6 Correlation between inventories of excess Pb-210 and Cs-137 in sediments from Lake Shinji, Lake Suwa, Chinese lakes, Nepal lakes and Japan Sea.

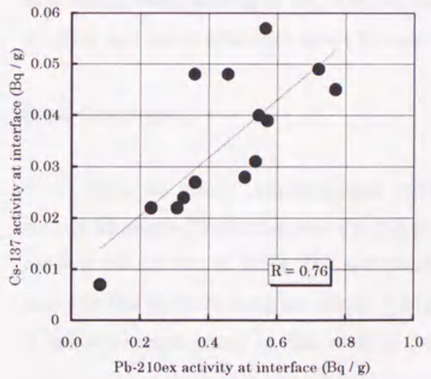

Fig.3-5-7 Correlation between excess Pb-210 activity and Cs-137 activity in surface sediment in Lake Shinji.

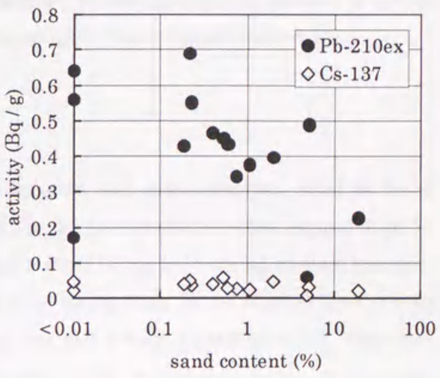

Fig.3-5-8 Correlation between sand content and activities of excess Pb-210 and Cs-137 in surface sediment in Lake Shinji.

Mixing and bioturbation

As was observed in Fig.3-5-3, some profiles of excess Pb-210 showed non-exponential change. In such case, mixing of sediment or bioturbation is probable. Distribution of excess Pb-210 is approximately expressed as some equations proposed by many researchers (for example, Goldberg and Koide, 1962; Christensen, 1982;Edgington and Robbins, 1976; Nozaki *et al.*, 1977;Officer and Lynch, 1982). One is a Berger and Heath model that expresses complete mixing of surface sediment (Berger and Heath, 1968). This is in the case of fast mixing rate compared with sedimentation rate. Another is a model that is expressed by diffusion coefficient D.

As fast mixing rate is expected in the case of Lake Shinji, the Berger & Heath model is applied. Supposing the complete mixing till depth of d, the profile of excess Pb-210 activity becomes as follows:

$X \leqq d \quad A(x) = F/(w+\lambda \cdot d)$

$X \geqq d \quad A(x) = F/(w+\lambda \cdot d) \cdot \exp(-\lambda /w \cdot (x-d))$

From the equation, the slope of logarithm of excess Pb-210 vs. depth at depth deeper than d becomes the same as that of non-mixing model. Therefore the rate of sedimentation is calculated by the same way of non-mixing model. Some results are obtained in Table 3-5-2.

In case of diffusion type mixing, the profiles of logarithm of excess Pb-210 sometimes become linear although the result is more complicated. Therefore, whether the sediment is suffered from mixing or not, cannot be decided by the logarithmic profiles of excess Pb-210, and much attention must be paid to calculate the sedimentation rates.

3.5.3 Conclusion

In order to study sedimentation environments and sedimentation rates in Lake Shinji, Shimane Prefecture, the Pb-210 and Cs-137 radioactivities were measured in 15 cores taken on Oct. in 1994. The sedimentation rates in the lake varied at each location; those in the western area are about 0.25g/cm^2/y, larger than in the eastern area (about 0.1g/cm^2/y), and those in the central area are the lowest ($\leqq$0.05g/cm^2/y). This fact indicates that most of the sediments supplied by the Hii River deposited in the western area and little amount was transported to the central area. The inventories of excess Pb-210 and Cs-137 that indicate the amount of accumulation were larger in the western area, which is the same tendency as the sedimentation rate. They are in a positive

correlation (correlation coefficient (R) is 0.78), and their relationships are different from that observed in offshore sediments of Japan sea, in Lake Nakaumi, and several lakes in China. The concentrations of excess Pb-210 and Cs-137 in surface sediments are in a good correlation (R=0.76), which indicates that both nuclides in sediment grains may exist in a constant ratio. The bioturbation and mixing of sediment changes the profile of radionuclides in sediment. Some sedimentation rates were obtained using Berger and Heath model that assumes complete mixing of surface sediment.

Chapter 4 Conclusion

In this dissertation, I elucidated the geochemical behavior of natural radioactive uranium series nuclides. As these nuclides exist everywhere in nature, they are very useful tracers for geochemical and geological events. Several useful applications of them to sedimentology were shown.

At first, the geochemical behavior of uranium, radium and radon in the Masutomi spring district, Yamanashi Prefecture, central Japan, were studied. This is a case study on water-rock interaction and water geochemistry. The results of the first section correspond with many studies at other locations such as groundwater geochemistry at the Tono uranium mine. The uranium concentrations in the Masutomi spring waters range from 0.01 to 2.07 ppb (average 0.27 ppb). The U-234/U-238 activity ratios (ARs) in the spring waters range from 0.98 to 2.42, and show an inverse correlation with the U-238 concentrations. As the waters are reductive because their redox potentials were low, this fact may be the reason for the low uranium concentrations. Alpha recoil dissolution of Th-234 explains the inverse correlation of ARs with U-238. Radioactive disequilibria are also observed in Ra-226/U-238, Rn-222/U-238, and Rn-222/Ra-226 ratios. Highly exceeded radon is attributed to both the source granite rocks and the Ra-226 rich precipitates near the surface. On the other hand, the behavior of Ra-226 as well as other general ions such as sodium is explained by mixing or dilution of deep water with surface waters. In this way, a part of the water-rock system is elucidated.

Secondly, the concentrations of uranium and other elements in bauxite deposits at Yangwa mine in China were determined, and geochemical behavior of uranium isotopes and sedimentation process were studied. In this section, uranium contents were determined not only in bulk but also in fraction obtained by chemical leaching method. Two major components of the bauxite samples, Al_2O_3 and Fe_2O_3, had an inverse correlation, and U as well as Ti, Cr and V had a strong correlation with Al_2O_3. Most of U in the bauxite is in the silicate fraction (18-75 %). 20-36 % of the U was in "resistate fraction". The ARs of those fractions were less than unity, and have a good correlation with the fractional U content. It is revealed that U-234 was depleted from the surface of the mineral grain. On the other hand, the activity ratios of HCl soluble U were more than unity, have an inverse correlation with the fractional U content. This suggests that almost constant amount of mobile U-234 was present in the ore deposits. The bauxite ore deposit is thought to be sedimentary in origin, and its formation process is

estimated as follows. It was at first formed as a terra rossa deposit on the karstic Ordovician limestone. The deposit was rich in Fe_2O_3 under relatively oxidative condition. Afterwards, the weathered materials of Pre-Cambrian basement were transported and deposited repeatedly. The deposition condition became reducing, favoring for the concentration of U. The clay minerals such as kaolinite changed reversibly to gibbsite and diaspore, depending on the H_4SiO_4 concentration. Th-234 was ejected from the surface of U-containing mineral grain and was adsorbed as HCl soluble form in the ore deposits.

Uranium has two major oxidation states; tetravalent and hexavalent. Thirdly the study on oxidation states is conducted. As a case study, the diagenetic behavior of uranium(IV, VI) in sedimentary rocks associated with apatite deposits at Nakamaruke, central Japan, was studied to examine the process of redistribution of uranium under the mild climate of the temperate zone. Uranium content (4-89 ppm) in the strata showed two peaks, the most prominent one at the phosphatic layer and another small one at the lower part of the outcrop, which suggests some amount of uranium has vertically migrated through the strata. The ARs of total U were < 1 in the phosphatic layer, and > 1 in the lower part (>0.3 m away from the phosphatic layer) of the outcrop. "U(IV)", "U(VI)" and "residue" fractions were obtained. About 50 % of total U was in "U(VI) fraction". The ARs of "U(VI) fraction" were > 1 in all the samples, so hexavalent U (U(VI)) is inferred to be bound relatively weakly and move easily. The ARs of "U(IV) fraction" and "residue fraction" showed the same trend as total U. The ARs of the "residue fraction" composed of silicate and clay minerals suggest that some uranium moved and was adsorbed by phyllosilicates.

Next a selective chemical leaching technique was applied to the samples for the detailed study. Uranium series nuclides in the granitic conglomerate from the Tono uranium mine, central Japan, were determined, and the uranium migration behavior through geological media was studied microscopically. The bulk contents of U and Th in fine-grained sample are larger than those of coarse-grained ones, and have positive correlation with the abundance of biotite. A large amount of U leached in sodium acetate/ acetic acid (pH 5.0) soluble, and hydroxylamine hydrochloride soluble fractions. It is inferred that carbonate minerals and iron oxides play an important role in U ore genesis. More than half of U was eluted by the leaching process. The percentage of the leached U of fine-grained sample is less than that of coarse-grained ones, suggesting that the U concentration in the residue of the fine-grained sample is much higher than expected from the soluble fractions that may correlate with the surface area. The

adsorption density tends to increase with decreasing grain size, which suggests that the fine U minerals are abundant and/or the U concentration around the complexing site of iron oxyhydroxides may have become high. The bulk AR is 0.95±0.05, and the bulk Th-230/U-234 activity ratio is 1.36±0.06. For most of the sieved samples, ARs are < 1, and Th-230/U-234 activity ratios are > 1, showing that U moved from the sediments. The uranium nuclides in the matrix of conglomelate are inferred to be not in equilibrium within 300,000 y. The ion exchangeable U, whose AR was > 1, is bound weakly and exchangeable with U in the surrounding water such as interstitial water and groundwater with AR > 1. The ARs of residue fraction are less than 1 (fine-grained sample) and larger than 1 (coarse-grained sample), indicating that the injection effect is advantageous for the coarse-grained sample while the ejection effect is advantageous for the fine-grained sample. The ARs of other fractions are less than 1, which is like the bulk ratio. The ratio decreases in the order of carbonate > iron oxide > organic/sulfide fractions. The Th-230/U-234 activity ratios is very low in ion exchangeable fraction and > 1 in carbonate, iron oxide and residue fractions. For residue fraction, AR > 1 and Th-230/U-234 > 1 indicate the elution of U and enrichment of U-234 relative to U-238 by alpha recoil injection. The organic/sulfide complex fraction is depleted in Th-230 compared to U-234 and U-238. It suggests that U was secondarily enriched without Th and continued to elute. As U was enriched at the surface of pyrites, it is supposed that pyrites adsorbed a portion of the eluted U and helped the secondary fixation of U in modern times.

Finally I applied the radionuclides to the dating of sediments because they have their own clocks. The dating of geological events is very important, so the dating of sediments younger than a hundred years is conducted using natural and artificial radionuclides such as Pb-210 and Cs-137. In this section, the sedimentation rates and sedimentary environment in Lake Shinji, Shimane Prefecture, are studied and several cautions for application are elucidated. The sedimentation rates in the lake varied at each location; those in the western area are about 0.25g/cm^2/y, larger than in the eastern area (about 0.1g/cm^2/y), and those in the central area are the lowest (≦0.05g/cm^2/y). This fact indicates that most of the sediments supplied by the Hii River deposited in the western area and little amount was transported to the central area. The inventories of excess Pb-210 and Cs-137 that indicate the amount of accumulation were larger in the western area, which is the same tendency as the sedimentation rate. They are in a positive correlation (correlation coefficient (R) is 0.78), and their relationships are different from

those observed in offshore sediments of Japan Sea, in Lake Nakaumi, and several lakes in China. The concentrations of excess Pb-210 and Cs-137 in surface sediments are in a good correlation (R=0.76), which indicates that both nuclides in sediment grains may exist in a constant ratio. While the bioturbation and mixing of sediment change the profile of radionuclides in the sediment core, some sedimentation rates are obtained using Berger and Heath model that assumes complete mixing of surface sediment.

Acknowledgements

Most of the studies were conducted during my works in the Geological Survey of Japan (GSJ). All of the co-workers in GSJ are much acknowledged for their help and support. I would like to thank many anonymous reviewers for constructive comments and improving the manuscripts for the submitted papers. I acknowledge much to Drs. Tominaga, T., Makide, Y. (the University of Tokyo), Matsuhisa, Y., Togashi, S., Imai, N., Terashima, S., Mita, N., Sakata, S., Okai,T. (GSJ), Sakamoto, T., Shibata, K. (Nagoya University), Ando, A., Sakamaki, Y. and Fujinuki, T. who gave me encouragement and much precious advice. I wish to acknowledge with thank Dr. Tanaka, T. (Nagoya University) for warm guidance and support. And I also want to thank my family for supporting me.

References

Adams,J.A.S. and Richardson,K.A. (1960) Thorium, uranium and zirconium concentrations in bauxite. *Econ. Geol.,* **55**, 1653-1675.

Altschuler,Z.S., Clarke,R.S.,Jr. and Young,E.J. (1958) The geochemistry of uranium in apatite and phosphorite. *U. S. Geol. Sur. Prof. Paper*, **314-D**, 45-90.

Anderson,R.F. (1984) A method for determining the oxidation state of uranium in natural waters. *Nucl.Instrum.Methods in Physics Research,* **223**, 213-217.

Andrews,J.N. and Kay,R.L.F. (1983) The U contents and $^{234}U/^{238}U$ activity ratios of dissolved uranium in groundwaters from some Triassic sandstones in England. *Isotope Geoscience,* **1**, 101-117.

Bacon,M.P., Spencer,D.W. and Brewer,P.G. (1976) $^{210}Pb/^{226}Ra$ and $^{210}Po/^{210}Pb$ disequilibria in sea water and suspended particulate matter. *Earth Planet. Sci. Lett.,* **32**, 277-296.

Balistrieri,L.S. and Murray,J.W. (1982) The adsorption of Cu, Pb, Zn, and Cd on goethite from major ion seawater. *Geochim. Cosmochim. Acta,* **46**, 1253-1265.

Balistrieri,L.S. and Murray,J.W. (1983) Metal-solid interactions in the marine environment: estimating apparent equilibrium binding constants. *Geochim. Cosmochim. Acta,* **47**, 1091-1098.

Bardossy,Gy., Boni,M., Dall'Aglio,M., D'Argenio,B. and Panto,Gy. (1977) Bauxites of peninsular Italy: composition, origin and geotectonic significance. Monograph series on Mineral Deposits (No. 15). Gebruder Borntraeger, Berlin-Stuttgart, 61 p.

Barretto,P.M.C., Clark,R.B. and Adams,J.A.S. (1972) Physical characteristics of radon-222 emanation from rocks, soils and minerals; its relation to temperature and alpha dose. In The Natural Radation Environment II (Adams,J.A.S., Lowder,W.M., and Gesell,T.F. ed.), 731-740.

Berger,W.H. and Heath,G.R. (1968) Vertical mixing in pelagic sediments. *J.Mar. Res.,* **26**, 134-143.

Brookins,D.G. (1984) Geochemical aspects of radioactive waste disposal. Springer-Verlag, New York, 1-8.

Burnett,W.C. and Deetae,S. (1987) Distribution of natural decay-series radionuclides within a phosphate rock weathering sequence in Florida. In Proc. Sympos. on Natural Radiation and Technologically Enhanced Natural Radiation in Florida

(ed. W. Propetzio), pp. 17-37. Health Physics Society.

Burnett,W.C. and Veeh,H.H. (1977) Uranium-series disequilibrium studies in phosphorite nodules from the west coast of the South America. *Geochim. Cosmochim. Acta,* **41**, 755-764.

Chapman,N.A. and Smellie,J.A.T. (1986) Natural analogues to the conditions around a final repository for high-level radioactive waste. *Chem. Geol.,* **55**, 167-173.

Chen,J.H., Edwards,R.L. and Wasserburg,G.J. (1986) ^{238}U, ^{234}U and ^{232}Th in seawater. *Earth Planet. Sci. Lett.*, **80**, 241-251.

Chen,C.H., Liu,K.K. and Shieh,Y.N. (1988) Geochemical and isotopic studies of bauxitization in the Tatun volcanic area, Northern Taiwan. *Chem. Geol,* **68**, 41-56.

Christensen,E.R. (1982) A model for radionuclides in sediments influenced by mixing and compaction. *J. Geophy. Res.*, **87**, 566-572.

Clarke,R.S.,Jr. and Altschuler,Z.S. (1958) Determination of the oxidation state of uranium in apatite and phosphorite deposits. *Geochim. Cosmochim. Acta,* **13**, 127-142.

Comer,J.B. (1974) Genesis of Jamaican bauxite. *Econ. Geol.,* **69**, 1251-1264.

Edgington,D.N. and Robbins,J.A. (1976) Records of lead deposition in Lake Michigan sediments since 1800. *Environ. Sci. Technol.*, **10**, 266-274.

Elsinger,R.J. and Moore,W.S. (1983) ^{224}Ra, ^{228}Ra, and ^{226}Ra in Winyah Bay and Delaware Bay. *Earth Planet. Sci. Lett.,* **64**, 430-436.

Eyal,Y. and Fleischer,R.L. (1985) Preferential leaching and the age of radiation damage from alpha decay in minerals. *Geochim. Cosmochim. Acta,* **49**, 1155-1164.

Eyal,Y. and Olander,D.R. (1990) Leaching of uranium and thorium from monazite: I. Initial leaching. *Geochim. Cosmochim. Acta*, **54**, 1867-1877.

Finnegan,D.L. and Bryant,E.A. (1987) Methods for obtaining sorption data from uranium-series disequilibria. Los Alamos Nat. Lab., LA-11162-MS UC-70, 1-21.

Fleischer,R.L. (1980) Isotopic disequilibrium of uranium: alpha-recoil damage and preferential solution effects. *Science,* **207**, 979-981.

Fleischer,R.L. (1982) Alpha-recoil damage and solution effects in minerals: uranium isotopic disequilibrium and radon release. *Geochim. Cosmochim. Acta,* **46**, 2191-2201.

Fujimoto,U.,Shibata,H., Yoshitake,H. and Oki,Y. (1958) Geology of the neighbourhood of Mt. Kogarasu, Yamanashi Prefecture, with special reference to plutonic rocks. *Jour. Geol. Soc. Japan,* **64**, 250-257 (in Japanese).

Giresse,P., N'Landou,J.D. and Wiber,M. (1986) The conditions for uranium

concentration in the phosphates of Tchivoula, Congo. *Uranium,* **2**, 287-300.

Goldberg,E.D. and Koide,M.(1962) Geochronological studies of deep-sea sediments by the ionium / thorium method. *Geochim. Cosmochim. Acta*, **26**, 417-445.

Gorden,M. and Murata,K.J. (1952) Minor elements in Arkansas bauxite. *Econ. Geol.*, **47**, 169-179.

Hamachi,T. and Obi,I. (1969) Uraniferous phosphorite at Nakamaruke area, Sekigawa-mura, Iwafune-gun, Niigata Prefecture. *Geol. Sur. Japan Report,* **232**, 595-601 (in Japanese, with English abstract).

Hashimoto,T., Aoyagi,Y., Kudo,H. and Sotobayashi,T. (1985) Range calculation of alpha-recoil atoms in some minerals using LSS-theory. *J.Radioanal. Nucl. Chem.*, **90/2**, 415-438.

Horiuchi,K. and Murakami,Y. (1978) A new explanation on the presence of excessive amount of radon in mineral spring by the delta Rn term calculated from the amounts of radium and radon. *Chikyukagaku(Geochemistry),* **12**, 59-70 (in Japanese, with English abstract).

Hotz,P.E. (1964) Nickeliferous laterites in southwestern Oregon and northwestern California. *Econ. Geol.*, **59**, 355-396

Imai,N. (1986) Multielement determination of rocks by inductively coupled plasma emission spectrometry. *Bull. Geol. Surv. Japan,* **37**, 515-523 (in Japanese, with English abstract).

Itakura,T. (1968) Radiochemical Studies on some micro-components of mineral spring water and sinter deposit in Ishikawa Prefecture. *J. Soc. Eng. Mineral Springs, Japan,* **5**, 41-45 (in Japanese, with English abstract).

Ivanovich,M. and Harmon,R.S. (1982) Uranium series disequilibrium: application to environmental problems. Clarendon Press, Oxford, 571.

Ivanovich,M. and Harmon,R.S. (1992) Uranium-series disequilibrium: application to earth, marine, and environmental sciences, Oxford, Clarendon Press.

Iwasaki,I (1968) Distribution of radium and mechanism of strongly radioactive spring. *J. Soc. Eng. Mineral Springs, Japan,* **6**, 18-28 (in Japanese).

Kamitani,M. (1987) Bauxite deposits in China; high aluminous shale. *J. Clay Sci. Soc. Japan,* **27**, 62-71 (in Japanese, with English abstract).

Kanai,Y. (1986a) Determination of $^{234}U/^{238}U$ activity ratios in geological reference materials by alpha spectrometry. *Radioisotopes,* **35**, 601-604 (in Japanese, with English abstract).

Kanai,Y. (1986b) Investigation of sedimentary environment by selective chemical

leaching method. The 1986 annual meeting of the Geochemical Society of Japan, 236 (in Japanese).

Kanai,Y. (1989) Chemical composition of the spring deposits from the Masutomi spring, Yamanashi Prefecture. *Chikyukagaku(Geochemistry)*, **23**, 77-83 (in Japanese, with English abstract).

Kanai,Y. (1992a) Uranium distribution and $^{234}U/^{238}U$ activity ratios in a sedimentary bauxite deposit from Yangwa mine, China, and its implication for sedimentation process. *Geochem. J.*, **26**, 207-218.

Kanai,Y. (1992b) Uranium contents and $^{234}U/^{238}U$ activity ratios in aluminium reagents and bauxites. *Bunseki Kagaku*, **41**, T83-T86 (in Japanese, with English abstract).

Kanai,Y. (1993a) Well-type Ge detector for measuring small amount of environmental samples. *Radioisotopes*, **42**, 169-172 (in Japanese, with English abstract).

Kanai,Y. (1993b) Characterization of sediments using selective chemical leaching methods. *Bunseki*, **1993**, 980-982 (in Japanese).

Kanai,Y. (1994) A selective chemical leaching study of sediments from fresh-water lake, brackish-water lake and sea in the Japan areas. *Bull. Geol. Surv. Japan*, **45**, 625-654.

Kanai,Y. (1995) Analytical chemistry and characterization of amorphous materials in sediments -speciation by selective chemical leaching methods-. *Chishitsu News*, **496**, 36-49 (in Japanese).

Kanai,Y. and Ikehara,K. (1995) Sedimentation rates of offshore deposits in the Sea of Japan off Niigata Prefecture, using Pb-210 and Cs-137 radioactivity measurements. *Bull. Geol. Surv. Japan*, **46**, 269-282 (in Japanese with English abstract).

Kanai,Y., Imai,N. and Terashima,S. (1985) Determination of trace amount of uranium in geological reference samples by fluorimetry and extractive spectrophotometry. *Geostand. Newslett.*, **10**, 73-76.

Kanai,Y., Imai,N. and Terashima,S. (1986) Determination uranium in thirty-six geological rmaterials by extractive spectrophotometry using trioctylphosphine oxide and Arsenazo III. *Bunseki Kagaku*, **34**, 199-202 (in Japanese, with English abstract).

Kanai,Y., Kamitani,M. and Sakamaki,Y. (1990a) Behavior of uranium nuclides in residual deposits. The 1990 annual meeting of the Geochemical Society of Japan, 162-163 (in Japanese).

Kanai,Y., Sakamaki,Y. and Seo,T. (1990b) Geochemical behavior of uranium series

nuclides (^{238}U, ^{234}U, ^{226}Ra, ^{222}Rn) around the Tono uranium mine, Gifu Prefecture, central Japan. *Chikyukagaku(Geochemistry),* **24**, 123-132 (in Japanese, with English abstract).

Kanai,Y., Sakamaki,Y. and Sasada,M. (1993) Uranium content, $^{234}U/^{238}U$ activity ratio and water quqlity of seepage water in the Tsukuba Tunnel, Ibaraki, Japan. *Radioisotopes,* **42**, 143-150 (in Japanese, with English abstract).

Kanai,Y., Inouchi,Y., Katayama,H. and Saito,Y. (1995) Estimation of sedimentation rate at the lake Suwa in Nagano Prefecture determined by Pb-210 and Cs-137 radioactivities. *Bull. Geol. Surv. Japan,* **46**, 225-238 (in Japanese, with English abstract).

Kanai,Y., Okuyama,Y. and Sakamaki,Y. (1996) Speciation analysis of sediment by selective chemical leaching method -experimental study and its application to granitic conglomerate-. *Bull. Geol. Surv. Japan,* **47**, 413-425 (in Japanese, with English abstract).

Kanai,Y., Inouchi,Y., Katayama,H. and Saito,Y. (1997) Radioactivity measurements in bottom sediments from Lake Suwa, Nagano Prefecture, using a new low background system to estimate sedimentation rates. *Bull. Geol. Surv. Japan*, **48**, 277-295 (in Japanese, with English abstract).

Kanai,Y., Okuyama,Y., Seo,T. and Sakamaki,Y. (1998a) Geochemical micro-behavior of natural U-series nuclides in granitic conglomerate from the Tono mine, central Japan. *Geochem. J.*, **32**, 351-366.

Kanai,Y., Inouchi,Y., Yamamuro,M. and Tokuoka,T. (1998b) Sedimentation rate and environment in Lake Shinji, Shimane Prefecture. *Chikyukagaku(Geochemistry),* **32**, 71-85 (in Japanese, with English abstract).

Kanai,Y., Inouchi,Y. and Tokuoka,T. (1998c) Measurement of sedimentation rate at Daihai and Blackspring Lakes in China using radioactive nuclides and their sedimentary environment. *J. Sed. Soc. Japan*, **47**, 55-70 (in Japanese, with English abstract).

Kanai,Y., Inouchi,Y. and Tokuoka,T. (2000) Sedimentation rate and environment in mountain lakes in Nepal. *Bull. Geol. Surv. Japan,* **51**, submitted (in Japanese, with English abstract).

Kato,Y. (1968) On the Tertiary granitic rocks around Kohu basin, Yamanashi Prefecture. *Jour. Jap. Assoc. Mineral. Petrol. Economic Geol.*, **59**, 21-39 (in Japanese, with English abstract).

Katsuragi,Y. (1983) A study of ^{90}Sr fallout in Japan. *Pap. Met. Geophy.*, **33**, 277-291.

Katsuragi,Y. and Aoyama,M. (1986) Seasonal variation of Sr-90 fallout in Japan through the end of 1983. *Pap. Met. Geophy.*, **37**, 15-36.

Kigoshi,K. (1971) Alpha-recoil thorium-234: dissolution into water and the uranium-234 / uranium-238 disequilibrium in nature. *Science,* **173**,47-48.

Kim,K.H. and Burnett,W.C. (1985) ^{226}Ra in phosphate nodules from the Peru/Chile seafloor. *Geochim. Cosmochim. Acta,* **49**, 1073-1081.

Kobayashi,T. (1989) Geology and uranium mineralization in the eastern part of the Kani basin, Gifu, Central Japan. *Min. Geol.,* **39**, 79-94 (in Japanese, with English abstract).

Koga,A. (1959) Chemical studies on the hot springs of Beppu XIX. Trace elements in the hot springs of Beppu. Part 9. Distribution of uranium. *Jour. Chem. Soc. Japan,* **80**, 369-370 (in Japanese).

Kolodny,Y. and Kaplan,I.R. (1970) Uranium isotopes in sea-floor phosphorites. *Geochim. Cosmochim. Acta,* **34**, 3-24.

Kress,A.G. and Veeh,H.H. (1980) Geochemistry and radiometric ages of phosphatic nodules from the continental margin of northern New South Wales, Australia. *Mar. Geol.*, **36**, 143-157.

Kronberg,B.I., Fyfe,W.S., Leonardos,W.S.,Jr. and Santos,A.M. (1979) The chemistry of some Brazilian soils: element mobility during intense weathering. *Chem. Geol.*, **24**, 211-229.

Kronberg,B.I., Fyfe,W.S., McKinnon,B.J., Couston,J.F., StilianidiFilho,B. and Nash,R.A. (1982) Model for bauxite formation: Paragominas(Brazil). *Chem. Geol.*, **35**, 311-320.

Ku,T.-L., Knauss,K.G. and Mathieu,G.G. (1977) Uranium in open ocean: concentration and isotopic composition. *Deep-Sea Res.,* **24**, 1005-1017.

Kuroda,K. (1944) Strongly radioactive springs discovered in Masutomi. *Bull. Chem. Soc. Japan,* **19**, 33-83.

Lowson,R.T., Short,S.A., Davey,B.G. and Gray,D.J. (1986) ^{234}U/^{238}U and ^{230}Th/^{234}U activity ratios in mineral phases of a lateric weathered zone. *Geochim. Cosmochim. Acta,* **50**, 1697-1702.

Matsumoto,E. (1975) ^{210}Pb geochronology of sediments from Lake Shinji. *Geochem. J.* **9**, 167-172.

Matsumoto,E. (1987) Pb-210 geochronology of sediments. *Studies of the San'in region natural environment,* **No.3**, 187-194.

Maynard,J.B. (1983) Geochemistry of sedimentary ore deposits. Springer-Verlag, New

York, p.89-108.

McKelvey,V.E. (1967) Phosphate deposits. *U. S. Geol. Surv. Bull.*, **1252-D**, D1-D21.

Megumi,K. and Mamuro,T. (1977) Concentration of uranium series nuclides in soil particles in relation to their size. *J. Geophys. Res.*, **82**, 353-356.

Mihune,M. (1981) Radioactive spring and Misasa hot spring. *Onsenkagaku*, **31**, 81 (in Japanese).

Mitsuda,H., Tanaka,K., Kigoshi,K. and Nahgasawa,H. (1983) $^{234}U/^{238}U$ ratios in the groundwater samples from Musashino-daichi, western Tokyo. *Chikyukagaku (Geochemistry)*, **17**, 103-108 (in Japanese, with English abstract).

Mitsunashi,S. and Tokuoka,T. (1988) Lakes Nakaumi and Shinji. p.115.

Moore,D.G. and Scott,M.R. (1986) Behavior of ^{226}Ra in the Mississippi River mixing zone. *J. Geophys. Res.*, **91**, 14317-14329.

Nagaya,Y. and Nakamura,K. (1987) Artificial radionuclides in the western northwest Pacific (II): ^{137}Cs and $^{239,240}Pu$ inventories in water and sediment columns observed from 1980 to 1986. *J. Oceanogr. Soc. Japan*, **43**, 345-355.

Nakai,T. (1940) Radium content of mineral springs in Japan. *Bull. Chem. Soc. Japan*, 15, 333-426.

Nakanishi,M. (1948) Micro-determination of uranium by the fluorescence method II. *Jour. Chem. Soc. Japan*, **69**, 4 (in Japanese).

Noguchi,K. and Imahashi,M. (1967) Uranium content of acid hot spring waters in Japan. *Onsenkagaku*, **18**, 1-7 (in Japanese, with English abstract).

Nohara,T., Ochiai,Y., Seo,T. and Yoshida,H. (1992) Uranium series disequilibrium studies in the Tono uranium deposit, Japan. *Radiochim. Acta*, **58/59**, 409-413.

Nozaki,Y., Cochran.J.K., Turekian,K.K. and Keller,G. (1977) Radiocarbon and ^{210}Pb distribution in submersible-taken deep-sea cores from project FAMOUS. *Earth Planet. Sci. Lett.*, **34**, 167-173.

Ochiai,Y., Yamakawa,M., Takeda,S. and Harashima,F. (1989) Natural analogue study on uranium deposit in Japan. *CEC*, 126-138.

Officer,C.B. and Lynch,D.R. (1982) Interpretation procedures for the determination of sediment parameters from time-dependent flux inputs. *Earth Planet. Sci. Lett.*, **61**, 55-62.

Peirson,D.H. (1971) Worldwide deposition of long-lived fission products from nuclear explosions. *Nature*, **234**, 79-80.

Roe,K.K. and Burnett,W.C. (1985) Uranium geochemistry and dating of Pacific island apatite. *Geochim. Cosmochim. Acta*, **49**, 1581-1592.

Sakamaki,Y. (1985) Geologic environments of Ningyo-Toge and Tono uranium deposits, Japan. in "Geological environments of sandstone-type uranium deposits". *IAEA-TECDOC-328*, 135-154.

Sakanoue,M. and Hayashi,T. (1982) Study on Tatsunokuchi spring with extraordinaly $^{234}U/^{238}U$ and surrounding ground water. Abstract of the 1982 annual meeting of the Geochem. Soc. Japan. 297-298 (in Japanese).

Sandoval,D.N., Greaves,E. and Melendez,S. (1987) Uranium and thorium isotopic disequilibrium in Venezuelan hot springs. *Geochem. J.*, **21**, 43- 49.

Sato,C., Ochiai,Y. and Takeda,S. (1987) Natural analogue study of Tono sandstone type uranium deposit in Japan. Natural analogues in radioactive waste disposal. *CEC*, 462-472.

Schuller,A. (1957) Mineralogie und Petrographie neuartiger Bauxite aus dem Gun Distrikt, Honan-Provinz(china). Geologie, **6**, 379-399.

Sheng,Z.Z. and Kuroda,P.K. (1984) Alpha recoil effects of uranium isotopes in radioactive minerals. *Radiochim. Acta,* **37**, 93-98.

Sheng,Z.Z. and Kuroda,P.K. (1986a) Isotopic fractionation of uranium: Extremely high enrichment of ^{234}U in the acid-residues of a Colorado carnotite. *Radiochim. Acta*, **39**, 131-138.

Sheng,Z.Z. and Kuroda,P.K. (1986b) Further studies on the separation of acid residues with extremely high $^{234}U/^{238}U$ ratios from a Colorado carnotite. *Radiochim. Acta,* **40**, 95-102.

Shirvington,P.J. (1983) Fixation of radionuclides in the ^{238}U decay series in the vicinity of mineralized zones: 1.The Austatom Uranium Prospect, Northern Territory, Australia. *Geochim. Cosmochim. Acta*, **47**, 403-412.

Sugihara,K. (1967) Study on seasonal variation of Masutomi spring, Yamanashi Prefecture. *Memoirs of the Faculty of Liberal Arts and Edu. Yamanashi Uni.,* **18**, 221-230 (in Japanese).

Suzuki,E. (1993) ^{207}Bi and ^{137}Cs in nearshore marine sediments. 1. Distribution of ^{207}Bi and ^{137}Cs in coastal marine sediments collected from the Japan Sea. *Radioisotopes,* **42**, 503-510 (in Japanese, with English abstract).

Szabo,B.J. (1982) Extreme fractionation of $^{234}U/^{238}U$ and $^{230}Th/^{234}U$ in spring waters, sediments, and fossils at the Pomme de Terre Valley, southwestern Missouri. *Geochim. Cosmochim. Acta,* **46**, 1675-1679.

Talvitie,N.A. (1972) Electrodeposition of actinides for alpha spectrometric determination. *Anal. Chem.*, **44**, 280-

Taylor,S.R. (1964) The abundance of chemical elements in the continental crust a new table. *Geochim. Cosmochim. Acta*, **28**, 1273-1285.

Tessier,A., Campbell,P.G.C. and Bisson,M. (1979) Sequential extraction procedure for the speciation of particulate trace metals. *Anal. Chem.*, **51**, 844-851.

Tessier,A., Rapin,F. and Carignan,R. (1985) Trace metals in oxic lake sediments : possible adsorption onto iron oxyhydroxides. *Geochim. Cosmochim. Acta,* **49**, 183-194.

Topp,S.E., Salbu,B., Roaldset,E. and Jorgensen,P. (1984/1985) Vertical distribution of trace elements in laterite soil (Suriname). *Chem. Geol,* **47**, 159-174.

Turekian,K.K. and Wedepohl,K.H. (1961) Distribution of the elements in some major units of the earth's crust. *Geol.Soc.America Bull.,* **72**, 175-192.

Torii,T., Murakami,Y. and Murata,S. (1958) Uranium in mineral springs. *Onsenkagaku,* **9**, 91 (in Japanese).

Valeton,I. (1972) Developments in Soil Science 1. Bauxites. Elsevier, Amsterdam, 213 p.

Veeh,H.H. and Burnett,W.C. (1978) Uranium-series dating of insular phosphorite from Ebon atoll, Micronesia. *Nature*, 274, 460-462.

Veeh,H.H, Calvert,S.E. and Price,N.B. (1974) Accumulation of uranium in sediments and phosphorites on the South West Africa shelf. *Mar. Geol.,* **2**, 189-202.

White,A.H. (1976) Genesis of low iron bauxite, northwestern Cape York, Queensland, Australia. *Econ. Geol,* **71**, 1526-1532.

Wolfenden,E.B. (1965) Geochemical behaviour of trace elements during bauxite formation in Sarawak, Malaysia. *Geochim. Cosmochim. Acta,* **29**, 1051-1062.

Yamamoto,I., Shiota,T., Harashima,F., Fujimoto,J., Koinuma,M. and Hirono,S. (1974) Uranium exploration in the Tono district, Gifu Prefecture, Japan. *Min. Geol.,* **24**, 123-132 (in Japanese, with English abstract).

Yokoyama,Y. (1955) Studies on radio active springs in Japan. III Isotopes of radium in mineral waters. *J. Chem. Soc. Japan,* **76**, 558-562(in Japanese).

Yoshida,H. (1994) Relation between U-series nuclide migration and microstructural properties of sedimentary rocks. *Appl. Geochem.,* **9**, 479-490.

副　論　文

1．Geochemical micro-behavior of natural U-series nuclides in granitic conglomerate from the Tono mine, central Japan.
（中部日本東濃鉱山の花崗岩れきにおける天然ウラン系列核種の地球化学的微細挙動）
Kanai, Y., Okuyama, Y., Seo, T. and Sakamaki, Y.
Geochem.J., **32,** 351-366 (1998).

2．Uranium redistribution implied by $^{234}U/^{238}U$ disequilibrium study on apatite-bearing sedimentary rocks at Nakamaruke district, central Japan.
Kanai, Y. and Sakamaki, Y.
Appl. Geochem., **9,** 547-552 (1994).
（中部日本中東地域のリン灰石胚胎堆積岩における $^{234}U/^{238}U$ 非平衡から示されるウランの再移動）

3. Uranium distribution and $^{234}U/^{238}U$ activity ratios in a sedimentary bauxite deposit from Yangwa mine, China, and its implication for sedimentation process.
（中国 Yangwa 鉱山の堆積性ボーキサイト鉱床におけるウラン分布と $^{234}U/^{238}U$ 放射能比、およびそれから示唆される堆積過程）
Kanai, Y.
Geochem.J., **26**, 207-218 (1992).

4. Behavior of uranium-238 and its daughter nuclides in the Masutomi spring, Yamanashi Prefecture, central Japan.
（中部日本山梨県増富温泉におけるウラン-238 とその娘核種の挙動）
Kanai, Y.
Geochem.J., **22**, 285-292 (1988).

参　考　論　文

1. 茨城県中部域の源流部における浅層地下水・地表水の水質変動
　　金井　豊，上岡　晃，金沢康夫，関　陽児，濱崎聡志，月村勝宏，中嶋輝允
　　地調月報，**50**，591-610（1999）.

2. 水と地表物質との相互作用による水質について-福島・茨城県における湧水・地表水の調査例-
　　金井　豊，関　陽児，上岡　晃，金沢康夫，月村勝宏，濱崎聡志，中嶋輝允
　　地調月報，**49**，425-438（1998）

3. 島根県宍道湖の底質における堆積速度と堆積環境
　　金井　豊，井内美郎，山室真澄，徳岡隆夫
　　地球化学，**32**，45-59（1998）

4. 放射性核種を用いた中国 Daihai 湖および Blackspring 湖の堆積速度測定と堆積環境
　　金井　豊，井内美郎，徳岡隆夫
　　堆積学研究会報，**47**，55-70（1998）

5. 低バックグラウンド放射能測定システムによる長野県諏訪湖底質の放射能測定と堆積速度の見積り
　　金井　豊，井内美郎，片山　肇，斎藤文紀
　　地調月報，**48**，277-295（1997）.

6. 分別溶解法による堆積物中の元素の存在形態の研究－実験的検討と花崗岩質礫岩への応用－
　　金井　豊，奥山（楠瀬）康子，坂巻幸雄
　　地調月報，**47**，413-425（1996）.

7. 日本海東縁海域におけるタービダイトの化学組成と放射能変化
　　金井　豊，中嶋　健
　　地調月報，47，377-392（1996）.

8. 放射能測定などによって明らかにされる 1993 年北海道南西沖地震に起因する海底タービダイト

金井　豊，中嶋　健

Radioisotopes, 44, 856-864 (1995).

9. 1983 年日本海中部地震震源域でのタービダイトによる地震発生間隔の推定

中嶋　健，金井　豊

地震　第２輯，48，223-228 (1995).

10. 新潟沖大陸棚の Pb-210 および Cs-137 法による堆積速度

金井　豊・池原　研

地調月報，46，269-282 (1995).

11. ^{210}Pb，^{137}Cs 法による長野県諏訪湖底質の堆積速度の見積り

金井　豊，井内美郎，片山　肇，斎藤文紀

地調月報，46，225-238 (1995).

12. A selective chemical leaching study of sediments from fresh-water lake, brackish-water lake and sea in the Japan areas
(日本における淡水湖，汽水湖及び日本周辺海域の堆積物の選択的分別化学溶解法による研究)

Kanai, Y.

Bull.Geol. Surv. Japan, 45, 625-654 (1994).

13. 海水と間隙水におけるウランの地球化学　－鹿児島湾・八代海・甑島西方海水および底質間隙水の例－

金井　豊，望月常一，三田直樹

地調月報，45，267-277 (1994).

14. 微少量環境試料測定用井戸型 Ge 検出器の効率特性

金井　豊

Radioisotopes, 42, 169-172 (1993).

15. 筑波トンネル掘削に伴う湧水中のウラン，$^{234}U/^{238}U$ 放射能比および水質について

金井　豊，坂巻幸雄，笹田政克

Radioisotopes, 42, 143-150 (1993).

16. アルミニウム試薬及びボーキサイトに含まれる不純物ウランとそのウラン-234／ウラン-238 放射能比
金井　豊
分析化学，41，T83-T86（1992）.

17. 新潟県中束地区におけるウランの水文学的・地球化学的研究
金井　豊，坂巻幸雄
地調月報，42，261-274（1991）.

18. 岐阜県東濃地域におけるウラン系列核種の挙動とナチュラルアナログとしての有用性
金井　豊，坂巻幸雄，瀬尾俊弘
地調月報，42，249-260（1991）.

19. 岐阜県東濃ウラン鉱床における地下水・地表水中のウラン系列核種（^{238}U，^{234}U，^{226}Ra，^{222}Rn）の挙動
金井　豊，坂巻幸雄，瀬尾俊弘
地球化学，24，123-132（1991）.

20. 茨城県北東部那珂台地における新生界堆積物の化学組成と元素分布
金井　豊，坂本　亨，安藤　厚
地調月報，41，551-566（1990）.

21. Simultaneous determination of iron(II) and iron(III) oxides in geological materials by ion chromatography
（イオンクロマトグラフィーによる地質試料中 Fe(II)と Fe(III)の同時定量）
Kanai, Y.
Analyst, 115, 809-812 (1990).

22. Elemental concentrations in nine new GSJ rock reference samples "sedimentary rock series"
（9つの新しい GSJ 岩石標準試料" 堆積岩シリーズ" 中の元素濃度）
Terashima,S., Ando,A., Okai,T., Kanai,Y., Taniguchi,M., Takizawa,F. and Itoh,S.
Geostandards Newslett., 14, 1-5 (1990).

23. 山梨県増富温泉における温泉沈澱物の化学組成
金井　豊
地球化学，**23**，77-83（1989）.

24. 関東平野北東部における第四紀後期テフラの主成分及び微量成分組成
金井　豊，坂本　亨，安藤　厚
地調月報，**39**，783-797（1988）.

25. イオンクロマトグラフィーにおける陰・陽イオンの保持挙動と陸水分析への応用
金井　豊
地調月報，**38**，587-600（1987）.

26. Determination of $^{234}U/^{238}U$ activity ratios in geological reference materials by alpha spectrometry
（アルファスペクトロメトリーによる岩石標準試料中の $^{234}U/^{238}U$ 放射能比の定量）
Kanai, Y.
Radioisotopes, **35**, 601-604（1986）.

27. 茨城県茨城町におけるＧＳ６６試錐試料の化学組成（第２報）－粒度別及び分別溶解法によるフラクション別の化学組成－
金井　豊
地調月報，**37**，555-570（1986）.

28. Determination of uranium in thirty-six geological reference samples by fluorimetry and extractive spectrometry
（蛍光法と抽出/吸光法による36個の地質標準試料中ウランの定量）
Kanai, Y., Imai, N. and Terashima, S.
Geostandards Newslett., **10**, 73-76（1986）.

29. 茨城県茨城町におけるＧＳ６６試錐試料の化学組成
金井　豊，坂本　亨，安藤　厚
地調月報，**36**，173-189（1985）.

30. トリオクチルホスフィンオキシド抽出分離－アルセナゾ III 吸光光度法による地質試料中微量ウランの定量
金井 豊，今井　登，寺島　滋
分析化学，34，199-202 (1985).

31. Determination of bismuth in geological materials by anodic stripping voltammetry (アノーディック・ストリッピング・ボルタンメトリーによる地質試料中ビスマスの定量)
Kanai, Y.
地調月報，33，619-625 (1982).

32. Background atmospheric concentrations of halogenated hydrocarbons in Japan (日本におけるハロゲン化炭化水素の大気中バックグラウンド濃度)
Makide, Y., Kanai, Y. and Tominaga, T.
Bull.Chem.Soc.Japan, **53**, 2681-2682 (1980).

33. メタンのハロゲン置換体のガスクロマトグラフィーにおける保持挙動
金井 豊，巻出義紘，富永　健
日本化学会誌，**1980**，663-666 (1980).